

POLITECNICO DI TORINO

Master's Degree Course
in Biomedical Engineering



MULTIBODY MODELS FOR A COMPARATIVE ANALYSIS OF ULTRA-CONGRUENT VERSUS MEDIAL-PIVOT DESIGNS OF TOTAL KNEE ARTHROPLASTY

Supervisors:

Prof. C. Bignardi

Prof. M. Terzini

Candidate:

Gloria Ruocco
S221768

2017-2018

CONTENTS

ABSTRACT.....	1
CHAPTER 1.....	3
INTRODUCTION	3
1.1 <i>ANATOMY OF THE HUMAN KNEE JOINT</i>	3
1.1.1 BONE STRUCTURES	3
1.1.2 SOFT TISSUES	5
1.1.2.1 Menisci and joint capsule	5
1.1.2.2 Ligamentous structures and their roles	6
1.2 <i>JOINT BIOMECHANICS</i>	9
1.2.1 Generality.....	9
1.2.2 Knee Joint coordinate system	10
1.2.3 Knee joint Biomechanics	11
1.3 <i>KNEE INJURIES AND CAUSES FOR TOTAL KNEE REPLACEMENT</i>	14
1.3.1 Meniscal Damages	14
1.3.2 Ligaments injuries.....	15
1.3.3 Arthritis.....	16
1.4 <i>TOTAL KNEE ARTHROPLASTY (TKA)</i>	17
1.4.1 Implant Components	17
1.4.2 Implant Designs	18
1.4.2.1 History	18
1.4.3 Types of Knee Arthroplasty	20
1.5 <i>MULTIBODY MODELING</i>	21
1.5.1 Multibody knee models.....	22
CHAPTER 2.....	25
METHODS AND MATERIALS	25
2.1 <i>THE PROSTHESES</i>	25
2.2 <i>MODELS DEVELOPMENT</i>	26
2.2.1 GEOMETRIES	26
2.2.2 ARTICULAR SURFACES CONTACT MODELING	30
2.2.3 LIGAMENTS REPRESENTATION.....	32
2.2.3.1 Number of ligament springs	35
2.2.3.2 Origin points and insertion points of each ligament and their zero-load length.....	36
2.3 <i>SIMULATED PASSIVE MOTION</i>	39
2.3.1 CONSTRAINTS AND LOADS	40
2.3.2 EVALUATION OF THE INTERNAL ROTATION OF THE TIBIA.....	41
2.4 <i>SIMULATED ACTIVE MOTION</i>	42

2.4.1 CONSTRAINTS AND LOADS	43
2.4.2 QUANTITATIVE ANALYSIS OF THE KINEMATICS	48
2.4.3 CONTACT FORCES DISTRIBUTION	49

CHAPTER 3.....52

RESULTS AND DISCUSSIONS	52
3.1 RESULTS FOR PASSIVE KNEE MOTION	52
3.1.1 LIGAMENT FORCES	52
3.1.2 CONTACT FORCES	54
3.1.2 TIBIAL INTERNAL ROTATION	55
3.2 RESULTS FOR THE ACTIVE KNEE MOTION	56
3.2.1 CONTACT FORCES	56
3.2.1 TIBIAL INTERNAL ROTATION	58
3.2.2 QUADRICEPS FORCES	60
3.2.3 FORCES DISTRIBUTION DURING A SQUAT MOTION.....	62
.....	62
3.3 CONCLUSIONS AND FUTURE DEVELOPMENTS	64

APPENDIX.....67

LIST OF FIGURES

FIGURE 1. 1:LOWER LIMB	3
FIGURE 1. 2: KNEE JOINT ON THE FRONTAL PLANE. (A) FRONT VIEW; (B) REAR VIEW [SCHUNKE M. ET AL PROMETHEUS-ATLANTE DI ANATOMIA 2006].....	4
FIGURE 1. 3: CAVITÀ GLENOIDE CON MENISCHI E LORO PUNTI DI INSERZIONE VIEW [SCHUNKE M. ET AL PROMETHEUS-ATLANTE DI ANATOMIA 2006].....	5
FIGURE 1. 4: CRUCIATES LIGAMENTS. (A) FRONT VIEW; (B) REAR VIEW [SCHUNKE M. ET AL PROMETHEUS-ATLANTE DI ANATOMIA 2006]	6
FIGURE 1. 5: COLLATERAL LIGAMENTS. (A) MEDIAL VIEW; (B) LATERAL VIEW [SCHUNKE M. ET AL PROMETHEUS-ATLANTE DI ANATOMIA 2006].....	8
FIGURE 1. 6 : ANATOMICAL AXES AND PLANES	9
FIGURE 1. 7: THREE ROTATIONS OF THE KNEE (A) AND THE THREE TRANSLATIONS (B) [NOYES FR ET AL]	10
FIGURE 1. 8: ROLL-GLIDE MECHANISM DURING KNEE FLEXION: (A) PURE ROLLING; (B) PURE SLIDING; (C) COMBINED MOVEMENT [SMITH P.N. ET AL 2003]	11
FIGURE 1. 9: AXIAL ROTATION AND TRANSLATION OF CONTACT POINTS ON THE TIBIAL PLATEAU SHOWING THE MEDIAL PIVOTING MOTION[DENNIS D. A. ET AL 2005	13
FIGURE 1. 10 : MENISCAL FISSURES PATTERN [MORDECAI S. C. ET AL 2014].....	14
FIGURE 1. 11: SCHEMATIC COMPARISON BETWEEN A HEALTHY KNEE (A) AND AN ARTHRITIC KNEE (B) [ZAFFAGNINI P.S. ET AL 2017]	16
FIGURE 1. 12: REPRESENTATION OF A TOTAL KNEE REPLACEMENT IMPLANT	17
FIGURE 1. 13: HINGED PROSTHESIS	18
FIGURE 1. 14: DUOCONDYLAR KNEE	19
FIGURE 1. 15: THE TOTAL CONDYLAR KNEE	19
FIGURE 1. 16: TYPICAL MOBILE BEARING TKA.....	20
FIGURE 1. 17: MEDIAL PIVOT KNEE [SHIMMIN A. ET AL 2015]	21
FIGURE 1. 18: MULTIBODY MODELS OF INTACT KNEE DEVELOPED BY LI, GIL ET AL. IN 1999 (A) AND BY GUESS IN 2011 (B)	22
FIGURE 1. 19: TOTAL KNEE REPLACEMENT MULTIBODY MODEL [STYLIANOU AP ET AL 2013]	23
FIGURE 2. 1: K_MOD ULTRACONGRUENT FIXED BEARING INSERT	25
FIGURE 2. 2: K_MOD DYNAMIC CONGRUENCE FIXED BEARING INSERT	25
FIGURE 2. 3: TIBIAL AND FEMORAL COMPONENTS	25
FIGURE 2. 4: GEOMETRIES OF THE BONES AND PROSTHESES IMPORTED INTO ADAMS. IN DETAIL THE TWO PROSTHESES: IN RED THERE IS THE ULTRA CONGRUENT INSERT AND IN GREEN THE DYNAMIC CONGRUENCE INSERT	27
FIGURE 2. 5: LATERAL AND FRONTAL VIEW OF THE ELLIPSOIDE USED TO REPRESENT THE PATELLAR BONE.....	29

FIGURE 2. 6: RAPRESENTATION OF HOW THE IMPACT FORCE WORKS	30
FIGURE 2. 7: CONTACT FORCE DIALOG BOX.....	31
FIGURE 2. 8: THE FORCE-STRAIN (F-E) RELATIONSHIP FOR THE ELEMENTS MODELLING THE LIGAMENT FIBER BUNDLES [WISMANS J. ET AL 1980; KORHONEN K.R. ET AL 2011].	33
FIGURE 2. 9: TIBIAL INSERTS DIVIDED INTO MEDIAL AND LATERAL COMPARTMENTS	39
FIGURE 2. 10: BUSHING DIALOG BOX.....	40
FIGURE 2. 11: LOADS AND CONSTRAINTS USED FOR THE PASSIVE MOTION OF THE KNEE.....	41
FIGURE 2. 12: EVALUATION OF TIBIAL INTERNAL ROTATION.....	42
FIGURE 2. 13: LATERAL AND FRONTAL VIEW OF THE ORIGIN AND INSERTION POINTS OF THE PATELLAR TENDON AND PATELLOFEMORAL LIGAMENTS	43
FIGURE 2. 14: FEMUR HEAD AND THE SPHERICAL AND TRANSLATIONAL JOINTS TO SIMULATE THE PRESENCE OF THE HIP	44
FIGURE 2. 15: REVOLUTE JOINTS TO ALLOW THE TIBIA MOVEMENTS WITH RESPECT TO THE FOOT.....	45
FIGURE 2. 16: MODIFY CONTROL BLOCKS DIALOG BOX	47
FIGURE 2. 17: SPHERICAL SHAPE OF POSTERIOR FEMORAL CONDYLES.....	48
FIGURE 2. 18: TWO CONCENTRIC SPHERES REPRESENT THE TWO POSTERIORE FEMORAL CONDYLES.	49
FIGURE 2. 19: THE DISCRETIZED ULTRACONGRUENT INSERT	50
FIGURE 2. 20: THE DISCRETIZED DYNAMIC CONGRUENCE INSERT	51
FIGURE 3. 1: TREND OF THE LIGAMENT FORCES FOR THE LATERAL COLLATERAL LIGAMENT IN THE MODEL WITH ULTRA CONGRUENT INSERT	52
FIGURE 3. 2: TREND OF THE LIGAMENT FORCES FOR THE MEDIAL COLLATERAL LIGAMENT IN THE MODEL WITH ULTRA CONGRUENT INSERT	53
FIGURE 3. 3: TREND OF THE LIGAMENT FORCES FOR THE LATERAL COLLATERAL LIGAMENT IN THE MODEL WITH DYNAMIC CONGRUENCE INSERT	53
FIGURE 3. 4: TREND OF THE LIGAMENT FORCES FOR THE MEDIAL COLLATERAL LIGAMENT IN THE MODEL WITH DYNAMIC CONGRUENCE INSERT	53
FIGURE 3. 5: TREND OF THE MERDIAL AND LATERAL CONTACT BETWEEN THE FEMORAL COMPONENT AND THE ULTRACONGRUENT INSERT	54
FIGURE 3. 6: TREND OF THE MEDIAL AND LATERAL CONTACT BETWEEN THE FEMORAL COMPONENT AND THE DYNAMIC CONGRUENCE INSERT	54
FIGURE 3. 7: TIBIAL INTERNAL ROTATION AFTER TKA WITH ULTRACONGRUENT INSERT.....	55
FIGURE 3. 8: T: TIBIAL INTERNAL ROTATION AFTER TKA WITHDYNAMIC CONGRUENCE INSERT	56
FIGURE 3. 9: CONTACT FORCES DEVELOPPED BETWEEN THE FEMORAL COMPONENT AND THE MEDIAL AND LATERAL SIDE OF ULTRACONGRUENT INSERT	56

FIGURE 3. 10: CONTACT FORCES DEVELOPPED BETWEEN THE FEMORAL COMPONENT AND THE MEDIAL AND LATERAL SIDE OF DYNAMIC CONGRUENCE INSERT.....	57
FIGURE 3. 11: TIBIAL INTERNAL ROTATION (ULTRACONGRUENT INSERT).....	58
FIGURE 3. 12: TIBIAL INTERNAL ROTATION (DYNAMIC CONGRUENCE INSERT).....	58
FIGURE 3. 13 :QUADRICEPS FORCE DEVELOPPED IN THE MODEL WITH ULTRACONGRUENT INSERT.....	60
FIGURE 3. 14: QUADRICEPS FORCE DEVELOPPED IN THE MODEL WITH DYNAMIC CONGRUENCE INSERT.....	61
FIGURE 3. 18: FORCES DISTRIBUTION AT SOME FLEXION ANGLES.....	63
FIGURE 3. 19: ULTRA CONGRUENT AND DYNAMIC CONGRUENCE INSERT.....	64
FIGURE 3. 20: CONÌMPARING TIBIAL INTERNAL ROTATION DURING THE PASSIVE KNEE FLEXION ERRORE. IL SEGNALIBRO NON È DEFINITO.	
FIGURE 3. 21: COMPARING TIBIAL INTERNAL ROTATION DURING THE ACTIVE KNEE FLEXION ERRORE. IL SEGNALIBRO NON È DEFINITO.	

ABSTRACT

The knee joint is one of the most complex joints of the human body. It is one of the joints of the lower limb where tibiofemoral and patellofemoral sliding allows joint movements. The fluidity and amplitude of movements are guaranteed by the integrity of the soft tissues surrounding the joint (ligaments, menisci and articular cartilage). If the articular cartilage covering the articular surfaces involved in the knee is consumed or subjected to a degenerative process (arthrosis), then a total knee arthroplasty (TKA) implant could be required. The implant is composed of a femoral component, a tibial component and a polyethylene insert whose role is similar to that of articular cartilage. However, several models of TKA are available with different materials and shapes.

The aim of this thesis work is the comparison between two different prosthetic designs. The two types of prosthesis are two fixed bearing models and they differ in the shape of the insert: one has a perfectly symmetrical geometry between the medial and lateral sides (ultra-congruent insert); the other has an asymmetry between the two compartments (dynamic congruent insert).

The comparative analysis between the two inserts was carried out through the realization of multibody models of the knee joint. The multibody models of the knees (physiological or prosthetic) are widely used to try to understand the complex biomechanical function of the knee. These are schematic representations of the joint composed of different bodies interacting with each other through relative movements containing a mathematical representation of the soft tissues within the joint.

For each type of prosthesis analyzed, two multubody models were created in order to simulate a passive and an active flexion movement of the knee, respectively. After having imported all the involved geometries, the ligaments and the contacts between the articulating surfaces have been appropriately modelled. The models of the passive knee movement (with each of the inserts) have been used to obtain the position of the ligament bundles and the zero-load lenght of the ligaments to guarantee a correct balance of the articular contact forces. These forces were evaluated by a simmetrical division of the two inserts in a medial and in a lateral portion. After obtaining the ligaments balancing in the passive condition, the same parameters were used for an active model in which a knee flexion with a quadriceps muscle activation was simulated. To obtain the pattern of the force distribution on the surfaces of the inserts, both inserts were divided in several cell

elements to evaluate the single contact between each cell and the femoral component of the prosthesis during the whole flexion movement.

In addition, the tibial intrarotation that occurs during the knee flexion movement from extension up to 90 ° of flexion were calculated.

In both prosthetic models it is possible to observe a consistent internal rotation of the tibia. However, the greater range of rotation observed in the model with dynamic congruent insert is actually a proof that its geometry, with asymmetrical shapes, allows a kinematics more similar to the physiological kinematics.

CHAPTER 1

INTRODUCTION

1.1 ANATOMY OF THE HUMAN KNEE JOINT

The knee is one of the joints of the lower limb together with the hip joint and the ankle joint.

1.1.1 BONE STRUCTURES

The knee joint consists of three main bones:

- Distal end of the **femur**
- Proximal end of the **tibia**
- **Patella**.

The **femur** is a long bone (its longitudinal dimension is predominant compared to the other two) that forms the skeleton of the thigh. The femur consists of the central part (diaphysis) and the two ends (epiphysis). The proximal epiphysis (formed by the head and neck of the femur) is articulated with the hip bone forming the coxofemoral joint, while the distal one (formed of two medial and lateral condyles) is articulated with the patella and the tibia forming the knee joint.

The **tibia** is another long bone of the lower limb. As for the femur, a central body and two extremities are considered. Proximal epiphysis (upper extremity), expands a lot in the transverse direction forming the tibial condyles each of which is concave (glenoid cavity) to allow articulation with the femoral condyles

Below the lateral condyle the tibia interfaces with the upper side of the fibula. The distal epiphysis is involved in the ankle joint.

The **patella** is the largest sesamoid bone (the three dimensions are comparable) of the body and is located in the anterior region of the knee.



Figure 1. 1: Lower limb¹

¹ Prometheus-Atlante di Anatomia-Anatomia Generale e Apparato Locomotore- Utet 2006 p. 375

It has a triangular shape with the base placed at the top and the apex at the bottom. The posterior surface, coated with cartilage, is in relationship with the joint cavity. The two medial and lateral margins are the attachment regions to the wing ligaments of the patella. The front surface is also contained in the expansion of the femoral quadriceps which continues below in the superficial fibers of the patellar ligament

These three bones are articulated to form two articular joints: one between the femur and the tibia (**tibiofemoral joint**) and the other one between the femur and the patella (**patellofemoral joint**) [Abulhaan J. F. et al 2017] . The fibula is not considered part of the joint because it is firmly connected to the tibia and has negligible relative movements.

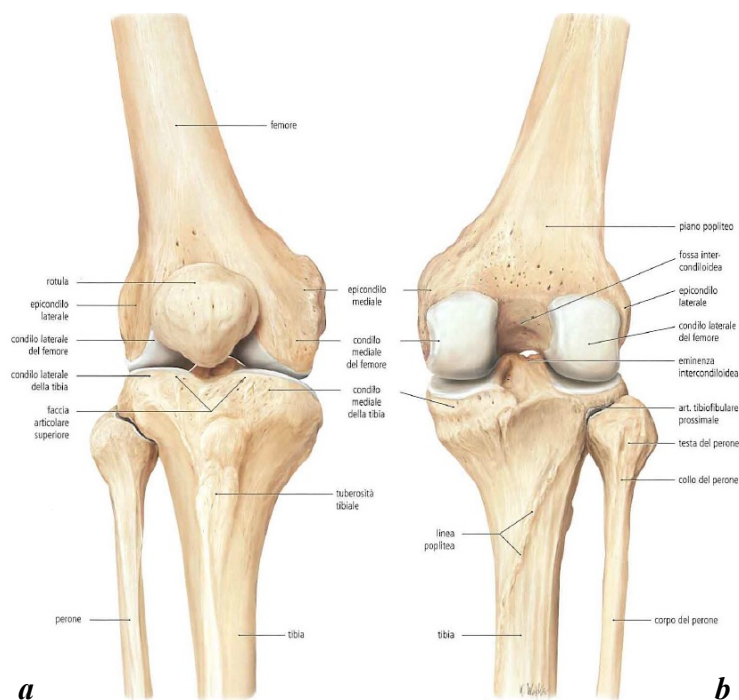


Figure 1. 2: Knee joint on the frontal plane. (a) Front view; (b) rear view [Schunke M. et al Prometheus-Atlante di Anatomia 2006]

The **tibiofemoral joint** has a medial and a lateral compartment [Chhajer B 2006]. It is the largest joint of the human body and includes two condylar joints: the medial and lateral femoral condyles, very convex, are articulated with the two almost flat tibial grooves (the upper face of the tibia is in fact generally called the tibial plateau). The femoral condyles have a curvature radius that decreases moving from the front to the back and the radius of curvature of the medial femoral condyle is wider than that of the lateral femoral condyle. Regarding the tibial compartments, they are not

congruent but asymmetrical structures: the medial one is more concave and oval while the lateral one is more convex [Goldblatt J. P. et al 2003].

The **patellofemoral joint** is a typical saddle joint between the patella and the femoral trochlea. The stability of the patella in the trochlear groove is a combination of bone, muscle and ligament containment [Goldblatt J. P. et al 2003]. The main role of this joint is played in the extensor mechanism: it allows the force of the extensors along the knee to be transferred to a greater distance from the axis of rotation.

1.1.2 SOFT TISSUES

1.1.2.1 Menisci and joint capsule

Between the articular surfaces of the femur and tibia there are the **menisci**, two cartilaginous semilunar disks that serve to improve joint compliance and assist knee rotation [Goldblatt J. P. et al 2003]. At the extremities (front and back horn) are attached to the bone at the level of the anterior and posterior intercondyloid areas by short ligaments. The medial meniscus is significantly larger posteriorly than when it is not anteriorly showing a sickle-like form [Schunke M. et al Prometheus-Atlante di Anatomia 2006]. The lateral meniscus has an almost complete circle shape with an approximately uniform thickness from the front to the back. Menisci have important **biomechanical functions**: they contribute to the transmission of loads, to the absorption of shock, to the stability and lubrication of the joint [Mordecai S. c. et al 2014]. Their function is also to reduce contact tensions and increase the contact area and make the articular surfaces of the femur and tibia congruent [Alice J. S. et al 2012].

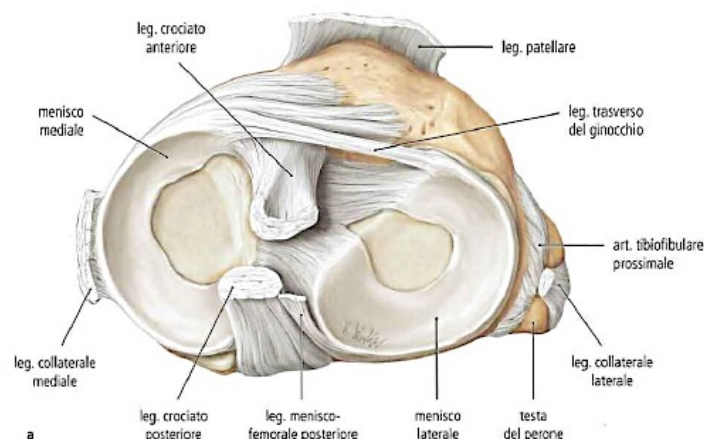


Figure 1. 3: Cavità glenoide con menischi e loro punti di inserzione view [Schunke M. et al Prometheus-Atlante di Anatomia 2006]

Like any diarthrosis (mobile joint), the knee is surrounded by a **joint capsule**. It is a fibrous sleeve composed of an internal and an external part. The internal membrane is the synovial membrane that delimits a cavity where synovial fluid is present, which normally functions as a biological lubricant to guarantee low friction between the articular surfaces [Tamer T. M. 2013]. There are also other capsules (four laterally and five medially [Abulhasan J. F. et al 2017]) filled with synovial fluid that help reduce friction between adjacent mobile structures. They are in fact distributed around areas characterized by large movements to ensure fluid and friction-free movements.

1.1.2.2 Ligamentous structures and their roles

Ligaments have a key role in providing **stability** to the knee joint during different activities, but even the muscles play an important role to guarantee the correct knee function [Abulhasan J. F. et al 2017]. The ligaments are bundles of fibers that connect two bones to each other providing support to joints; in the knee joint the ligaments link together the femur and tibia ([Abulhasan J. F. et al 2017], [Wismans J. 1980]). Each bundle of ligaments is responsible for stability in specific directions during a knee movement but the joint stability depends on the interactions of all ligaments [Bhaskar K. M. et al 2014]. There are different types of ligaments in the human knee but the most important, from a mechanical point of view, are the **cruciates** and the **collateral ligaments** [Wismans J. 1980]. Their main role is to avoid abnormal motions of the joint.

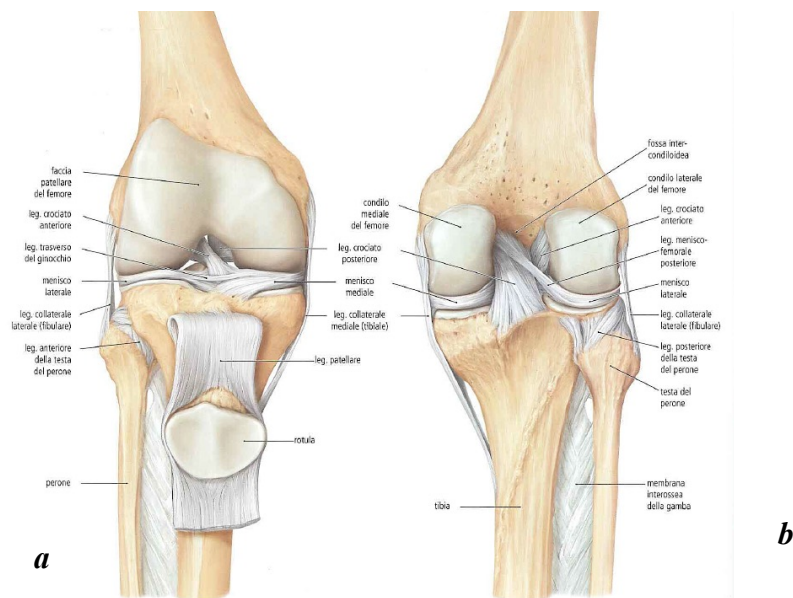


Figure 1. 4: Cruciates ligaments. (a) Front view; (b) rear view [Schunke M. et al Prometheus-Atlante di Anatomia 2006]

There are two **cruciate ligaments**: the anterior cruciate ligament (**ACL**) and the posterior cruciate ligament (**PCL**). They are both intra-articular ligaments; it means that they are located in the middle of the joint [Wismans J. 1980] and their tibial insertions suggest their name.

The **ACL** consists of two bundles: the anteromedial (AM) bundle and the posterolateral bundle (PL) ([Schunke M. et al Prometheus-Atlante di Anatomia 2006]; [Petersen W. et al 2006]). Infact the AM bundle originates from a deeper point in the posteromedial portion of the lateral femoral condyle and it arrives to its anteromedial tibial insertion, whereas the PL bundle has a more superficial, low and distal origin point on the femoral condyle and its tibial insertion between the intercondylar eminences of the tibia is more posterior and lateral.

The **PCL** is shorter than the ACL. Its femoral attachment is located on the lateral surface of the medial femoral condyle, while the tibial attachment is in the posterior intercondyloid area. The PCL is characterized by two bundles: the anterolateral bundle and the posteromedial bundle. These two ligaments are the most important stabilizer in the human knee joint and they provide a restraint to the anteroposterior slidings of the knee: the ACL limits anterior and rotational displacements of the tibia relative to the femur, while the PCL restricts posterior displacement ([Abulhasan J. F. et al 2017], [Petersen W. et al 2006]). This is possible because the anterolateral band of the PCL is tight in flexion (restricting the posterior tibial displacements in flexion position) and the posteromedial bundle is tight in extension (resisting posterior tibial displacement during the extension), whereas the recruitment of the ACL fibers is almost the opposite ([Kweon C. et al 2013], [Blankevoort L. et al 1991]).

Two **collateral ligaments** reinforce the joint: the **medial (or tibial) collateral ligament (MCL)** and the **lateral (or fibular) collateral ligament (LCL)**.

The **MCL**, as the name suggests, is located in the internal side of the joint. It's the largest of the collateral ligaments and it's a flat band attached proximally to the medial femoral epi-condyle and distally under the medial tibial plateau on the medial tibial surface (Figure 1.5.a). It's main role in the knee joint is to limit valgus rotations during the knee flexion; thus it's tight during full extension while its laxity increases during flexion. Otherwise, the **LCL** it's a strong round cord-like ligament originating from the lateral epicondyle of the femur to the fibular head (Figure 1.5.b).

The MCL and LCL limit respectively the valgus and varus rotations during flexion.

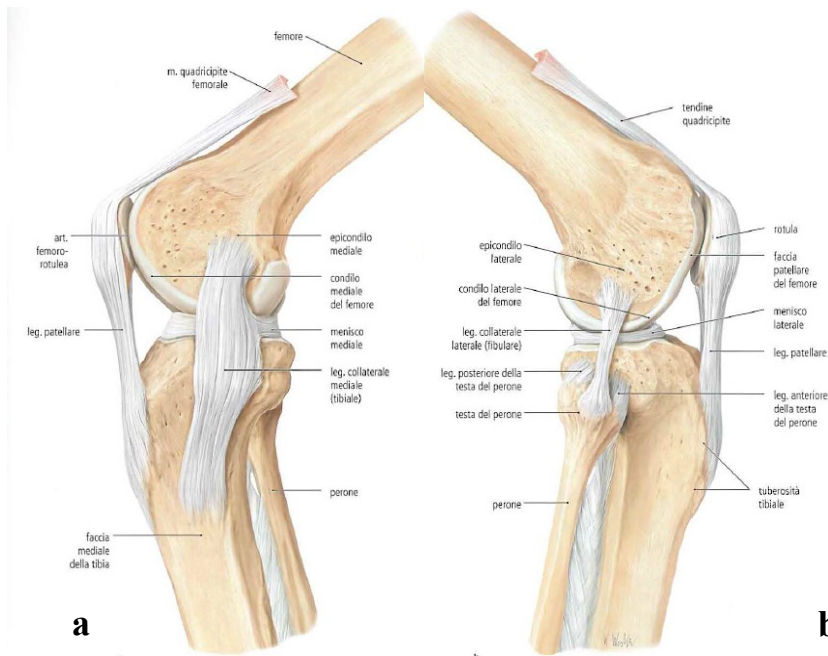


Figure 1. 5: Collateral ligaments. (a) Medial view; (b) Lateral view [Schunke M. et al Prometheus-Atlante di Anatomia 2006]

To perform this functions both collateral ligaments are tight when the knee is totally extended then, with increasing degrees of flexion, the LCL relaxes until full flexion whereas the medial collateral ligament remains in tension throughout the whole range of flexion changing its area of tension: in extension the whole ligament is involved then the posterior part of the ligament is relaxed in flexion and only the anterior portion remains in tension ([Otto B. Y. et al 1941], [Blankevoort L. et al 1991]).

Other important ligaments in the knee joint are those related to the stability of patellar bone. First of all the the **patellar ligament** is a broad, thick fibrous bundle extending from the apex of the patella (the most inferior portion of the patella) to the tuberosity of the tibia (**Figure 4**). This bundle of fibers is called *ligament* because connects two bones: the patella and the tibia; but from a morphological point of view, it represents the end of the quadriceps tendon that extends from the quadriceps and, incorporating the patella, arrives on the tibial tuberosity; thus it's also called patellar tendon . The patellar ligament is fundamental in the extension of the knee joint: patients with patellar ligament rupture are no longer able to extend the leg [Kricun R. et al 1980]. To restrain medial and lateral patellar dislocations, the knee joint is provided with two **patellofemoral ligaments**: the medial patellofemoral ligament (**MPFL**) and the lateral patellofemoral ligament (**LPFL**). The MPFL generally extends from the posterior region of the medial femoral epicondyle to the superomedial part of the

patella [Smirk C. et al 2003] and, on the opposite side, from the posterior and proximal region of the lateral femoral epicondyle to the superolateral facet of the patella the LCL originates and inserts [Navarro MS et al 2008].

1.2 JOINT BIOMECHANICS

1.2.1 Generality

The aim of all joints is to allow the movements of the bony structures that are part of the joint to guarantee mobility to the entire skeleton. The field of the science regarding the human body's movement due to the interaction of muscles, bones and ligaments, is called **biomechanics**.

Before describing the movements that affect the knee joint it is necessary to define some important anatomical references.

The movements of the human body take place in space, so it is important to associate a reference Cartesian tern to the human body:

- **Longitudinal axis:** it is the vertical axis that goes from the feet towards the head and is parallel to the force of gravity;
- **Middle-lateral axis:** it is the axis orthogonal to the longitudinal axis that goes from right to left;
- **Antero-posterior axis:** it is the axis perpendicular to the two previous axes that proceeds from the back of the body towards the front.

Coupling these three axes we can identify the three anatomical planes of the human body:

- **Sagittal plane:** plane orthogonal to the middle-lateral axis (axis of symmetry of the human body);
- **Trasversal plane:** plane orthogonal to the longitudinal axis;

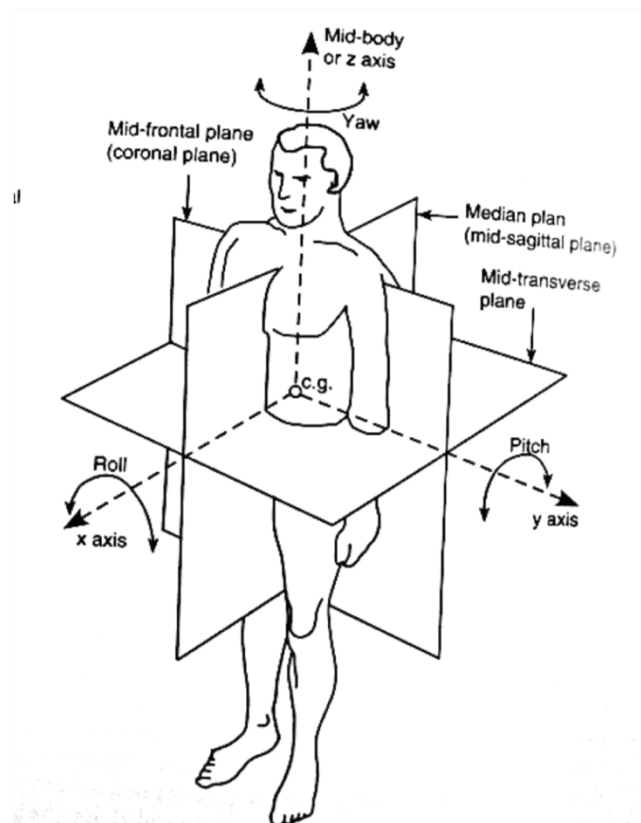


Figure 1. 6 : Anatomical axes and planes

- **Frontal plane:** plane orthogonal to the antero posterior axis.

Since the movements of the different body segments are defined starting from the mutual positions of the segments, it is advisable to identify for each skeletal segment a local reference system consisting of a longitudinal axis (parallel to the main axis of the considered segment), a mid-lateral axis (from the center of the segment to the outside) and an anterior-posterior axis (orthogonal to the previous two); then to define a coordinate system for the joint to which the segments belong.

1.2.2 Knee Joint coordinate system

By focusing on the knee joint, the relative movements between the femur and the tibia can be defined starting from a **joint coordinate system** [Grood E. S. et al 1983]. This coordinate system is defined by considering:

- An axis fixed to the first skeletal segment involved in the articulation (the femur) and coinciding with its mid-lateral axis (**flexion-extension axis**);
- An axis fixed to the second skeletal segment involved in the articulation (tibia) and coinciding with its longitudinal axis (**axial rotational axis**);
- An axis mutually orthogonal to the previous two defined "floating axis" because it does not belong to any of the two skeletal segments (**abduction-adduction axis**).

A rotation can occur around each of these axes and a translation can take place along each axis. From a kinematic point of view, the knee is a joint with six degrees of freedom (DOF): three translations and three rotations[Blankevoort L. et al 1988] schematically illustrated in the Figure 1.7.

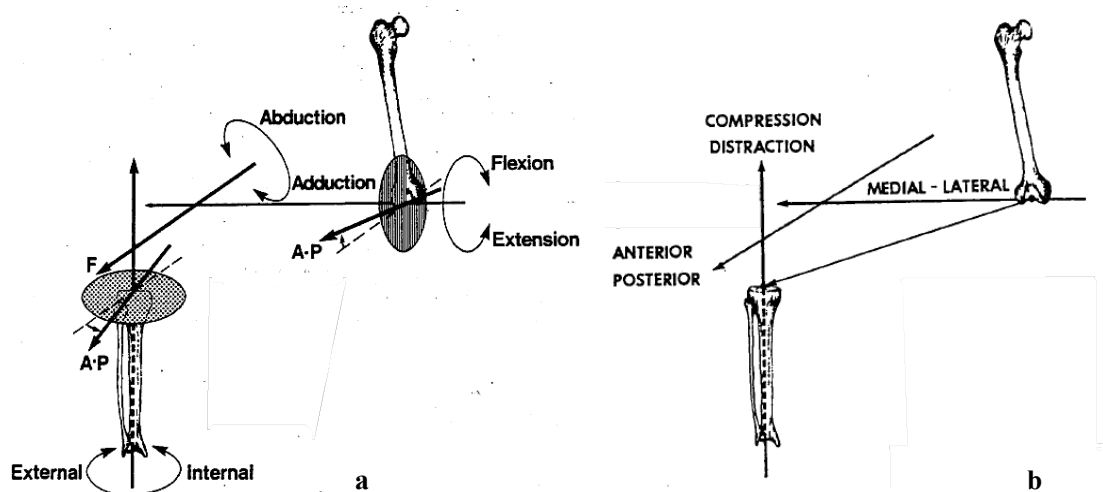


Figure 1. 7: Three rotations of the knee (a) and the three translations (b) [Noyes FR et al]

1.2.3 Knee joint Biomechanics

The knee joint is essentially a mechanical linkage whose components like ligaments, menisci, cartilages and muscles allow complex mechanical responses to different applied loads ([Banks SA et al 1996], [Bhaskar K. M. et al 2014]).

The key movement of the knee joint is the flexion-extension; the others take place to a lesser extent and are generally coupled with it. The translations are limited by the capsule-ligamentous apparatus and by the muscles, therefore they occur in a very reduced way.

The joint kinematics during flexion extension movement is mainly determined by the geometry of the articular surfaces. The rounded shape of the femoral condyles may lead to imagine a pure rolling movement ("roll") of the femoral condyles on the tibial glenoid cavities as a pure hinge joint. However, it has been widely demonstrated that joint movement is driven by a combined **rolling and sliding mechanism** [Kapandji I. et al 1970; Muller P.N. et al 1983; O'Connor J. Et al 1990; Smith P.N. et al 2003]. If the movement were pure rolling, a dislocation of the knee would be observed: the femur moves backwards with respect to the tibia (Figure 6.a). If, on the contrary, there was only sliding, the flexion would be impeded due to premature contact of the femur with the posterior surface of the tibia (Figure 6.b). A combination of the two movements allows to obtain a wide flexion and to maintain the contact between the articular herpes (Figure 6.c). The ratio of the sliding-rolling phenomenon during flexion and extension is variable. Starting from complete extension, the femoral condyles begin to roll, without slipping up to 20 ° -30 ° of flexion; as the degree of flexion increases, the sliding movement becomes preponderant until the end of the flexion. With regard to pure rolling, the two femoral condyles have different characteristics because of their asymmetry: the rolling occurs first on the medial condyle and then on the lateral condyle.

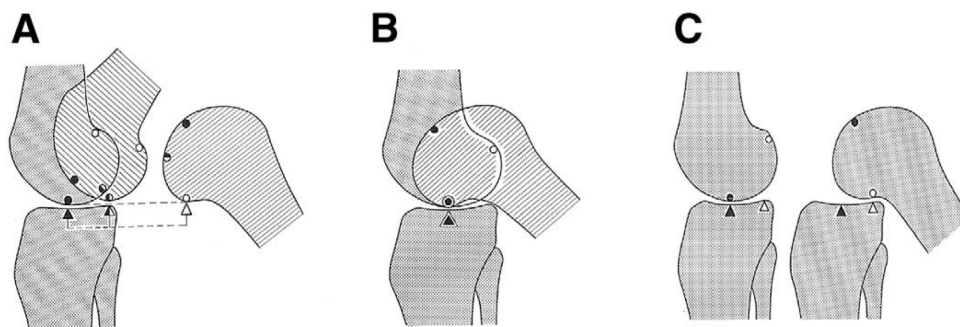


Figure 1. 8: Roll-glide mechanism during knee flexion: (A) pure rolling; (B) pure sliding; (C) Combined movement [Smith P.N. et al 2003]

The flexion-extension movement is characterized by some important features. It has been highlighted that during the flexion of the knee there is a minimal movement of the medial femoral condyle while the lateral femoral condyle moves backwards. This pattern is determined by the occurrence of two events: while the knee flexes around an epicondylar axis, the tibia rotates around its vertical axis towards the inside of the joint (tibial internal rotation) [Hollister A. M. et al 1993; Churchill D. L. et al 1998; Walker P.S. et al 2009].

Several studies have highlighted these characteristics: in 1999, Todo S. et al in an *in vivo* study of unloaded normal knees measured the femoral condyle antero-posterior translation on the tibia connecting the centers of the two femoral condyles and showed that, in a flexion range up to 90 °, the lateral femoral condyle rolled back more than the medial condyle; further demonstrations of this have been reported from **in vitro studies** on unloaded cadaver knee [Iwaki H. et al 2000; Wilson D. R. et al 2000] also simulating deeper knee bends up to 150 ° of flexio [Li G. eta al 2004], and **in vivo studies** on loaded knees during weight-bearing activity like squatting [Hill P.F. et al 200] or normal gait, rising from and sitting in a chair [Komistek R. D. et al 2003]. A comparative study on tibio-femoral kinematics in living knees under unloaded and loaded conditions analyzed through direct imaging revealed that in both conditions the medial side of the joint is more stable showing minimal translations and is accompanied by an internal rotation of the tibia (external femoral ration). However, this rotation, which increases as the bending angle increases, is greater in the weight-bearing conditions [Johal P. eta al 2005].

Different authors use different techniques for the evaluation of relative movements: Asano T. et al in 2001 using a biplanar image-matching technique analyzed the kinematics of the knee by evaluating the movement of the geometric center axis ((axis connecting the centers of the two femoral condyles) to the surface of the tibia. Iwaki H. et al (2000) evaluated tibiofemoral movements in unloaded cadaver knees. These measurements were made on MRI images by drawing, at each bend angle, the segment that connected the tangent to the posterior cortex of the tibia with the center of each posterior femoral condyle (FFC). The same technique was used in the study of Johal P. et al in 2005 conducted on living knees and the results obtained confirmed those of cadaveric experiences.

In 2005 Dennis D. a et al proposed a method of tibiofemoral kinematics analysis based on contact points: for each flexion angle the minimum contact point of each

femoral condyle on the tibia was automatically calculated and projected onto the tibia surface (**Figure 1.9**).

Despite these different methods, the one on which most of the studies converge is that the main movement of the knee joint (flexion-extension) is not only a rotation movement around an intercondylar axis, limited to the sagittal plane, but there is an internal axial rotation of the tibia: it's the so called **physiological medial-pivot pattern** [Feng Y. et al 2015; Asanto T. et al 2001; Johal P. et al 2005; Moro-oka T. et al 2008] classically defined as the “**screw-home**” **pattern** (Meyer H. in 1853 was the first to introduce this concept).

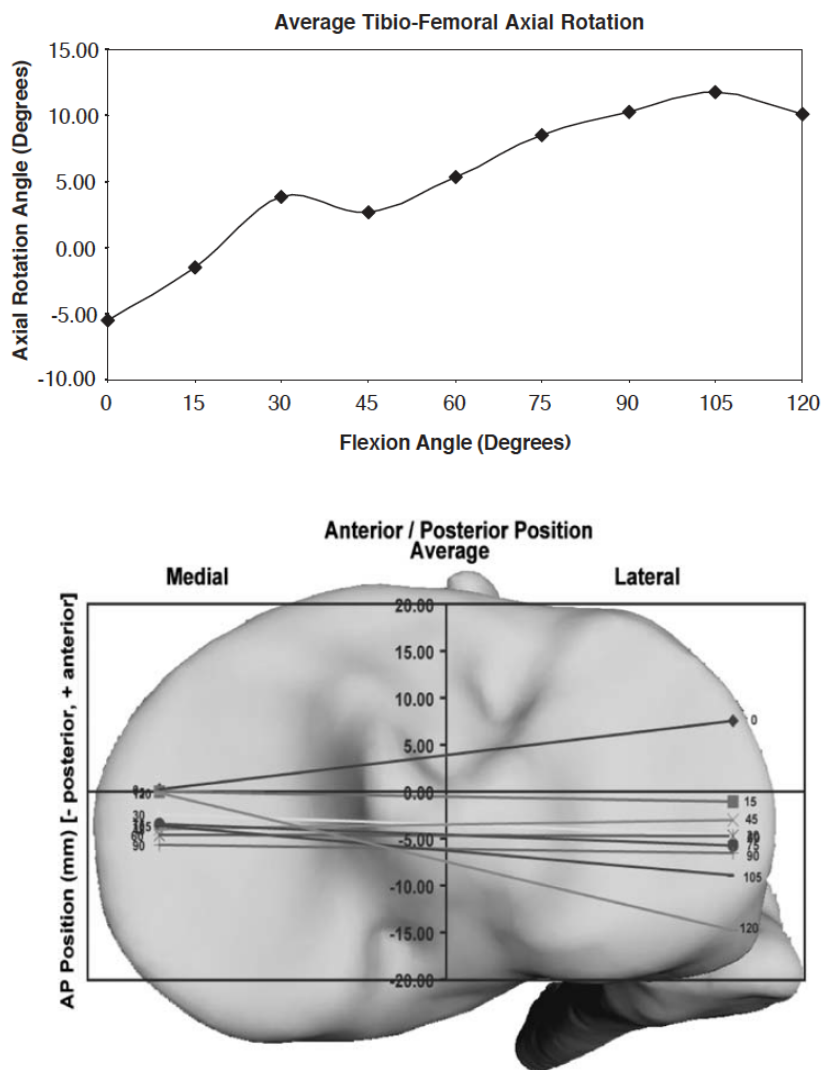


Figure 1. 9: Axial rotation and translation of contact points on the tibial plateau showing the medial pivoting motion [Dennis D. A. et al 2005]

1.3 KNEE INJURIES AND CAUSES FOR TOTAL KNEE REPLACEMENT

The knee joint is subjected to a very high mechanical demand providing its support function. This is why any problems that affects one of its components can compromise the entire functionality of the joint.

The most common injuries that affect the knee are total or partial ligament or meniscus ruptures, bone fractures and osteochondral injuries [Trilha JM et al 2009].

1.3.1 Meniscal Damages

Meniscal fractures are the most common orthopedic diseases and a distortion trauma (a violent rotation of the femur on the tibia) is usually the main cause of meniscal injuries.

Depending on the location of the fractures, they can be divided in longitudinal, horizontal, vertical and complex lesions (Figure 6). Complex injuries are degenerative and are created by the coexistence of two or more fissure patterns.

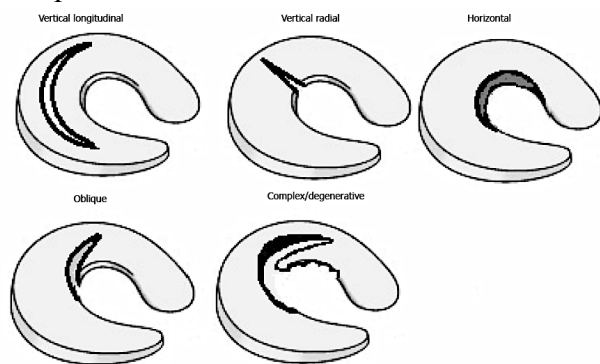


Figure 1.10 : Meniscal fissures pattern [Mordecai S. C. et al 2014]

With age, degenerative problems can occur caused by wear. They are different from a meniscal rupture because not caused by a traumatic event occurred generally during a sport activity but it's only an effect of aging of tissues. In both of these situations the meniscus most often affected is the medial one because it has a reduction of motion [Alice J. S. et al 2012] compared with the lateral one thus, because of a traumatic event it is less able to react to sudden loads and, if a degenerative process is occurring, the medial meniscus will be the most damaged because it is subjected to greater loads.

Different treatment of meniscal injuries exist: non-operative treatment, meniscectomy (total or partial) and meniscal repair [Mordecai S. C. et al 2014]. The first choice is a conservative method and it can be satisfying in the short term because specific physical exercises can increase muscle strength and flexibility but, when the symptoms come back and persist, meniscectomy could be the solution. However,

total meniscectomy (total removal of the damaged meniscus) is not recommended because the total absence of the menisci causes punctual loads and drastic changes in the biomechanics of the joint. On the other hand removing only the damaged part (partial meniscectomy) or repairing the meniscus (using the modern arthroscopy techniques) can help to save some meniscal function [Mordecai S. C. et al 2014].

1.3.2 Ligaments injuries

Ligaments injuries are common in people practicing sport activities. When the ligaments are underwent to excessive tension, they first stretch, then gradually tear off until complete rupture.

The worst case is the total rupture of the tissue that may occur either at a central point of the bundle or at the points of attachment with bones; this situation can compromise the stability and balance of knee movement [Bhaskar K. M. et al 2014]. Collateral ligament rupture (MCL, LCL) usually occurs when the leg is urged inwards (resulting in a medial collateral ligament tears) or outwards ((resulting in a lateral collateral ligament tears) . It is particularly common because these abnormal movements occur in many sports activities when the foot is on the ground and a force is applied to the side of the knee. The ligaments are well vascularized so they can heal themselves if helped by a good rehabilitative activity. Therefore, usually surgery is not necessary to repair damage to a collateral ligament.

It's not always the same for the cruciate ligaments. During sport activities or as a result of car accident [Trilha JM et al 2009, excessive hyperextension or sudden back force can cause tearing of the ACL (anterior cruciate ligament). The PCL (posterior cruciate ligament) is mostly damaged when the flexed knee receives a strong blow that push the tibia posteriorly. This occurs for example during a car accident when the knee bumps against the dashboard (it's called the 'dashboard injury' [Jones O.]) or during different sports. The posterior cruciate ligament, being well vascularized, is able to heal after an accurate rehabilitative activity. On the contrary, ACL has insufficient vascularity to withstand the repair process and therefore the ligament irreversibly degenerates. For this reason, in young patients with intense physical activity, arthroscopic surgery is a specific treatment with which the damaged ligament can be replaced with a tendon graft generally from the patellar tendon.

1.3.3 Arthrosis

The most common cause of pain in the various joints of the human body is osteoarthritis which causes a reduced functionality of the joints themselves. Knee joint is definitely one of the joints most affected by this disease because of the mechanical stress to which it is subjected.

The osteoarthritis of the knee, **gonarthrosis**, is most frequently defined as the “*change involving damage of the articular cartilage of the knee joint, emergence of abnormal knee tissue, reactive changes in synovial membrane, and pathological synovial fluid*” [Kasumovic M. et al 2015].

Therefore it is not an inflammatory disease but a chronic degenerative rheumatic disease related to joint wear. With the degenerative process of arthrosis there is a thinning of the articular cartilage (**Figure 7**) that covers the femoral condyles and the tibial plates. As articular cartilage is a non-vascularized tissue, it can not regenerate and its progressive degeneration will lead to expose the underlying bone that reacts producing sharp growths called osteophytes. The resulting pain is accompanied by rigidity and limitation in movements.

The onset of osteoarthritis is generally caused by trauma that can damage the joint, degenerative joint diseases [Moti LT et al 2015] (typically rheumatoid arthritis), abnormal loadings and mechanopathology [Felson DT et al 2009] such as joint instability or joint malalignment.

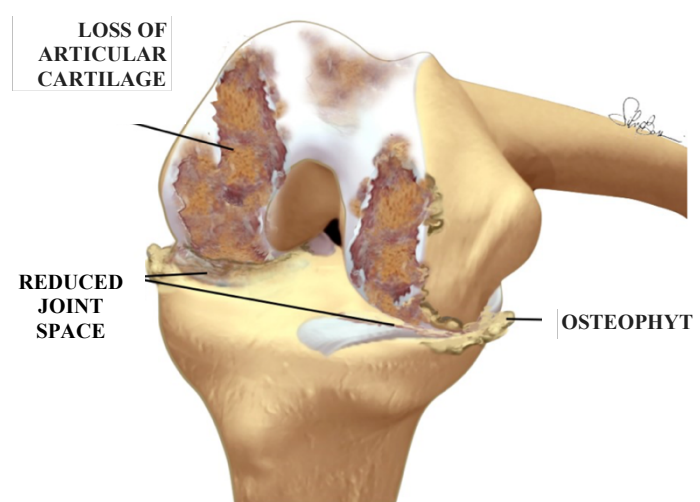


Figure 1. 11: schematic comparison between a healthy knee (a) and an arthritic knee (b) [Zaffagnini P.S. et al 2017]

To treat osteoarthritis, an initial approach includes drug therapy, physiotherapy or infiltration of cortisone and hyaluronic acid whose goal is to reduce inflammation and pain. Because of the progressive nature of the disease, these treatments could not be able to control symptoms, thus many patients undergo surgery with the replacement of the entire joint.

1.4 TOTAL KNEE ARTHROPLASTY (TKA)

1.4.1 Implant Components

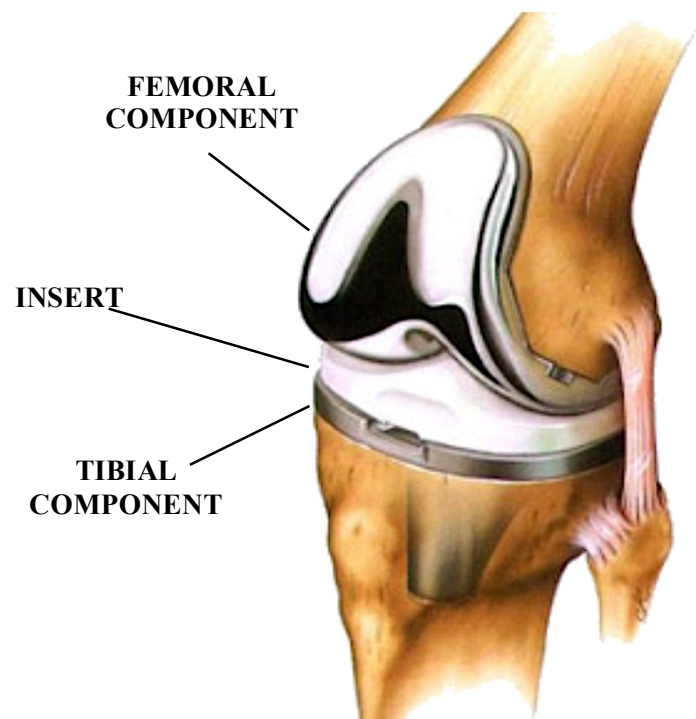


Figure 1. 12: Representation of a total knee replacement implant

Total knee replacement surgery involves replacing damaged bone portions with implantable components.

The first prosthetic implants were based on the idea that the knee was a pure hinge joint so that they included a hinge connection between the components. More recent implants try to replicate the most complex movements and to the support of the ligaments.

Many types of prosthetics for the TKR are commercially available, but all have the following common elements (Figure 8):

- a **femoral component**, consisting of a large metal component used to cover the surface of the distal part of the femur (the two condyles). This component, on its anterior part, has a furrow inside which the patella can move so that the knee can flex and extend;
- a **tibial component**, represented by a metallic flat surface that is fixed on the proximal part of the tibia;
- an **insert** made of plastic material (polyethylene), which allows the femur to articulate with the tibia. It may have a complex profile that mimics the natural articular surface.
-

1.4.2 Implant Designs

The main objective of a total knee arthroplasty is to restore lost knee functions and normal joint kinematics. The design of a total knee replacement has to satisfy anatomic congruence (conformity) of the contacting areas between the femoral and tibial surfaces, it has to reproduce the normal constraint (opposition to a movement in a particular degree of freedom) and the anatomical laxity [Walker PS et al 2000].

1.4.2.1 History

([Vivian P. P. et al 2018], [Causero A. et al 2014])

The development of total knee arthroplasty dates back in 1860, when the German surgeon, Themistocles Gluck, implanted the first hinge joints (the prosthesis allowed only the flexion of the joint, a limited extension and lateral stability) made of ivory. The failure due to infections led to different modifications of the prosthetic model, especially from the point of view of materials, reaching the early seventies with the Guaper prosthesis composed of a cobalt-chrome alloy hinge.

The hinged prostheses (**Figure 1.13**) were highly constrained limiting the movements to the sole flexion-extension and they had short duration.



Figure 1. 13: Hinged Prosthesis

Guenston nel 1965 fu tra i primi a realizzare una protesi totale di ginocchio policentrica: a unhinged knee with separate condylar components on both sides (medial and lateral) of the joint.

In 1971 the first Duocondylar Knee (**Figure 1.14**) was implanted; it was composed of two separated tibial components and it provided the retention of both cruciate ligaments. This model was then

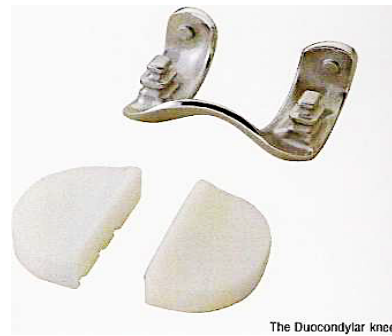


Figure 1. 14: Duocondylar knee

replaced by the Duopatella Knee and Total Condilar Knee in 1974. The Duopatella Knee, continuing to preserve the cruciate ligaments, included a femoral component with an anterior lip for the patellar articulation and a singular tibial component (for a better stability) with a posterior rectangular cut for the PCL. The surgical results were positive but the surgeons preferred the Total condilar Knee (**Figure 1.15**)



Figure 1. 15: The total condylar knee

created by Isnall, Ranawat and Walker and Scott. It was a posterior stabilized implant including sacrificing of the cruciate ligaments. It was made of a Cobalt Chrome femoral component, polyethylene tibial component and a patellar component. The conformity of femoral and tibial components allowed sliding and rotation during flexion of the knee. A second version of this prosthesis was developed in 1976 (The Insall-Burstein Prosthesis) to solve some manufacturing problems and instability of the first version.

For a better posterior stabilization of the joint a “tibial-wedge-shaped post” [Papas PV et al 2018] was added and it articulated with a femoral cam between the two condyles. The tibial component, with a metaphyseal stem, was originally in polyethylene but then was backed with metal to guarantee a more homogeneous loading distribution to the surrounding bone preventing polyethylene deformation [Causero A et al 2014].

Modern and advanced designs still contain some of this characteristics.

1.4.3 Types of Knee Arthroplasty

The first classification among the different types of knee prostheses concerns **total knee prostheses** and **partial knee prostheses**. Partial knee replacements are more conservative because they only replace the damaged articular region, making the intervention less invasive; with the total knee prosthesis all the articular components are replaced with artificial components.

During a total knee replacement surgery, the condition of the surrounding tissues must be checked. If the posterior cruciate ligament (PCL) is in good condition and can continue to perform its stabilizing functions, it is not removed but retained and in this case the chosen prosthesis category is that of the **cruciate retaining TKA (CR)**. In case of PCL removal, the prostheses are called **posterior-stabilized TKA (PS)**. The difference between the two types of prosthesis is the design: the tibial component of a PS design has a central post that work together a cam in the femoral component to do what the PCL does: prevent abnormal sliding of the femur during knee flexion. The opinions on which of the two types offer better results are controversial: some authors have concluded that between the two types of prosthesis there are no clinically significant differences in functional outcome [Conditt M. A. et al 2004], range of motion or pain reduction [Verra W.C. et al 2014].

Another important classification in total knee prostheses concerns **mobile bearing** or **fixed bearing prostheses**. As the name suggests, these are prosthetic designs in which the polyethylene insert is mobile with respect to the metal tibial component or fixed with it respectively. The reason why mobile-bearing design was introduced, was to avoid wear and excessive stressed caused by the fixed-bearing models. However studies about short-terms [Kaikmaz B. et al 2015] , mid-terms [Kim YH eta al 2001] or long-terms results [Kim YH et al 2007] have shown that the range of motion recovered after the operation wa satisfactory for both models. The main difference found was in the duration of the intervention that is longer for mobile bearing.



Figure 1. 16: Typical Mobile Bearing TKA

The extensive studies conducted on kinematics of the knee and the continuous research of a prosthetic implant increasingly conforming to human anatomy led to the realization of **medial pivot knees**. They are implants in which the insert presents the medial and lateral compartments with non symmetric but asymmetric shapes: the



Figure 1. 17: Medial Pivot Knee [Shimmin A. et al 2015]

medial compartment has a spherical surface ("ball in socket design" [Shimmin A. et al 2015]), while the lateral side presents a wider and less conformant surface. These geometrical characteristics allow the medial femoral condyle rotation during flexion but limiting its antero-posterior translation; the lateral femoral condyle can freely translate

posteriorly respecting the "screw-home mechanism" (2.3 paragraph) of physiological kinematics.

The choice of the kind of prostheses to implant is based on the patient's characteristics (eg age, weight, physical activity), on the conditions of surrounding tissue (especially ligaments), on implant characteristics and, in the end but not least, on the surgeon's experience and familiarity with the device.

1.5 MULTIBODY MODELING

In this paragraph the multibody models will be briefly introduced: what they are and how they can be used in the study of the biomechanics of the knee joint.

Multibody models are the schematic representation of more complex mechanical systems composed of different bodies (rigid or flexible) interacting with each other through relative movements. Through the study, analysis and simulations of multibody models of interconnected bodies it is possible to understand their dynamic behavior. Among the various engineering fields in which multibody models are used (especially aerospace engineering, robotics or vehicle engineering), Biomechanics is also included.

In this field multibody dynamics (**MBD**) models are used to represent simplified kinematics of the human joints and their anatomical range of motion, to reproduce the constrained movements between different anatomical segments and a realistic representation of the contacts between anatomical geometries [Ambrósio J., Silva M. 2005].

1.5.1 Multibody knee models

In the field of the analysis of the mechanical behavior of the knee joint and of the interaction between the various structures that make it up, the dynamic multibody models of the knee are an important tool used today. Dynamic simulations of these models with applied external loads (forces or moments) and appropriate constraints between the articulating surfaces, allow to make considerations on mechanical contacts in articulation and joint kinematics. Over the years, multibody knee models have been developed relating to both the natural knee and the prosthetic knee.

The first studies related to the healthy knee were focused on the development of simplified mathematical models of the knee for the analysis of the relative movements and of the forces present in the human knee (Wismans 1980) verifying their correspondence with experimental results.

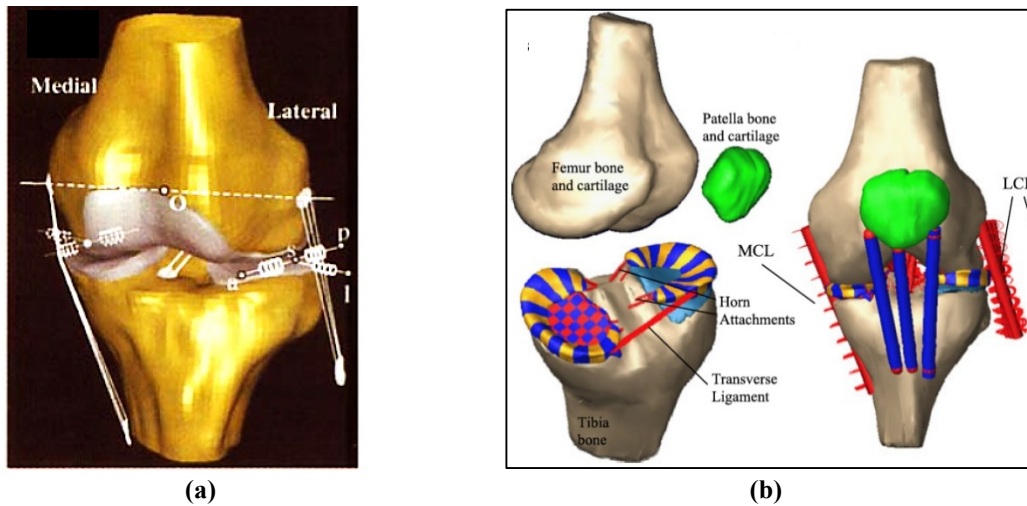


Figure 1.18: Multibody Models of intact knee developed by Li, Gil et al. in 1999 (a) and by Guess in 2011 (b)

Thanks to the technological progress, more and more complex and refined models have been developed (**Figure 11**), including articular cartilage, meniscus, muscles and ligaments [Blankevoort L., Kuiper et al 1991; Blankevoort, Huiskes et al. 1991; Bei et al 2004; Guess Trent , Thiagarajan et al 2010; Bloemker K. H., Trent M. Guess et al 2012;] applying both static and dynamic loading conditions, axial loads, anterior posterior loads or simulating simple or more complex knee-like tasks such as simple flexion-extension, the models have been used to correctly replicate and analyze joint contacts, ligament properties and especially the joint kinematics and joint loads.

When a knee is no longer healthy and requires a prosthetic intervention, the specific knowledge of joint kinematics and joint loads is essential to ensure the success of the surgery and understand the features that can improve the designs of total knee replacement [Walker P.S et al 2009]. A knee prosthesis in fact has to allow a kinematic that is as physiological as possible and loads (contact forces) that fall within the physiological ranges. Abnormal loads are in fact harmful elements that help not only the progress of rheumatic diseases, but can be the triggering cause of wear and subsequent failure of the knee implant.

In TKA multibody models the articular cartilage (femoral and tibial) and the menisci are removed and the prosthetic components are inserted (**Figure12**) into their place. If the type of prosthesis provides it, the modelling of cruciate ligaments can be sacrificed or preserved.

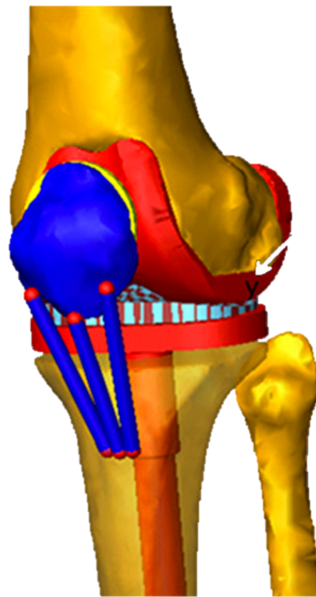


Figure 1. 19: Total knee replacement Multibody model [Stylianou AP et al 2013]

These models can be used to predict contact forces, joint movements (g.e. internal and external rotation and anteroposterior translations) and muscular activations during one of the most daily activities carried out: a normal walking [Chen et al 2014; Marra et al 2015; Chen et al 2016]. However, after a knee prosthesis implantation, it is expected to be able to perform, in addition to the normal walking, many more activities that however require the achievement of greater angles of flexion.

The dynamic simulations of multibody models during weight-bearing deep knee bend activities like squatting [Stylianou A. P. et al 2013] allow to obtain the contact forces between the prosthetic components that have higher values than those recorded

for a normal walking cycle falling within a range between 2 and 5 times the body weight [Innocenti B. et al 2011; Mizu-uchi H. et al 2015] confirming the results of other dynamic simulations of multibody models but related to intact knees [Nagura T. et al 2006; Smith S. et al 2008; Kutzner I. et al 2010; Bersini S. et al 2015].

The contact forces transmitted between the articulating surfaces (metal component and polyethylene insert) have a direct impact on the distribution of the tensions between the components and the surrounding bone. Since a non-homogeneous transmission of tensions or the birth of punctual loads are among the main causes of failure of the knee prosthesis implants, a later analysis with a finite elements model (FEM) would allow to obtain information about the stress conditions at the bone-implant interface.

CHAPTER 2

METHODS AND MATERIALS

The aim of this thesis work is the comparison and analysis of the behavior of two different total knee prostheses.

2.1 THE PROSTHESES

The two prostheses analyzed are two models of the Bioimpianti group of Milan belonging to the K_MOD family (Knee Modular Solution). What differentiates them is the type of insert:

- **Ultra-congruent (Fixed Bearing) insert:**
insert used in case of resection of the posterior cruciate ligament. The two medial and lateral compartments are symmetrical; unlike traditional posterior stabilizer implants, it requires less bone resection and the raised anterior part avoids front sliding which could lead to anterior dislocation.
- **Dynamic Congruence (Fixed Bearing) insert:**
insert characterized by the asymmetry of the medial and lateral compartments with a spheroidal surface of the medial compartment. This guarantees a natural tibiofemoral kinematics. Also in this design the raised anterior part avoids front sliding which could lead to anterior dislocation.

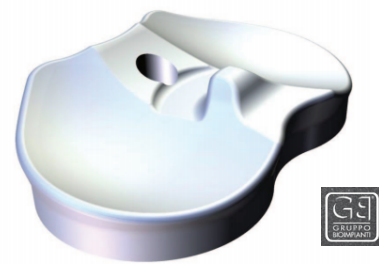


Figure 2. 1: K_MOD ultracongruent fixed bearing insert



Figure 2. 2: K_MOD dynamic congruence fixed bearing insert

The femoral component and the tibial (fixed) component were provided to complete the two prosthetic designs.



Figure 2. 3: Tibial and femoral components

2.2 MODELS DEVELOPMENT

To study the dynamic behavior of the two different types of prostheses, two multibody models of the knee joint were assembled in a specific multibody dynamics simulation software: **MSC ADAMS**[®] (*Automated Dynamic Analysis of Mechanical Systems*).

This kind of software performs the analysis of the motion of multibody systems. More precisely, it's able to analyze both the kinematics and the dynamics of the system after defining:

- The bodies constituting the model (parts)
- The system of loads acting on each part (forces)
- The constraints and relative movements between the various parts.

In this thesis work the knee joint assembled models have been used to simulate a passive motion and an active motion (squatting activity) to analyze the joint kinematics in an unloaded and loaded left knee after total knee arthroplasty.

2.2.1 GEOMETRIES

In order to create the knee models, the complete geometry of the bone elements that compose it was necessary: the femur, the tibia and the patella. Furthermore, since prosthetic knees are also present, the geometries of the prosthetic elements have also been considered.

Two **Sawbones standard geometries** were used for the bone elements of the femur and tibia. Their CAD, together with the CADs of the prosthetic components, were first imported into Solidworks[®] to obtain a correct alignment between the parts, and then the assembly was imported into Adams in Parasolid format. In **Figure 2.4** the geometries imported into Adams are shown in their correct positions. *Fixed joints* were placed between the femoral component and the femur, the insert and the tibial component, the tibial component and the tibia. Doing this, no relative movements were allowed between the locked parts.

When the geometries are imported into Adams, the software recognizes them as rigid bodies and automatically assigns the material: steel. However, to make the model more accurate, it is necessary to associate specific properties or material with the individual

parts. Adams allows both to create a new material to associate with the parts and to assign certain mass properties opening the dialog box referred to each part.

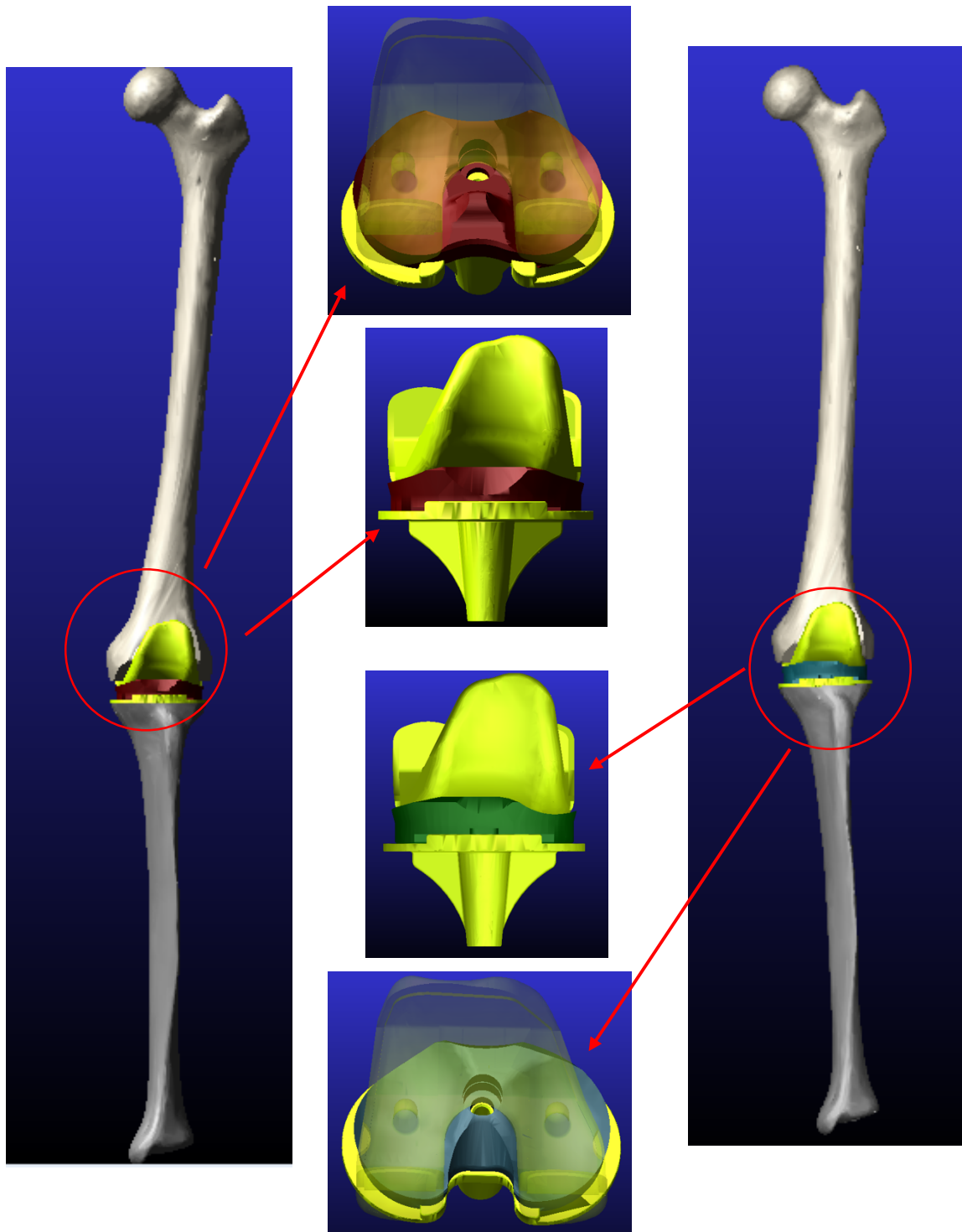


Figure 2. 4: geometries of the bones and prostheses imported into Adams. In detail the two prosthesis: in red there is the ultra congruent insert and in green the dynamic congruence insert

Disregarding the difference between cortical bone and cancellous bone, two densities in the Geometry and Density box in the Adams dialog box have been associated with the bony parts of the femur and tibia:

- Femoral density: $1.6 \cdot 10^{-6} \text{ kg/mm}^3$
- Tibial density: $2.74 \cdot 10^{-6} \text{ kg/mm}^3$.

The materials used for the three components of the prostheses are:

- Titanium for the femoral component;
- High molecular weight polyethylene (UHMWPE) for the two inserts;
- Titanium for the tibial component.

The characteristics of these materials have been included in the Geometry and Material Type box defining Young's module, Poisson ratio and density of each material. The properties of titanium have been defined starting from those present in Adams' browser; instead, for UHMWPE, a new material was created and associated with the inserts. The specifications of the materials included in the models are shown in **Table 2.1**.

	Femoral Component	Inserts	Tibial Component
	Titanium	UHMWPE	Titanium
Young's Module (MPa)	$1024 \cdot 10^5$	800^2	$1024 \cdot 10^5$
Poisson Ratio	0,3	$0,46^3$	0,3
Density (kg/mm^3)	$4,85 \cdot 10^{-6}$	$9,3 \cdot 10^{-7(4)}$	$4,85 \cdot 10^{-6}$

Table 2.1: Material properties specified for the prosthetic components

To finish the description of the different geometries present in the models, the **patella** is missing. The patella was inserted only in the model for the simulation of active flexion of the joint. With no CAD drawings available for this component, a new part was added to the model from an ellipsoid. To define the dimensions of the ellipsoid representative of

² <http://www.dielectriccorp.com/downloads/thermoplastics/uhmw.pdf>;

https://www.kmsbearings.com/media/wysiwyg/pdfs/UHMW_properties.pdf

³ <http://www.goodfellow.com/E/Polyethylene-UHMW.html>

⁴ <http://www.dielectriccorp.com/downloads/thermoplastics/uhmw.pdf>

the patella, reference was made to various morphological studies on the height, width and thickness of the patella (Table 2.2).

	Width (mm)	Length (mm)	Thickness (mm)
Shlenzka D. et al 1991	(45-51) ±2.1	(41-49)±2.1	(27-32) ±1.6
Yoo Ho J. Et al 2007	45.8±3.6	44.6±3.7	22.3±1.9
Iranpour F. et al 2008	44.8±4.8	34.3±3.8	22.4±2.3
Kayalvizhi I. et al 2015	41.3±3.4	42.9±4.8	20.7±1.5

Table 2.2: Patellar dimensions from morphological studies

In order that the ellipsoid representative of the patella could move easily in the troclear groove, the following dimensions (Table 2.2) were chosen and a density of $1.6 \cdot 10^{-6}$ kg/mm³ was assigned to the patellar bone.

Width (mm)	Length (mm)	Thickness (mm)
41.3	42.9	20.7

Table 2.2: Patellar dimensions chosen for the models

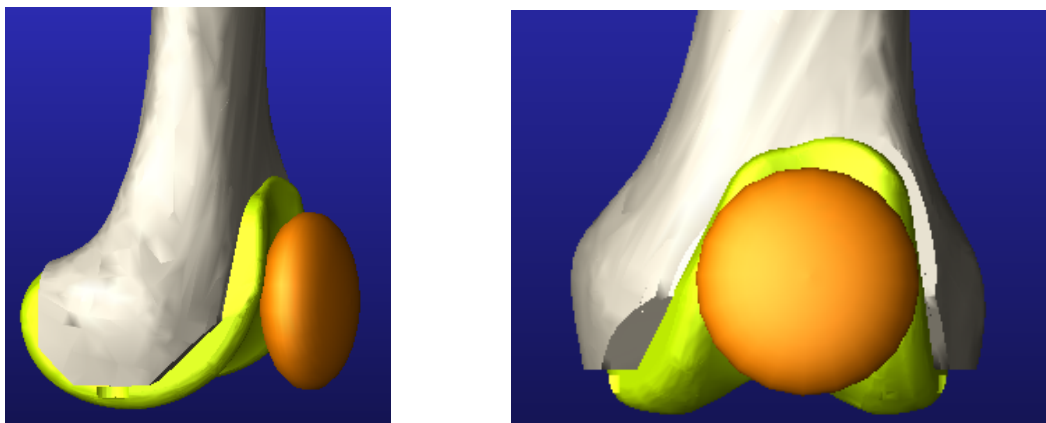


Figure 2. 5: lateral and frontal view of the ellipsoide used to represent the patellar bone

Once the materials have been defined for each part of the model, Adams automatically calculates the mass and the coordinates of the center of mass (CM) of each body.

2.2.2 ARTICULAR SURFACES CONTACT MODELING

Now that all the bodies are in the model, it's important to set the **contact's force** between the bodies to describe the interactions between the components.

Adams provides two ways to set up a contact force:

- **Impact** function model;
- Coefficient of **restitution** or the POISSON model.

In the Impact function model a sort of damped spring is considered between the bodies. Adams evaluates the total intersection volume and calculates its center of mass. From this point the nearest points on the surfaces of the two bodies are calculated and the line connecting the these two points is used as the direction of the force. The force applied originates from the center of mass of the intersection volume and extends towards the nearest surfaces of the contact bodies

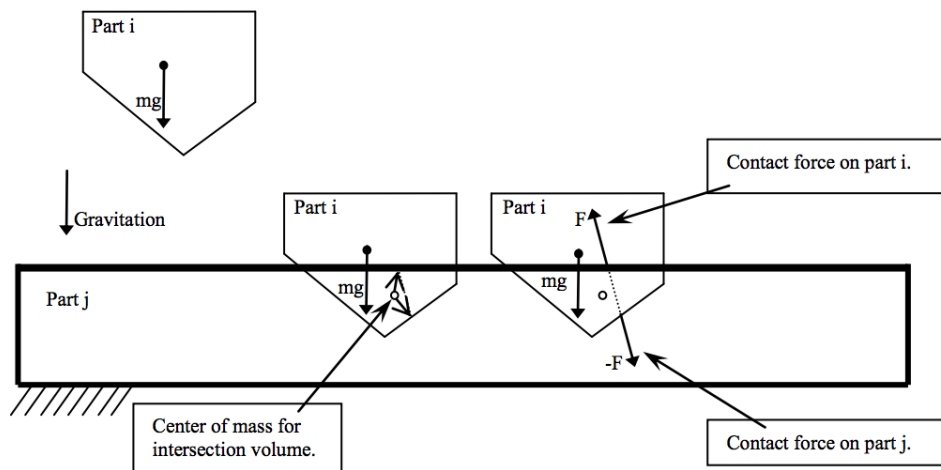


Figure 2. 6: Representation of how the Impact force works⁵

The general form of Impact force is:

$$F_c = k\delta^n + B(\delta)\dot{\delta} \quad (2.1)$$

where F_c is the contact force, n is an exponent that allows to modify further the force, δ is the depth of penetration and $\dot{\delta}$ is the penetration velocity at the point of contact. $B(\delta)$

⁵ <http://www.diva-portal.org/smash/get/diva2:531245/FULLTEXT01.pdf>

is the damping coefficient; it's not constant but it is variable and depending on penetration velocity, on penetration distance (d_{max}) at which the damping is maximum (B_{max}). It's a ramp function defined by the equation 2.2 [Stylianou A. P. et al 2013]. The damping is introduced to take into account the amount of energy dissipation associated with the internal damping of materials [Machado, M. et al 2012].

$$B(\delta) = \begin{cases} 0 & \delta \leq 0 \\ B_{max} \left(\frac{\delta}{d_{max}-\delta} \right)^2 \left(3 - \frac{2\delta}{d_{max}-\delta} \right) & 0 < \delta \leq d_{max} \\ B_{max} & \delta > d_{max} \end{cases} \quad (2.2)$$

The other kind of contact provided by Adams is the Restitution function used to define inelastic contact. When the contact is modelled with the restitution function, the penalty factor and a restitution coefficient are required. The first one represents the contact stiffness that should be able to eliminate the penetration between the bodies. It's required that this coefficient is high enough to make the penetration negligible, but non so high to bring instability [Doyle J. 2012]. The restitution coefficient specifies the energy dissipated during the contact and it can varies between 0 and 1: the value 1 indicates a purely elastic contact (the energy is conserved); instead, the value 0 indicates a purely inelastic contact.

In general the restitution method is used when the parameters required for the impact force are unknown and the restitution contact can be derived from material references or physical testing. Furthermore the impact method guarantees greater contact control thanks to the possibility of varying the damping or the exponent to obtain better results.

With this in mind, thanks to the availability of different contact parameters from previous studies, it was decided to set all the contacts between the surfaces of the models as **impact**.

After selecting the two bodies in contact, the *stiffness*, the *force exponent*, the *damping* and *penetration depth* have to be set.

While in some studies regarding models of intact knees the friction between the articular surfaces is neglected [Wismans J. et al 1980; ; Blankevoort L. et al 1991; Guess T. M. et

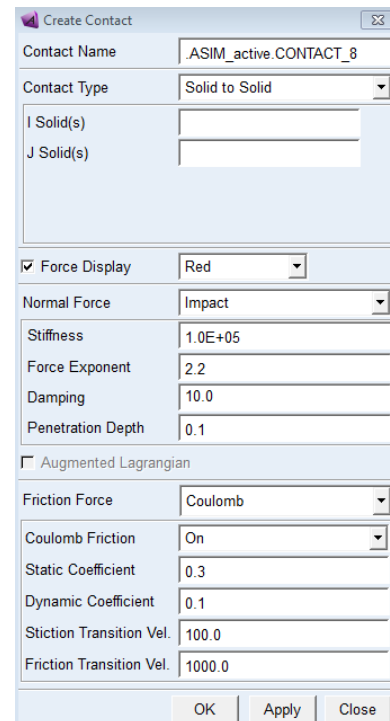


Figure 2. 7: contact force dialog box

al 2010,] it is not advisable to neglect it when modeling a knee with an implanted prosthesis. For this reason *static and dynamic friction coefficient* have been setted in the models.

A contact force has been created for these couples of articulating surfaces:

- Femoral component and the polyethylene inserts;
- Femoral component and the patellar bone.

The choice of contact parameters will be discussed later in the paragraphs relating to the two passive and active flexion models of the knee.

2.2.3 LIGAMENTS REPRESENTATION

After assembling the prosthetic components with the bones, the connecting elements between the bones have to be added: the **ligaments**. Since the models realized concern a knee with total knee arthroplasty, surely two ligaments have not been included in the models:

- the anterior cruciate ligament has not been included because it is resected during the operation;
- the posterior cruciate ligament has been omitted because the two types of prostheses analyzed do not provide for its retaining; furthermore the cutting on the tibia has been performed without preserving the bone part of the ligament insertion.

The two collateral ligaments (medial and lateral) between the femur and tibia, the two patellofemoral ligaments (medial and lateral) between the femur and the patella, and the patellar ligament between the patella and the tibia have been instead included in the models.

Thinking of the flexion-extension movement, it might think of representing the ligaments as linear springs elements. However, this representation of the ligaments would be too much forcing since the springs work both in compression and in extension instead the ligaments work only when tensioned. Moreover, unlike the springs, the ligaments do not have a purely linear force-strain relationship because of their composition: they are composed of elastin fibers that form a disordered network and collagen fibers which, in the absence of loads, are rolled up and instead, when external loads are applied, they align themselves in the direction of the load. Thus all ligaments were represented as **nonlinear springs** [Wismans J. et al 1980 ; Blankevoort L. et al 1991] with a force-deformation curve shown in the **Figure 2.6**.

In this curve we can identify 4 characteristic regions [Wismans J. et al 1980]:

- **region 1:** region corresponding to the unrolling of collagen. Therefore the stiffness is given by the elastin fibers (**zero strain region**);
- **region 2:** stiffness (slope of the curve) increases as the fibers become aligned this process ends at the end of this phase (**toe region**).

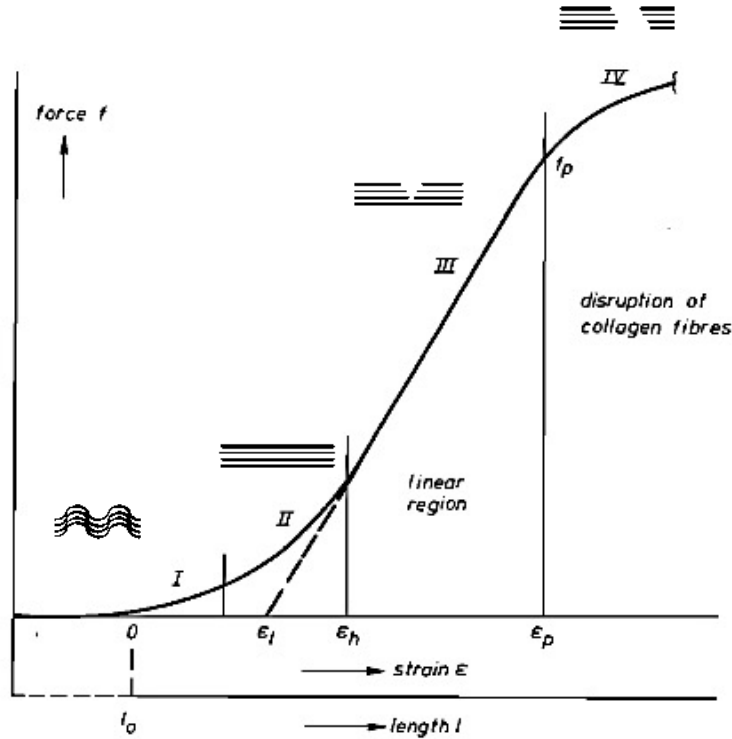


Figure 2. 8: The force-strain (f-ε) relationship for the elements modelling the ligament fiber bundles [Wismans J. et al 1980; Korhonen K.R. et al 2011].

- **region 3:** in this region the ligament stiffness is constant and it depends on the stiffness of collagen (**linear or elastic region**).
- **region 4:** increasing the strength, there is a breakdown of some of the fibers followed by the complete tearing of the entire tissue (**plastic region**).

For low strains values (region 1 and 2) the force-displacement curve is a quadratic curve (equation 2.1); in the region 3 the relation is linear (equation 2.2) [Wismans J. et al 1980]

$$f = c * \varepsilon^2 \quad 0 \leq \varepsilon < \varepsilon_h \quad (2.1)$$

$$f = k * (\varepsilon - \varepsilon_l) \quad \varepsilon_h \leq \varepsilon < \varepsilon_p \quad (2.2)$$

k represents the experimentally determined ligament stiffness and ε_l represents the strain

at which the linear portion of the force-strain curve would cross the strain axis, if it was extended (Figure 2.6).

To ensure continuity between the toe region and the linear region, equaling equations 2.1 and 2.2, the condition to be respected is: $\epsilon_h = 2\epsilon_l$.

By imposing the condition of continuity between the different regions, the expression of the force of the ligaments is thus obtained as a function of the ϵ_l and of the k [Wismans J. et al 1980 ; Blankevoort L. et al 1991]:

$$f = \begin{cases} 0 & \epsilon < 0 \\ -\frac{1}{4}k \frac{\epsilon^2}{\epsilon_l} & 0 \leq \epsilon \leq 2\epsilon_l \\ -k(\epsilon - \epsilon_l) & \epsilon > 2\epsilon_l \end{cases} \quad (2.3)$$

ϵ is the strain of each bundle of ligaments defined as

$$\epsilon = \frac{L - L_0}{L}. \quad (2.4)$$

$$L_0 = \frac{L_r}{\epsilon_r + 1}. \quad (2.5)$$

where L is the length of the ligament and L_0 is the “**zero-load length**” [Blankevoort L. et al 1991] defined as “the length of the ligament when it first becomes taut” [Bloemker K. H. 2012]. This ligaments’ activation length is a function of the **reference strain** (ϵ_r) and **reference length** (L_r) which are the ligament strain and ligament length at the reference position of the joint : extension (equation 2.5).

Since the ligaments, from the mechanical point of view, are not purely elastic but viscoelastic elements, following what reported by the study of Guess et al 2010 concerning a specific patient specific multibody model of an intact knee, a damper was added in parallel with each ligament spring. Thus the total force for each ligament spring is the sum of two terms: the first is the force given by equation 2.3 and the second is the dissipative term given by the product of the friction coefficient (C) for the deformation speed of the fiber from oringin point to the insertion point of each ligament:

$$F_{TOT} = f + C \frac{dL(t)}{dt} \quad (2.6)$$

2.2.3.1 Number of ligament springs

The mathematical modeling of the ligaments requires the choice of the **number of springs** that characterize the single ligaments.

In the literature, different choices have been adopted. Wismans J. et al 1980 in their three dimensional mathematical model of the human knee joint used seven springs: one spring for both cruciate ligaments and for the lateral collateral ligament; two springs for the medial collateral ligament (anterior and posterior) and posterior part of the capsule. In the three dimensional model of knee realized by Blankevoort L. et al in 1991 the number of springs increased: three springs were used for each collateral ligament, two springs for each cruciate ligaments and the capsule. This is the most common choice used in the computational models of the knee. In 1997 Pandy M. G. et al realized a three dimensional musculoskeleton model of human knee to simulate first the passive flexion of the knee and then different activities like anterior-posterior draw, axial rotation. In this model they used twelve elements to represent the ligaments. This high number was due to the fact that the MCL was separated into an upper portion and a deeper one each with three bands; LCL was schematized with only one fiber; the two cruciates and the posterior capsule were each described by two fibers. In the models containing the patella, other three fibers are also considered for the patellar ligament [Guess T. M. et al 2010]. When a total knee arthroplasty is added in the model the fibers of the anterior cruciate ligament disappear and in many studies the medial and lateral patellofemoral ligaments are also added with two [Chen Z. et al 2014] or three [Marra et al 2015] bundles.

It is clear that the greater the number of fibers with which each bundle of ligaments is represented, the more correct the modeling will be. However, there is a danger of complicating the models a lot.

In this thesis work the following choice was made: each ligament was represented with **three springs**. Depending on the orientation of the ligaments, the following choices were made:

- Ligaments that develop mostly in the longitudinal direction on the sagittal plane have been represented with an anterior fiber, a posterior fiber and a central fiber;
- Ligaments with predominantly vertical orientation on the frontal plane were represented with a medial fiber, a lateral fiber and a central fiber;
- Ligaments with a more horizontal orientation were represented by a superior fiber, a lower fiber and a middle fiber.

MEDIAL COLLATERAL LIGAMENT		LATERAL COLLATERAL LIGAMENT	
Anterior bundle	aMCL	Anterior bundle	aLCL
Intermediate bundle	iMCL	Superior bundle	sLCL
Posterior bundle	pMCL	Posterior bundle	pLCL

MEDIAL FEMORO-PATELLAR LIGAMENT		LATERAL FEMORO-PATELLAR LIGAMENT	
Superior bundle	sMPFL	Superior bundle	sLPFL
Middle bundle	mMPFL	Middle bundle	mLPFL
Inferior bundle	iMPFL	Inferior bundle	iLPFL

PATELLAR LIGAMENT	
Medial bundle	mPL
Intermediate bundle	iPL
Lateral bundle	lPL

Table 2.3: ligament bundles considered in the models.

2.2.3.2 Origin points and insertion points of each ligament and their zero-load length

Once it was decided how to represent the ligaments, they have been inserted into the models. In Adams this is done with a *Single component force* acting along the direction line between two bodies: the action body and the reaction body. On the action body there are the **origin points** of the ligaments, whereas on the reaction body the **insertion points** of the ligaments are located. How a single component force is created for each ligament is shown in a futur paragraph (dopo aver detto che calcolo la Lr dal modello a 180 e dopo aver definito le design variables)

In order to insert ligaments into a computational knee model it is necessary to identify the points of origin and insertion. Traditionally these points are derived from MRI images of individual [Guess T. M. et al 2013; Hosseini A. et al 2015] or experimentally obtained on cadaveric knees [Bloemker K. H. 2012]. In other studies, starting from the insertion and origin sites identified by radiographic images, the centroides of these areas were directly considered as points of origin and insertion for the single ligaments [Wismans J. et al 1980; Li G. et al 1999; Bersini S. et al 2015]; or in other studies the values present

in the literature were used and then manually adjusted to find the right correspondence with the geometry of the considered bones [Chen Z. et al 2014].

In this thesis work we did not start with radiographic images of the knee. CADs of the bones from which the models were created were provided. Therefore starting from anatomical atlases [Schunke M. et al Prometheus-Atlante di Anatomia 2006] and comparing different knee models present in the literature, the points of origin and insertion of the three fibers for each considered ligament were positioned.

For the positioning of the points of origin and insertion of each ligament and for the determination of the correct Lo, an optimization process was carried out, whose purpose was to obtain ligaments whose forces allowed a correct balancing of the loads between the medial and lateral compartments of the prosthesis. The recommended range of values for the correct bicompartamental balance is 5-40 lbf which corresponds to a range of 22-178 N (1 lbf = 4.44 N) maintaining a difference between the two compartments of less than 15 lbf [Gustke K. A. et al 2014 a; Gustke K. A. et al 2014 b].

The Lo Ligament has been evaluated by making the following considerations [Guess TM and Razu 2017]:

- Throughout the range of motion there must not be fibers that do not produce force;
- The force produced must be less than 50 N so that the working region of the ligament remains the non-linear region (toe-region);
- Each fiber of each ligament has been recruited according to what was reported by Blankevoort L. et al 1991:
 - The anterior fibers are active in flexion: aLCL after 50 ° of flexion, aMCL after 30 ° of flexion
 - Central fibers are active for almost the entire ROM;
 - The posterior fibers are active in extension: pLCL up to 30 ° of flexion, pMCL up to 40 ° of flexion.

To achieve this, two models were created in which, for each knee prosthesis, the femur and tibia were positioned at 180 ° to represent the reference position: complete extension. In each of these models the points of origin and insertion of the ligaments and the respective forces (single component) between action body and reaction body were inserted. To calculate the Lo of each ligament a vertical force was applied to the tibia at its center of mass and with a value equal to 800 N (once body weight) to compact the model. The tibia has been constrained to the ground with a parallel joint in order to allow it to adapt freely during the simulation.

At the end of the simulation lasting 1 s, the point to point distances were measured between each point of origin and insertion. These distances represent the L_r of each ligament ie the reference length calculated in full extension. These calculated length values, combined with the values of the reference strains (ϵ_r), allowed to calculate the value of L_0 for each ligament according to the quation 2.5.

Ligament bundle	K (N)	ϵ_r	L_0 (mm)
aLCL	2000	-0,25	60,99
sLCL	2000	-0,05	47,95
pLCL	2000	0,08	42,76
aMCL	2750	0,04	62,42
iMCL	2750	0,04	63,64
pMCL	2750	0,03	65,4
mPL	58000	/	36,48
iPL	58000	/	26,10
IPL	58000	/	39,24
sMPFL	2000	0,12	49,15
mMPFL	2000	0,08	47,61
iMPFL	2000	0,08	49,45
sLPFL	1000	0,06	44,82
mLPFL	1000	0,06	42,99
iLPFL	1000	0,06	44,60

Table 2.4: the stiffness parameters, reference strains and zero-load length of the ligament elements

After that, a multibody model of the knees has been assembled to simulate a passive motion (paragraph 2.2.3). In this model the parameters of stiffness, reference strain and zero-load length were inserted for each ligament defining *Design variables* in the Adams framework and implementing the functions 2.3 and 2.6 for each ligament with the damping coefficient $C= 0.5$ Ns/mm [Guess T. M. et al 2010] and the ϵ_1 strain assumed equal to 0,03 for all the ligaments [Butler T. L eta al 1986] .

Table 2.4 summarizes the parameters that made it possible to obtain a good balance between the two compartments: the values of stiffness and reference strain have been obtained from the literature [Blankevort L. et al 1991; Piazza J. S. and Delp S. L 2001; Marra A. A. et al 2015]; the L_0 values are the result of the optimization process.

2.3 SIMULATED PASSIVE MOTION

In this section it will be describe how the knee models with total arthroplasty were realized for the simulation of **passive motion**.

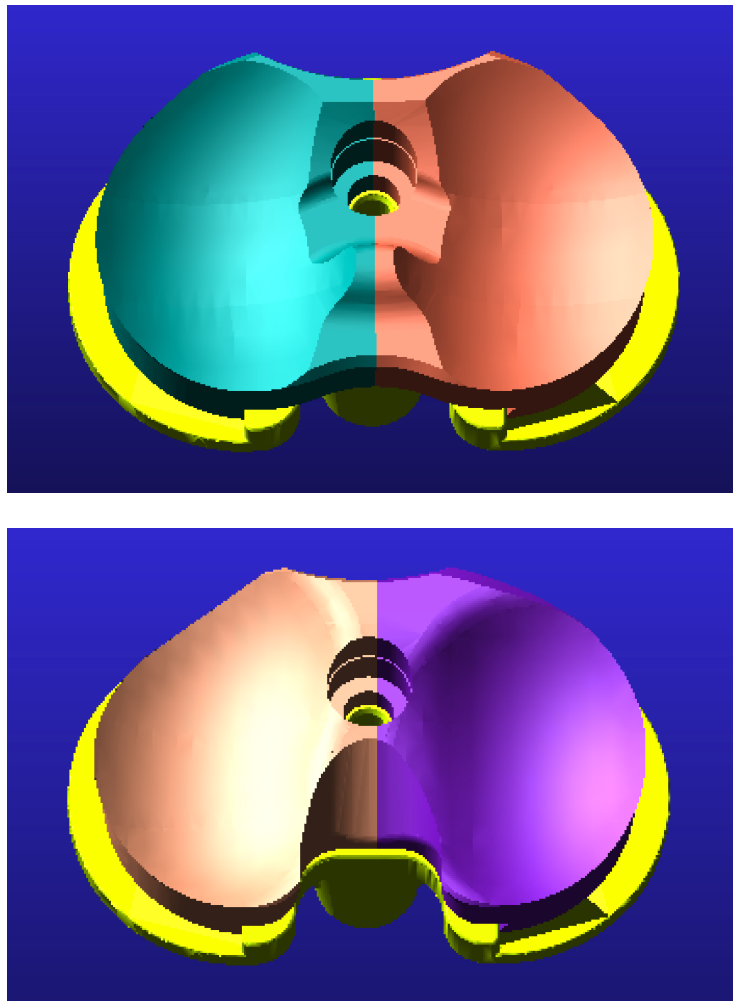


Figure 2. 9: tibial inserts divided into medial and lateral compartments

First of all we have divided the two inserts into two compartments: medial and lateral. The reason for this is related to the possibility of being able to evaluate the loads generated by the interactions between the femoral component and the insert both in the medial compartment and in the lateral compartment.

The contact parameters chosen derive from considerations on:

- Duration of the simulation
- Depth of conpenetration
- Respect of the limit ranges for medial and lateral loads and ligament strengths.

The values of stiffness, damping and exponent that led to a simulation of reasonable duration (5s), contact forces and ligament forces that respected the imposed limits and an interpenetration of 0.001 mm are reported in Table 2.5.

CONTACT PARAMETERS	
Stiffness	10000 N/mm
Force exponent	2.2
Damping	1000 Ns/mm

Table 2.5: Contact parameters for passive knee flexion

In Figure 2.9 the two inserts with the divisions are shown: at the top there is the ultracongruent insert and at the bottom the dynamic congruence insert. The right side of the images represents the medial compartments, the left side the lateral compartments.

2.3.1 CONSTRAINTS AND LOADS

Passive flexion of the knee was accomplished by imagining that, for example, during surgery the patient's femur is fixed and the tibia is moved by flexing the knee. For this purpose a *fixed joint* was placed between the femur and the ground at the center of mass of the femur so that all the translations and rotations were inhibited to this segment. To simulate the passive movement of the tibia a cylinder was added distally on the tibia in order to apply a bushing between this cylinder and the tibia.

Bushing represents a spring and damper force acting between two s possible to define the amplitude of force and momentum (Fx, Fy, Fz, Tx, Ty, Tz) that are linear functions of the translational and rotational displacements between the two parts. In order to flex the tibia, the only non-zero stiffness component has been assigned to the z component of the translational stiffness (Figure 2.11).

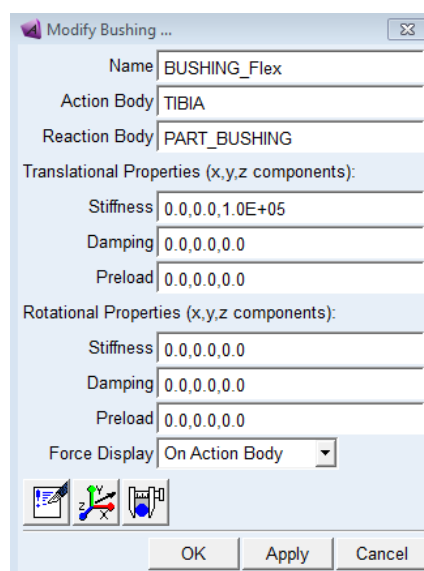


Figure 2. 10: bushing dialog box

In this way the force of the bushing would tend to push the tibia in the z direction. In order to simulate the bending movement, a joint was created and a movement was defined for the same joint. Specifically, a *revolute joint* was positioned at the center of the joint. This kind of joint allows the rotation of one part respect to another one about a common axis.

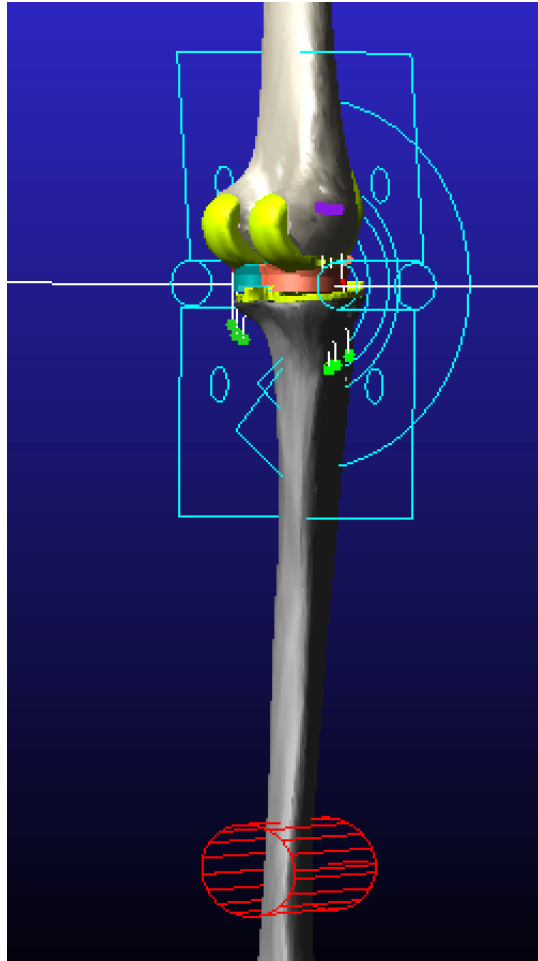


Figure 2. 11: loads and constraints used for the passive motion of the knee

2.3.2 EVALUATION OF THE INTERNAL ROTATION OF THE TIBIA

A dummy element was used to evaluate the internal rotation of the tibia in this model: a sphere positioned at the center of the tibial plate surface. The sphere has been constrained to the tibia through a spherical joint in order to block the translations and allow only the rotations. The idea was to make this sphere follow the tibia in the bending movement but not in the internal rotation so as to be able to evaluate how much the tibia, with respect to this reference (the sphere), rotated. Then to the sphere were assigned:

- Very small mass (1g) to prevent its mass from creating interference in the simulations

- Null moment of inertia around the x axis so as not to oppose to the movement around the x axis (bending)
- Very high inertia moments of the order of 10^5 around x and z so that it could remain still in those directions.

Finally, with a parallel axes joint, the sphere was forced to remain parallel to the longitudinal axis of the tibia. In this way, while the tibia flexes, the ball follows it in flexion, but while the tibia bends internally, the sphere remains still. The angle between the y-axis of the cm of the reference sphere and the z-axis of the marker on the tibial plateau, gives the measure of tibial intrarotation (Figure 2.12).

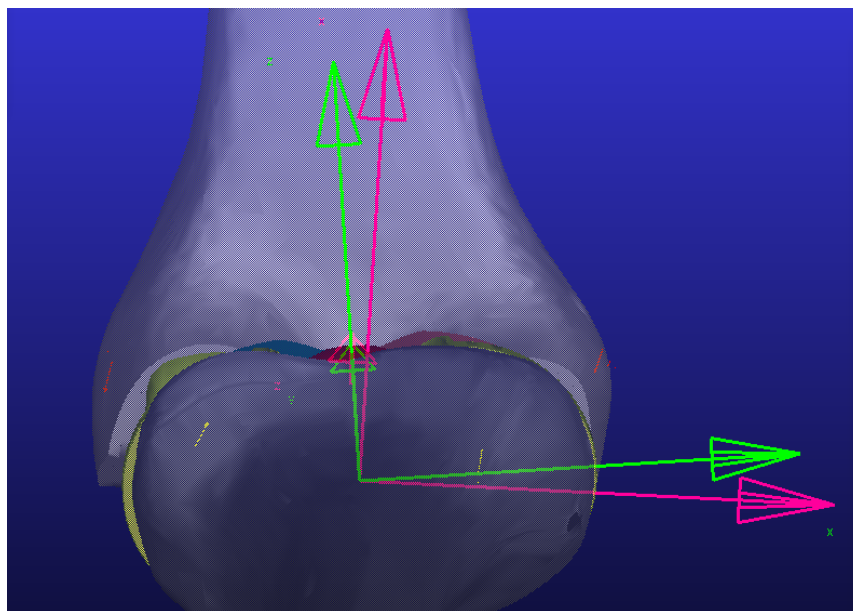


Figure 2. 12: Evaluation of tibial internal rotation

2.4 SIMULATED ACTIVE MOTION

After choosing the contact parameters that allow a bilateral balance of the joint, a new model was implemented in which the two knee prostheses were tested.

In this model, in addition to the collateral ligaments used in the previous passive knee flexion model, the two patellofemoral ligaments (medial and lateral) and the patellar ligament (or patellar tendon) were considered. In fact, in this second model another geometry has been inserted: the patella, so that we can actually simulate the muscular activation of the quadriceps whose tendon is inserted on the upper base of the patella.

The patellar tendon was modeled through three bundles (medial, central and intermediate) [Guess T.M. et al 2011] that originate from the apex of the patella up to the tibial tuberosity. For the positioning of these beams, a study on the biomechanical function of

the patellar tendon during a weight bearing activity was considered [DeFrate L.E. et al 2007]. Considering what reported in this study, in the sagittal plane, the three bundles of the patellar tendon in complete estension have a certain inclination with respect to the logitudinal axis of the tibia: the medial bundle has an inclination of $22.2^{\circ} \pm 7.9^{\circ}$; the central beam is inclined at $22.9^{\circ} \pm 9.5^{\circ}$ and the side beam is $21.6^{\circ} \pm 8^{\circ}$.

As for the two patellofemoral ligaments, these were inserted considering that their sites of attachment on the patella are in correspondense of the superior two thirds of the patella and converge on the surfaces of the femoral condyles [Saper G. A. et al 2014]. In addition, considering a study related to a subject specific model of the prosthetic knee [Marra M. A. et al 2015] were modeled with three beams each (upper, intermediate, lower).

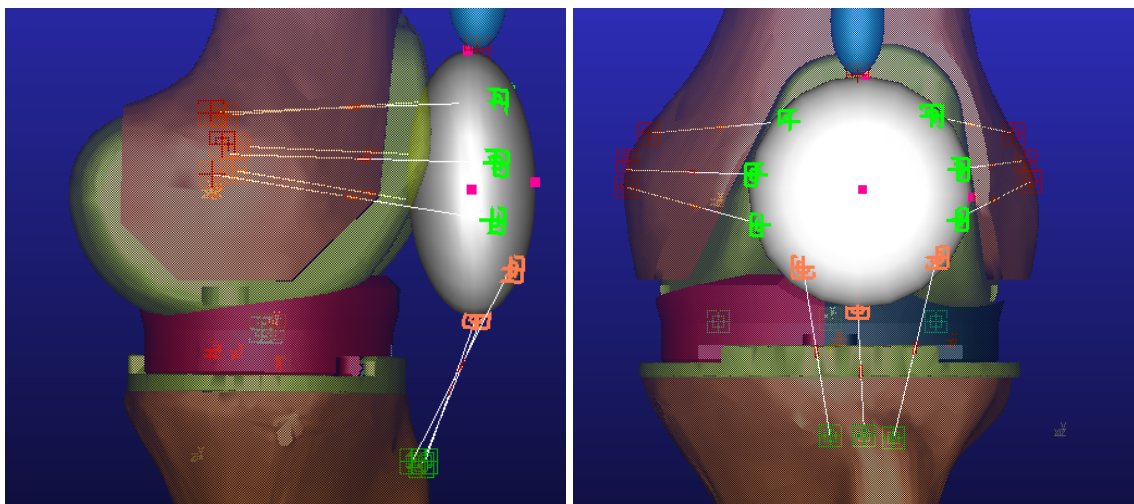


Figure 2.13: Lateral and frontal view of the origin and insertion points of the patellar tendon and patellofemoral ligaments

The contact pramameters used to model the contact between the femoral component and the patella were derived from a study on a multibody model created for the simulation of a squat movement. [Stylianou A. P. et al 2013]: $K=30000\text{N/mm}$, $d_{\text{max}}=0.1$, $n=1.5$, $B_{\text{max}}=40\text{Ns/mm}$, static friction coefficient of 0.03 and a dynamic coefficient of 0.01.

2.4.1 CONSTRAINTS AND LOADS

To obtain this pattern several changes were necessary compared to the passive flexion model. During a weight-bearing activity the main driving force is the weight force. To consider it, a sphere has been inserted into the head of the femur. Adams, as usual, assigns default steel as a material. However, to simulate the weight of the body associated with only one of the lower limbs, a mass was arbitrarily defined for the new part. Specifically,

assuming a subject with a body weight of 80 kg, a mass of 400 N, that is half of the body weight (0.5 BW), was assigned to the head of the femur.

The femur, in its proximal part, is articulated with the hip. In particular the head of the femur can rotate inside the acetabulum (enartrose). To model this physiological situation, a *spherical joint* was inserted between the head of the femur and the ground; in this way the head of the femur is free to rotate in all directions but not to translate. Finally, to ensure only vertical translation of the endpoint of the femur in order to allow proper lowering to perform the bending movement, a *translational joint* has been imposed between the head of the femur and the ground (it is a constraint that allows a part to translate along a one specific direction relative to another part).

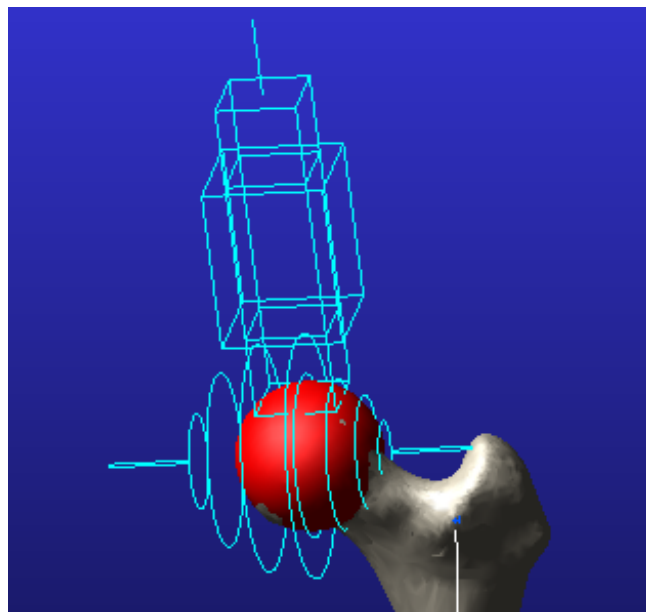


Figure 2. 14: Femur head and the spherical and translational joints to simulate the presence of the hip

On the opposite side of the lower limb, the most distal part of the tibia is articulated with the ankle. During a weight-bearing activity such as the squat the tibia flexes relative to the foot (the joint angle decreases) and can rotate around its axis. To simulate these two rotations a cylinder was inserted whose center of mass was made to coincide with the central point of the end of the tibia and, between this new part and the tibia, two revolute joint were applied to allow the rotations described above (Figure 2.14).

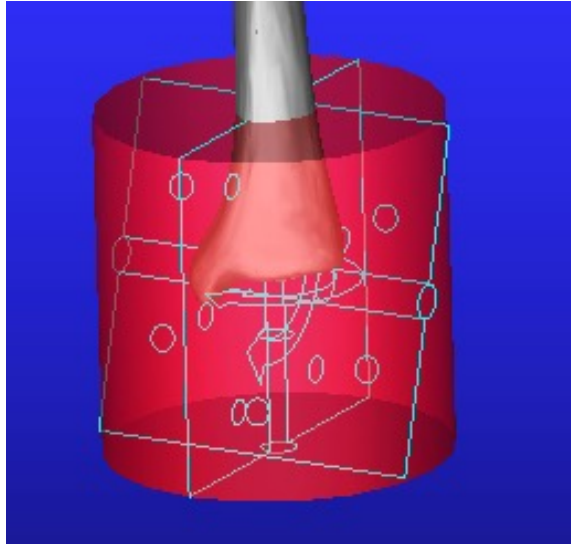


Figure 2. 15: revolute joints to allow the tibia movements with respect to the foot

As regards the muscular component, the quadriceps muscle has been inserted as the main responsible for the flexion-extension movement of the knee joint. The quadriceps, as the name implies, is a muscle composed of four parts: rectus femoris, vastus medial, vastus intermediate and vastus lateral. These do not all have the same point of origin (the rectus femoris originates from the anterior iliac spine, the vastus medial from the neck of the femur, the vastus intermediate from the harsh line of the femur and the vastus lateral from the lateral region of the great trochanter). However they all end in a single tendon that fits into the patella.

In the model the origin attachment of the muscle has been settled on the great trochanter while its insertion on the patella was modeled with the addition of three ellipsoids (Figure 2.15 in green). These three ellipsoids schematize the quadriceps tendon; they were assigned a density of 2.68 g / cm^3 obtained from a study on the mechanical properties of the patellar tendon [Hashemi J. et al 2005]. The different ellipsoids are connected to each other and with the patella through spherical joints that allow each part only three degrees of freedom (the three rotations) blocking all the translations.

The reason why this chain of ellipsoids was introduced is that, during knee flexion, the quadriceps tendon comes physiologically in contact with the trochlear groove by wrapping it. The presence of these three additional elements allows to reproduce this physiological winding of the tendon during the flexion (Figure 2.10).

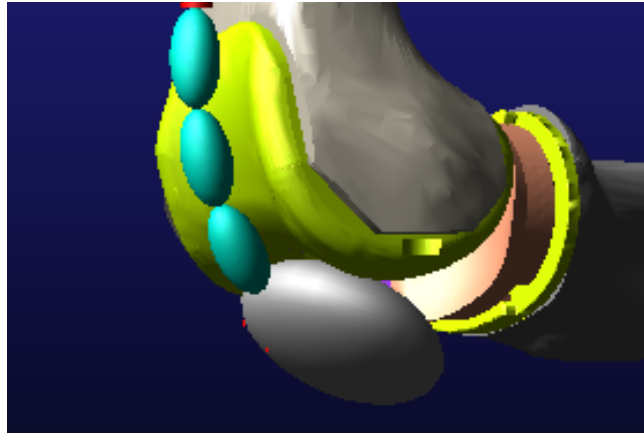


Figure 2.15: how the chain of ellipsoids works during knee flexion

The quadriceps is modelled as a single component force applied between the femur and the first ellipsoid simulating the quadriceps tendon. The quadriceps force was obtained through the modulation of a PID controller (Proportional Integral Derivate controller).

The PID controller adjusts the output based on the value of the error signal (proportional action), the past values of the error signal (integral action) and the variation of the speed of the error signal (derivative action). It is therefore necessary to set the value of three coefficients to obtain an optimal response. In a closed loop system such as the pid controller, the set point is defined as the desired value of the measured process variable; the error is the difference between the process variable and the set point; it is used to determine the value of the controller output variable.

The process to set the optimal values of the gains is called tuning. There are several methods for setting the control parameters of a PID controller. We have chosen to use a trial and error method. This method involves setting the integral and derivative gains initially to zero and then increasing the proportional gain (P) until the controller output oscillates (avoiding setting such a high value that the system is unstable). This value is then halved to set the K_p gain of the controller. Finally, the integral and derivative gains (I and D) are manually adjusted so that the offset between the set point and the measured process variable is reduced to a minimum and the variable quickly reaches its reference.

In the model realized, the set point is the height at which the head of the femur is to arrive during flexion. If the set point is set to 0 it means that the knee should not flex. The controlled variable is the displacement in the vertical direction of the femoral head. In Adams, to create a pid controller, two inputs are needed: a proportional input and a derivative input that is consistent with the proportional input. In the specific case of knee flexion, the proportional input is the position of the femoral head, then the derivative input will be its velocity (Figure 2.15 shows the dialog box to modify the control block).

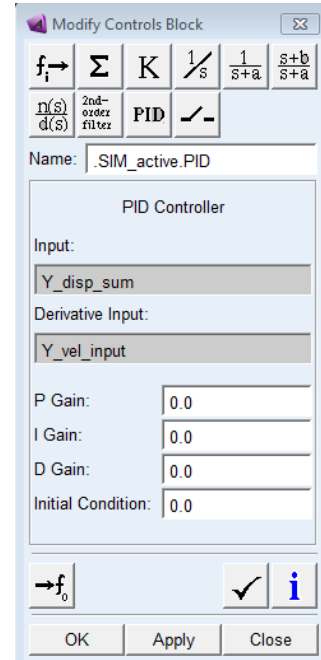


Figure 2. 16: Modify control blocks dialog box

The output of a pid controller in general has the form of the one reported in equation 2.7: sum of the three proportional, integral and derivative terms.

$$(2.7) \quad u(t) = K_p e(t) + K_I \int_0^t e(\tau) d\tau + K_D \frac{de(t)}{dt}$$

The pid controller output is used to modulate the quadriceps force. Therefore, by optimizing the PID control parameters, it is possible to optimize the force required for the quadriceps.

The values of the three gains used for the two models are shown in Table 2.5:

	DYNAMIC CONGRUENCE INSERT	ULTRA CONGRUENT INSERT
K_p	150	150
K_I	2	2
K_D	1	1

Table 2.5: Proportional, Integral and Derivative gains used

2.4.2 QUANTITATIVE ANALYSIS OF THE KINEMATICS

After the tuning of the pid controller, the analysis of the joint kinematics has been evaluated by the internal rotation of the tibia which, during active flexion, is observed with the two different types of prosthesis.

For the quantitative evaluation of the kinematics of the knee joint during flexion, a method widely reported in the literature was used. This method starts from the considerations that Iwaki H. et al 2000 conducted in a study on unloaded cadaver knee on the shape of the bone surfaces that make up the knee joint. In this study the imaged and dissected knees

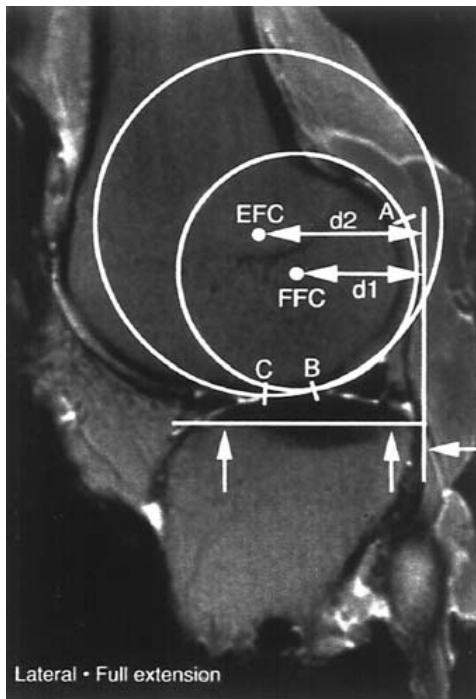


Figure 2. 17: Spherical shape of posterior femoral condyles

involved were analyzed in the sagittal plane revealing a spherical shape of the posterior femoral condyles. The geometric centers of these balls called FFC (flexion facet center) were used to evaluate the posterior antero translation of the femoral condyles on the tibia as the distance of each center from the posterior cortex of the tibia.

The geometric centers of the posterior femoral condyles have also been used in in vivo studies during cycles of flexion extension [Feng Y. Et al 2015] to study the movements of the femoral condyles. In this case the two centers were projected on the transverse plane of the tibia and the smallest distance between the center of the condyle and the mediolateral axis of the tibia was

considered representative of the antero-posterior translation.

In the present thesis work, in order to evaluate the tibiofemoral kinematics during active flexion, two spheres coincident with the posterior femoral condyles were realized. Considering that anatomically the medial condyle is slightly larger than the lateral one, the sphere corresponding to the medial condyle is larger and moreover the two centers of the two spheres, seen in a lateral view, are concentric (Figures 2.18) [Asano T. et al 2001]. The joint kinematics was evaluated by calculating for each simulation instant the components on the tibial plate of the distance of the centers of the femoral condyles from a point in the center of the tibial plateau. The internal rotation of the tibia this time has been calculated as the angular coefficient of the line which at each instant of time links the projections of the centers of the two femoral condyles.

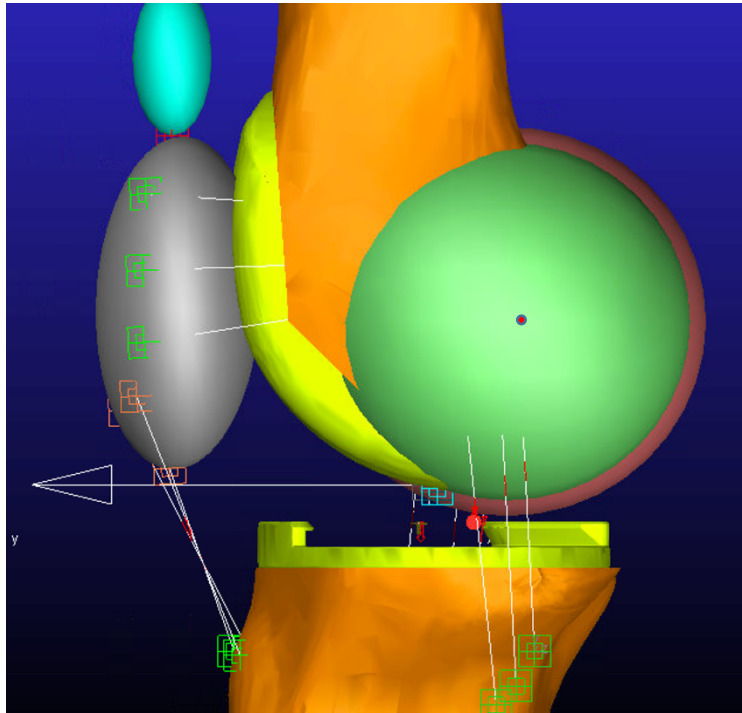


Figure 2. 18: two concentric spheres represent the two posteriore femoral condyles.

2.4.3 CONTACT FORCES DISTRIBUTION

The distributed contact forces were obtained through the discretization of polyethylene inserts in multiple elements. To achieve this, a specific macro (indicated in the Appendix) was created. A macro is a single command that the user defines to execute a series of Adams commands. For the discretization of the inserts, a box has been created such as to:

- Completely incorporate the insert;
- Having the base coinciding with the insert base.

The discretization elements are the result of Boolean intersection operations between the created box (splitter box) and the insert (geometry to split). Cells have been created so that, on the transverse plane of the tibia, they had a 3 mm x 3 mm dimension for a total of 278 cells for the dynamic congruence insert and 266 cells for the ultracongruent insert. Within the macro each cell was bound to the tibial plateau with a *fixed joint* and an impact contact was created between each cell and the femoral component.

The parameters of contact between the femoral component and the discretized insert were estimated using the Elastic Foundation Theory [Blankevoort L. et al 1991; Pandy M. G. et al 1997; Bei Y. Ta al 2004]. According to this contact modeling, independent springs are distributed on the contact surface representing a single elastic layer between two bodies. In the models of artificial knees it is assumed that the deformations are small and

the equation (2.8) is used for calculating the contact pressure of each spring on the surface of the insert [Bei Y. Ta al 2004; Stylianou A. P. et al 2013].

$$p = \frac{(1 - \nu)E}{(1 + \nu)(1 - 2\nu)} \frac{d}{h} \quad (2.8)$$

In this expression E and h respectively represent the Young's modulus and the thickness of the elastic layer, ν the Poisson coefficient and d the spring deformation. To estimate the contact stiffness parameter (k), the p / d ratio has been multiplied by the area of each element discretized in the transversal plane (3x3 mm²). Considering that the average thickness of the inserts is 10 mm, the Young modulus of 800 MPa and Poisson coefficient of 0.46 (Table 2.1), the estimated K value is 3328 N / mm. For the values of maximum penetration depth, damping and exponent the following values were used: $d_{\max}=0,01$, exponent $n=1,2$ and maximum dampinc coefficient $B=30$ Ns/mm (almost 0.01K).

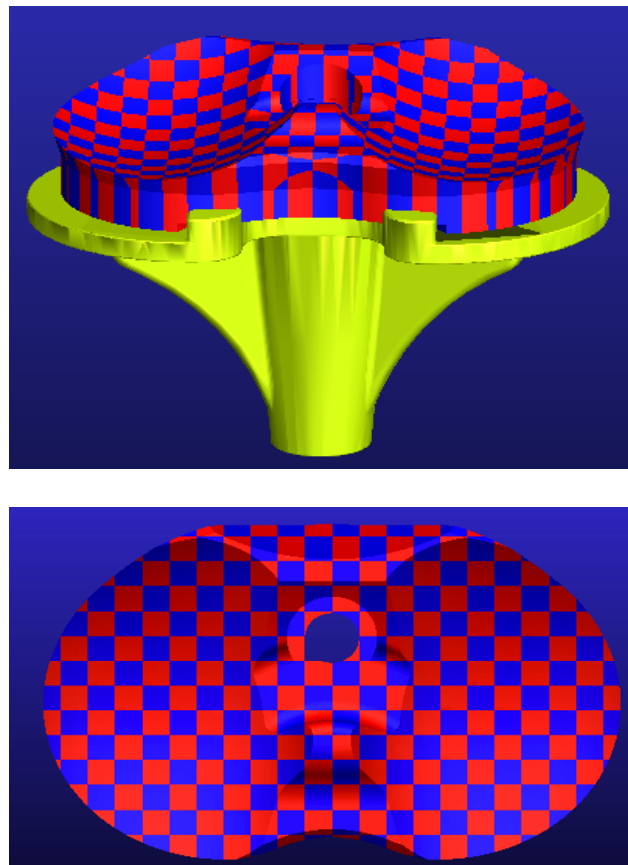


Figure 2. 19: The discretized ultracongruent insert

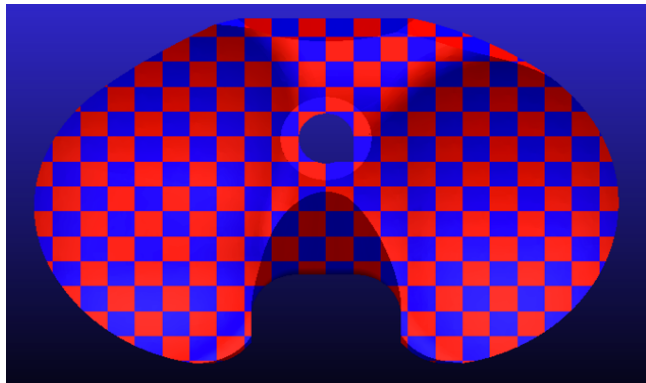
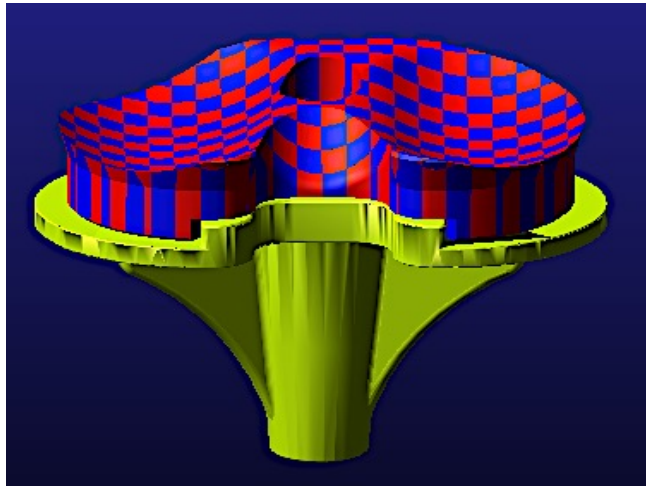


Figure 2. 20: The discretized dynamic congruence insert

CHAPTER 3

RESULTS AND DISCUSSIONS

The following chapter will show the results obtained after the simulations. The results will concern the trends of the bicompartamental contact forces, the forces developed by the ligaments and the internal tibia rotations observed during the passive knee flexion after the implantation of the two types of knee prostheses with ultracongruent and dynamic congruent inserts.

Moving on to the active knee flexion model, in this case the trends of the force developed by the quadriceps, of the medial and lateral compressive forces and of the observed intrarotations will be reported. Finally, maps representing the distribution of forces during a squat movement will be reported.

3.1 RESULTS FOR PASSIVE KNEE MOTION

The knee model realized to simulate a **passive flexion** of the joint was used to obtain ligament forces that allowed a balance of the loads applied to the medial and lateral compartments. This balance, as reported in the literature, is obtained if all the ligament strengths do not exceed 50N [Guess TM et al 2017] and if the forces applied on the two compartments maintain a difference of less than 15 lbf for the whole flexion range [Gustke K. A. et al 2014 a; Gustke K. A. et al 2014 b].

3.1.1 LIGAMENT FORCES

In the following figures are shown the trends of the forces developed by collateral ligaments (medial and lateral) after choosing the final configuration of points of origin and insertion for ligaments.

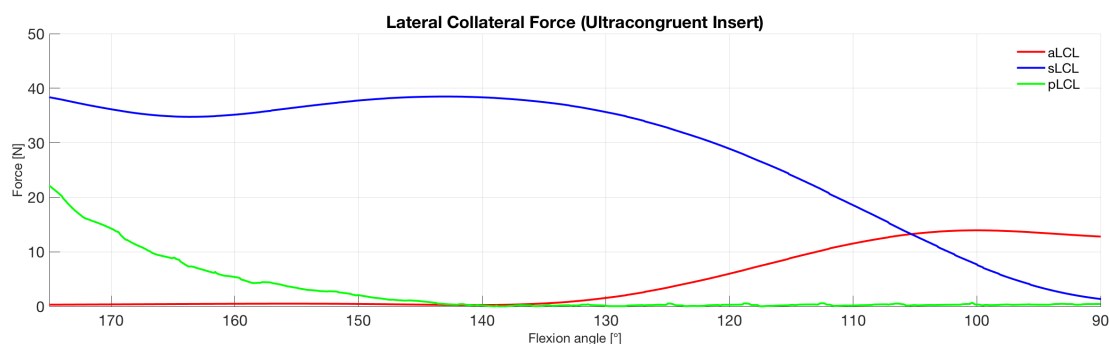


Figure 3. 1: Trend of the ligament forces for the lateral collateral ligament in the model with ultra congruent insert

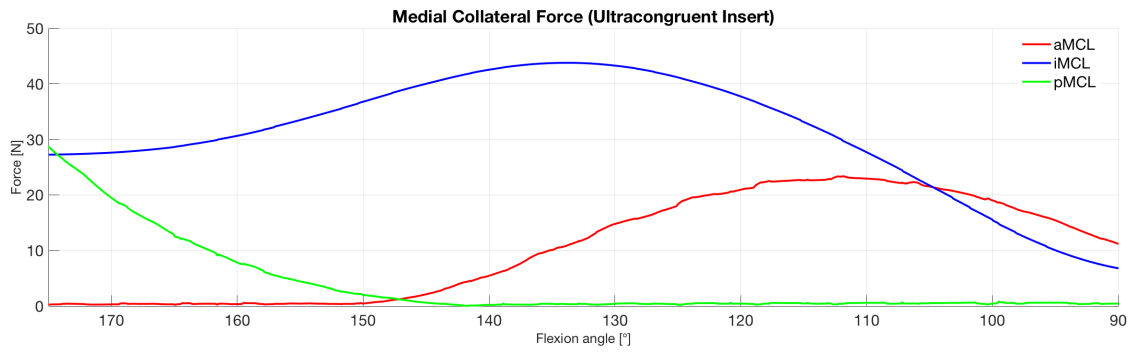


Figure 3. 2: Trend of the ligament forces for the medial collateral ligament in the model with ultra congruent insert

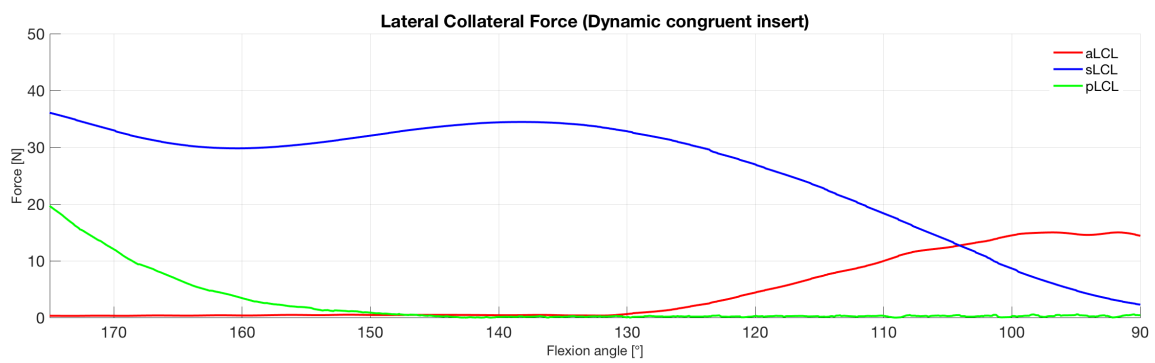


Figure 3. 3: Trend of the ligament forces for the lateral collateral ligament in the model with dynamic congruence insert

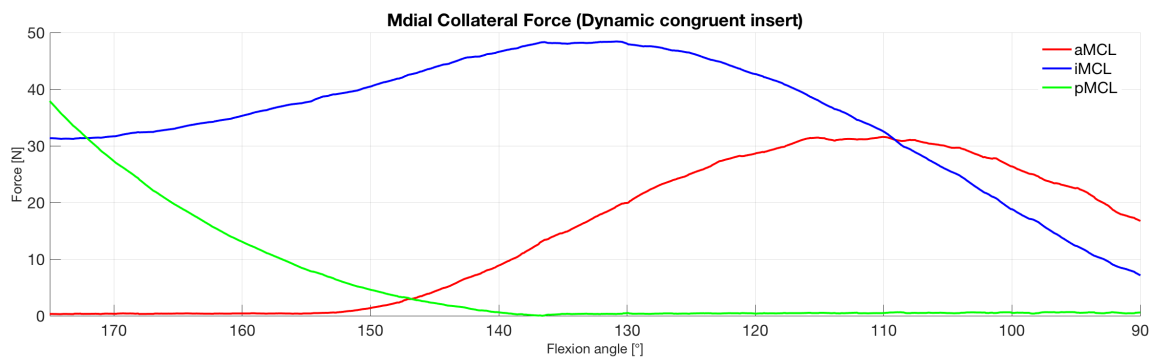


Figure 3. 4: Trend of the ligament forces for the medial collateral ligament in the model with dynamic congruence insert

With the choices made on the points of origin and insertion of the ligaments, this was achieved both in the model with ultracongruent insert and in the model with dynamic congruent insert. In Figure 3.1, Figure 3.2, for the model with ultracongruent insert, and in Figure 3.5 and Figure 3.6 for the model with dynamic congruent insert, it's possible to notice that:

- all the ligament bundles exert a force;
- these forces don't exceed 50N;

- the anterior bundles work in flexion, the posterior bundles work in extension and the central bundles are active for almost the whole flexion range. This complies with the recruitment laws reported in the literature [Blankevoort et al 1991].

3.1.2 CONTACT FORCES

The division of each insert into a medial and lateral compartment allowed the evaluation of the loads exchanged in the two compartments. The results are shown below.

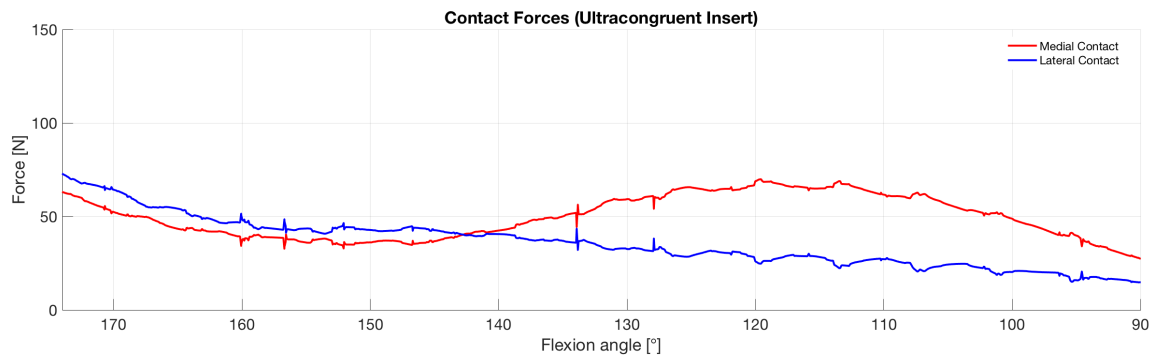


Figure 3. 5: Trend of the medial and lateral contact between the femoral component and the ultracongruent insert

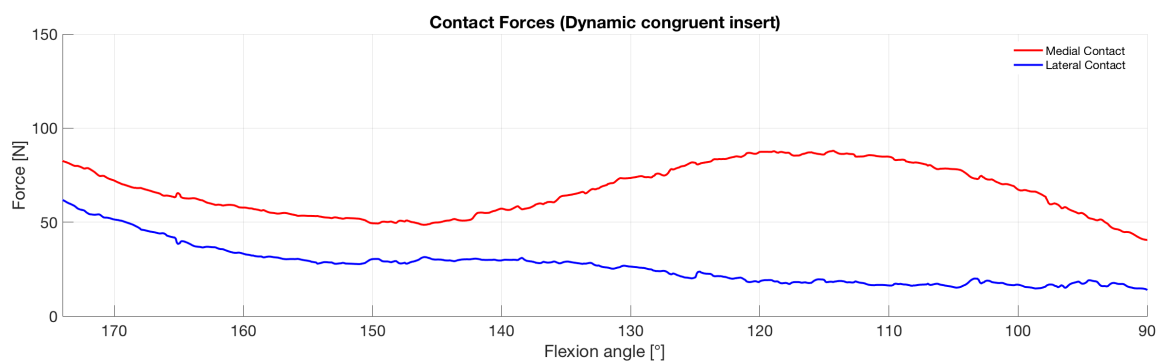


Figure 3. 6: Trend of the medial and lateral contact between the femoral component and the dynamic congruence insert

Trends in medial and lateral contact forces for the two insert models are different:

- the model with dynamic congruent insert shows a medial contact greater than the lateral contact throughout the whole flexion range maintaining the difference of 15 lbf [Gustke K. A. et al 2014 a; Gustke K. A. et al 2014 b]. Between the loads in the two compartments (at the beginning the medial force is 92.23 N; the lateral force is 59, 22N).
- the trend of the contact forces in the model with ultracongruent insert is totally different: the medial contact, at the beginning of the flexion is lower than the lateral contact (different of 15 N), therefore after 35 ° of flexion the tendency is reversed and

the contact medial grows beyond the lateral one until the end of the flexion movement.

Both the trends for medial and lateral contacts during a passive knee flexion are reported in the literature: Verstraete M. A. et al in 2017 reproducing through an experimental setup the same surgical conditions that can occur during a TKA surgery, had positioned sensors, in correspondence of the articular interface, for the measurement of compartmental loads. The results showed a greater medial load of the lateral load throughout the flexion range with a difference of less than 15 lbf [Verstraete M. A. et al 2017]. The trend found in the model with ultracongruent insert is consistent with the results reported in a successive study carried out on cadavers in which the results of the native knee with the portesized knee are compared [Salvadore G. et al 2018]. In this study, the results of the contact forces exchanged between the medial and lateral compartments of the knee joint show a greater lateral load of the medial load up to about 35 ° and an opposite pattern throughout the remaining flexion range.

3.1.2 TIBIAL INTERNAL ROTATION

The quantitative evaluation of the internal tibia rotation, observable during a knee flexion movement, was carried out by using a 1 g mass sphere positioned in the center of the tibial plateau. This sphere can not translate on the plate but follows the tibia in its bending. By evaluating the angle that the axes of its center of mass form with the axes of a marker placed at the center of the plate, it is possible to quantify the axial rotation of the tibia.

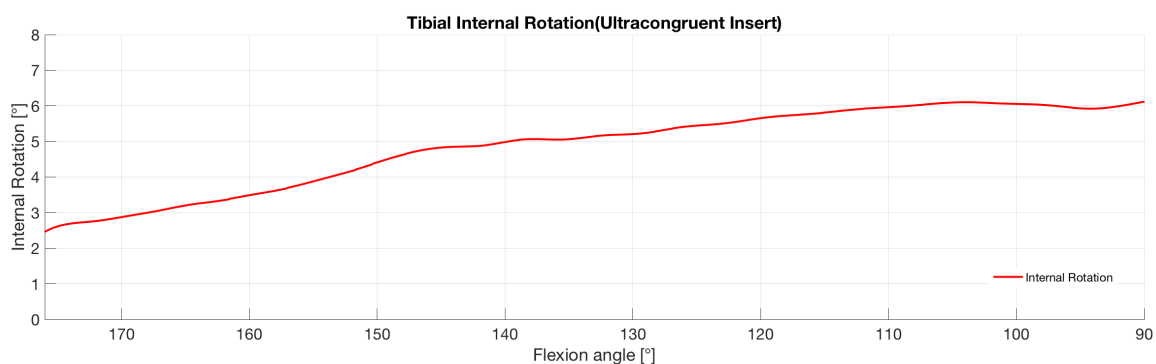


Figure 3. 7: Tibial internal rotation after TKA with ultracongruent insert

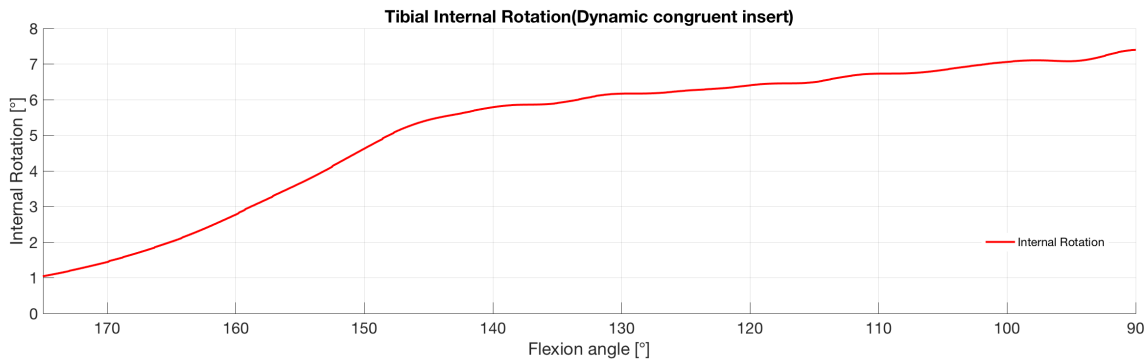


Figure 3. 8: T: Tibial internal rotation after TKA withdynamic congruence insert

A medial contact greater than the lateral contact (Figure 3.5 and Figure 3.6) is linked to the screw home mechanism. In the model with dynamic congruent insert, the intrarotation increases as the flexion angle increases from 1° to a maximum of 6.97 °; in the model with ultracongruent insert the tibia's internal rotation reaches 5,76 ° starting from 2.6°.

Different studies show several values of the angles of internal rotation of the tibia during a knee flexion after total knee replacement. On average, after a knee prosthesis implant, from 1 to 10 ° of internal tibia rotation can be observed depending on the type of prosthesis and the surgical technique used for the implant [Stiehl J. B. 2009].

3.2 RESULTS FOR THE ACTIVE KNEE MOTION

3.2.1 CONTACT FORCES

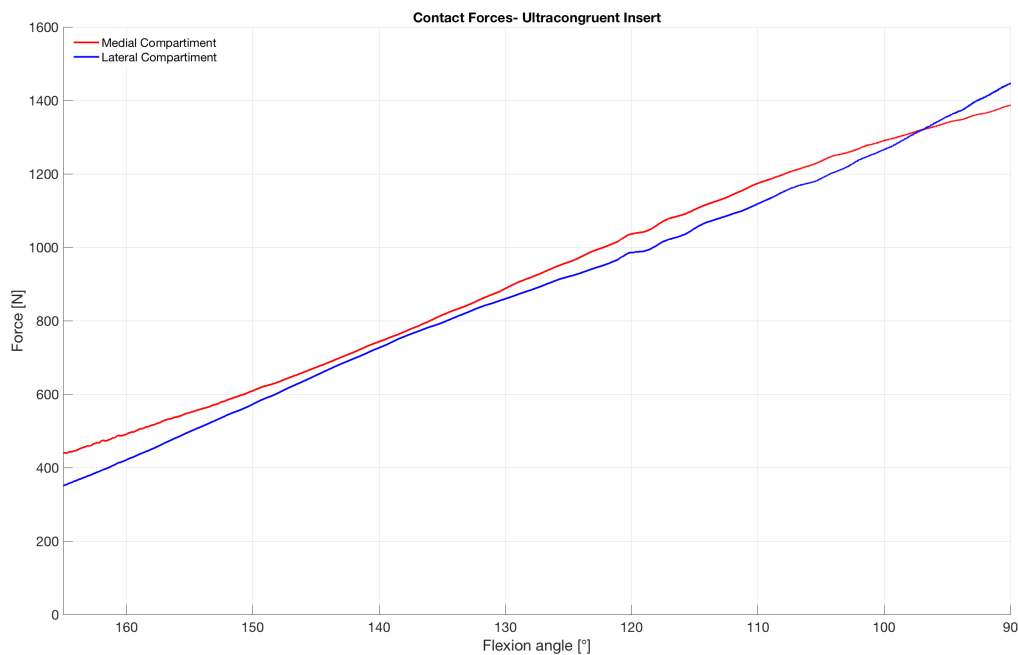


Figure 3. 9: Contact forces developed between the femoral component and the medial and lateral side of ultracongruent insert

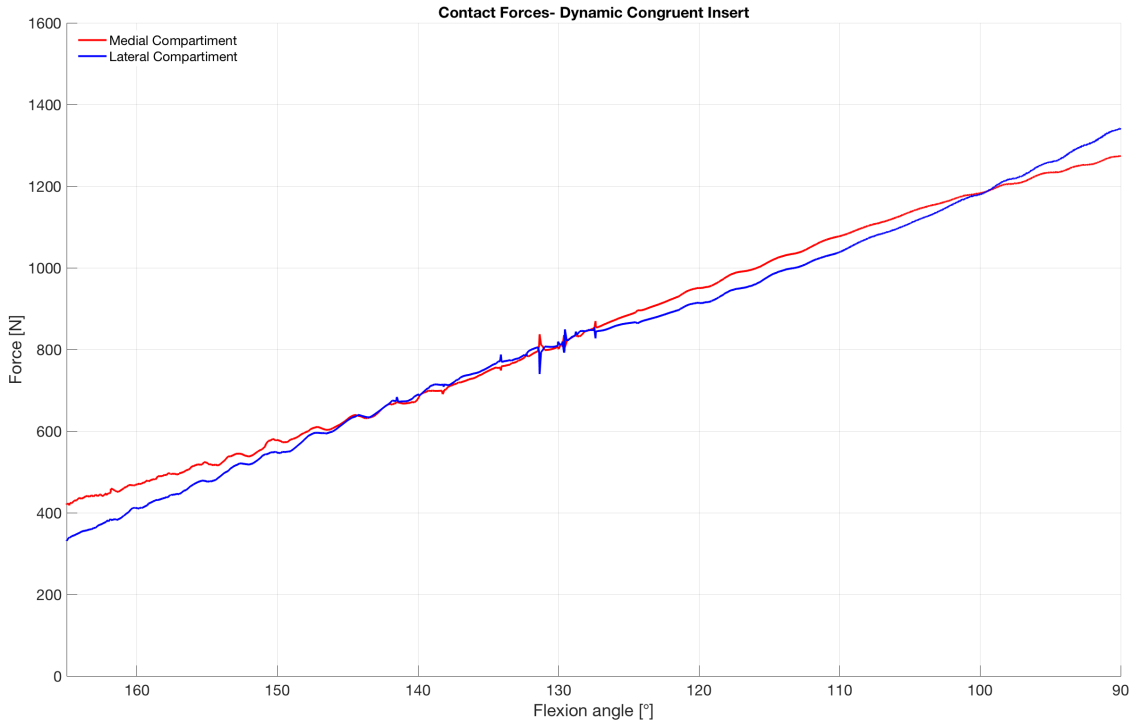


Figure 3. 10: Contact forces developed between the femoral component and the medial and lateral side of dynamic congruence insert

The multibody model created to simulate a knee flexion with muscle activation is much more complex because in addition to the prosthetic components inserted in the femur and tibia, it also includes the patella with its ligaments and a schematization of the quadriceps and its tendon. In this case the amount of forces exerted in correspondence of the medial compartment and of the lateral compartment is certainly greater than that obtained in the case in which the joint was not loaded. To test the correctness of the results obtained, these were compared with those of another multibody model present in the literature [Bersini S. et al 2015]. This model was created for the simulation of a squat activity in a physiological knee model. In this study it was shown that the tibiofemoral contact force increases with increasing flexion angle (in a nonlinear way) reaching a peak at 90 ° equal to 4.2 BW (4.2 times the body weight). A range of tibio-femoral contact forces between 2 and 5.5 BW was reported from a study in which a multibody knee model was made to simulate a squat movement when different types of implants were implanted [Innocenti B. et al 2011].

In the present study, for the model with dynamic congruent insert, a maximum medial contact of 1366.3 N and a maximum lateral contact of 1507.50 N (Figure 3.9 upper image) was achieved for a total of 2873 N corresponding to 3.5 BW. For the model with ultracongruent insert (Figure 3.9 lower image), a maximum value was reached for the medial contact of 1441.46 N and for the lateral contact of 1567.62 N, reaching a total contact force

of 3009.08 N equal to 3.76 BW. The results obtained from the point of view of the contacts are therefore consistent with that reported in the literature.

3.2.1 TIBIAL INTERNAL ROTATION

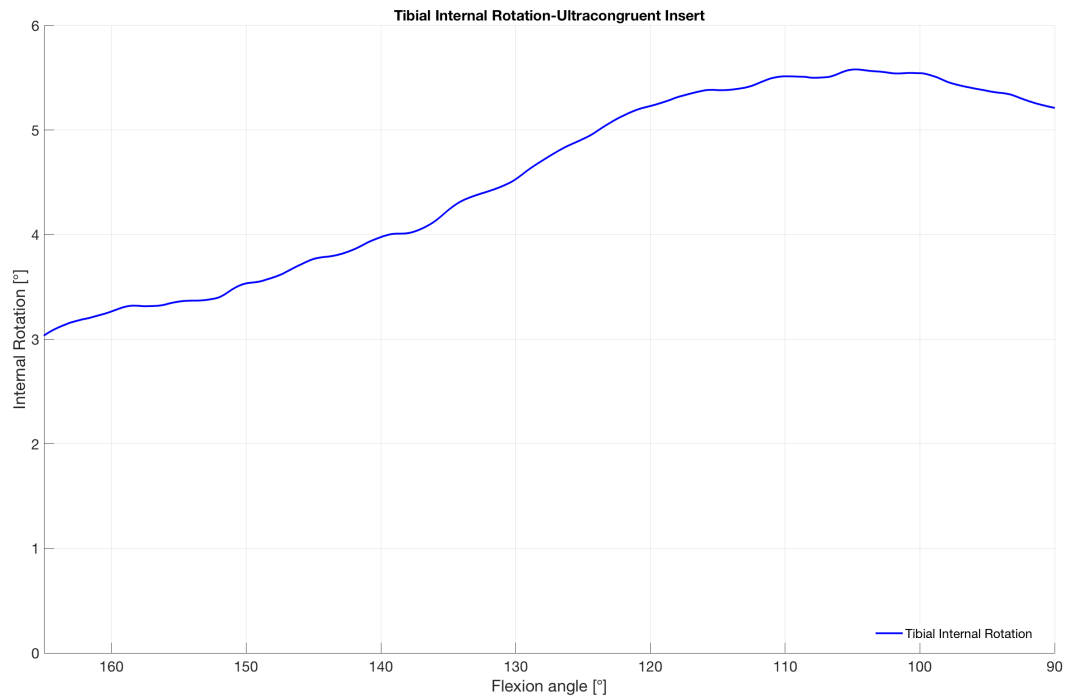


Figure 3. 11: Tibial Internal rotation (ultracongruent insert)

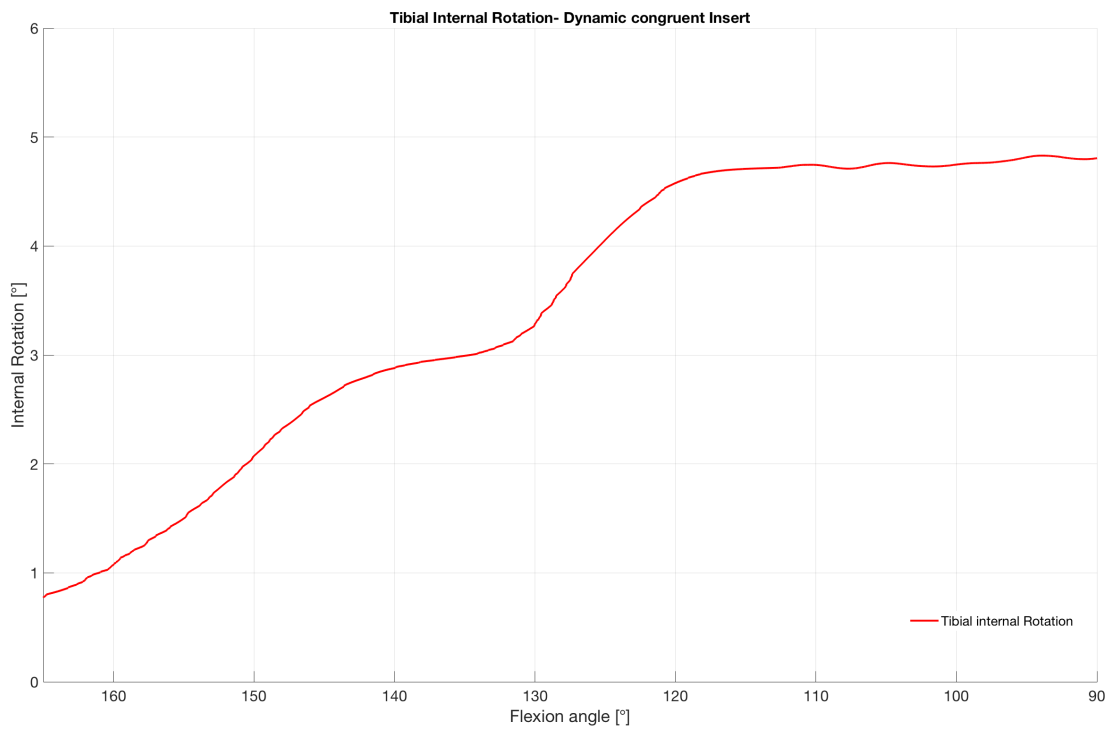


Figure 3. 12: Tibial Internal rotation (dynamic congruence insert)

The internal rotations obtained in the two models during active knee flexion are shown in Figure 3.10 and Figure 3.13. Internal tibial rotation during active knee flexion was assessed using two spheres corresponding to medial and lateral femoral condyles. The angular coefficient of the line linking the projections of these centers on the transverse plane of the tibial plate was used to estimate the axial rotation of the tibia. Apparently it seems that the rotation achieved in the model with ultracongruent insert is greater. Actually, the starting value is the one at which the rotation stabilizes after the initial oscillations. In the case of ultracongruent insert this occurs at the 3 ° and then reaches 5.3 ° at 90 ° of bending making a 2.3 ° rotation overall. Observing the curve relative to the model with dynamic congruent insert, on the other hand, it can be noted that here the rotation stabilizes around 0.8 ° and reaches 4.7 ° making a total of 3.9 ° of internal tibial rotation.

Figures 3.18 and 3.19 represent comparisons of these rotations that can be observed respectively during passive and active flexion of the knee with distinction of what happens using one type of insert rather than the other one.

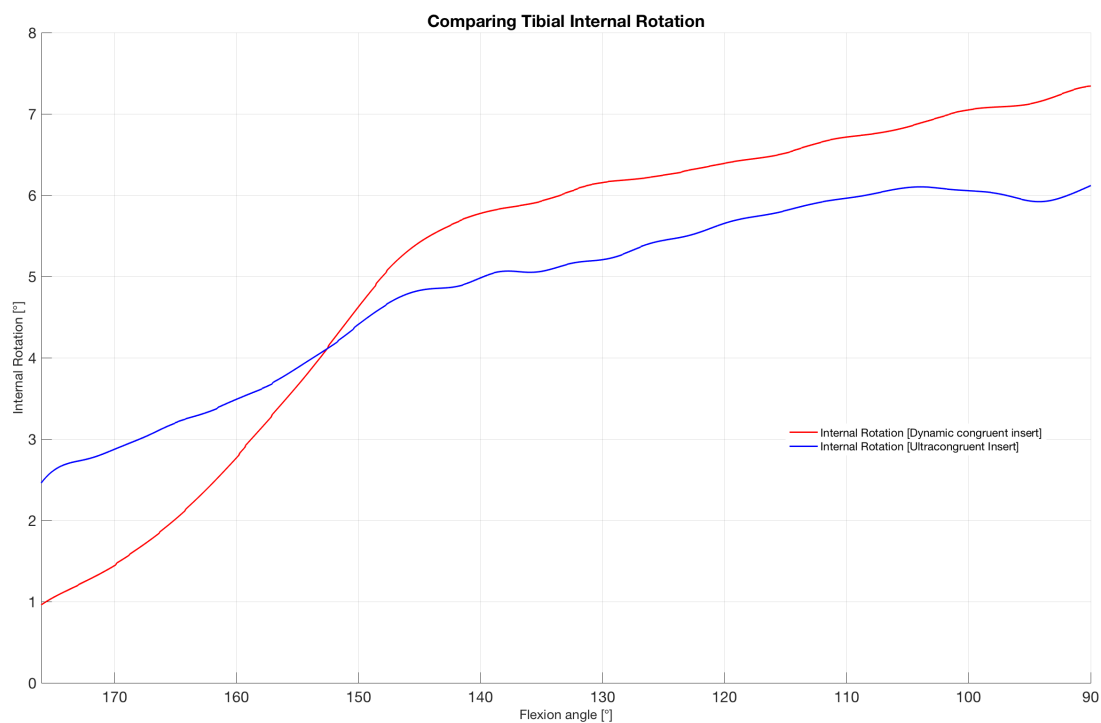


Figure 3. 13: Comparing tibial internal rotation during the passive knee flexion

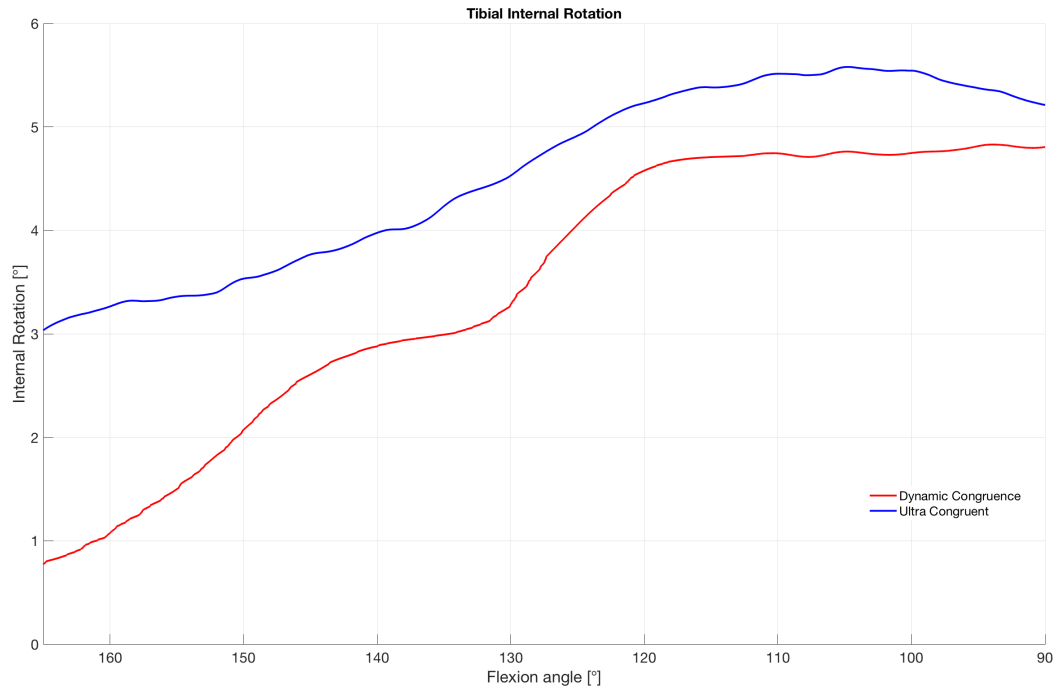


Figure 3. 14: Comparing tibial internal rotation during the active knee flexion

3.3.2 QUADRICEPS FORCES

The following graphs illustrate the quadriceps forces developed in both models with the two different inserts.

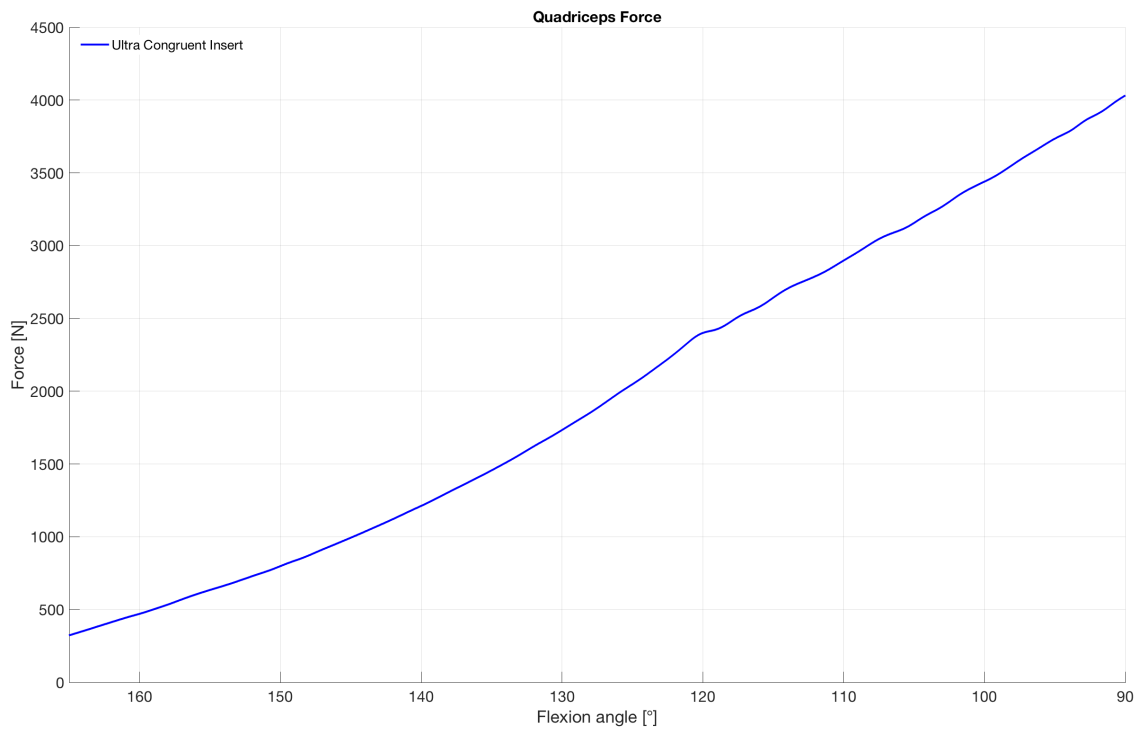


Figure 3. 15 : Quadriceps force developed in the model with ultracongruent insert

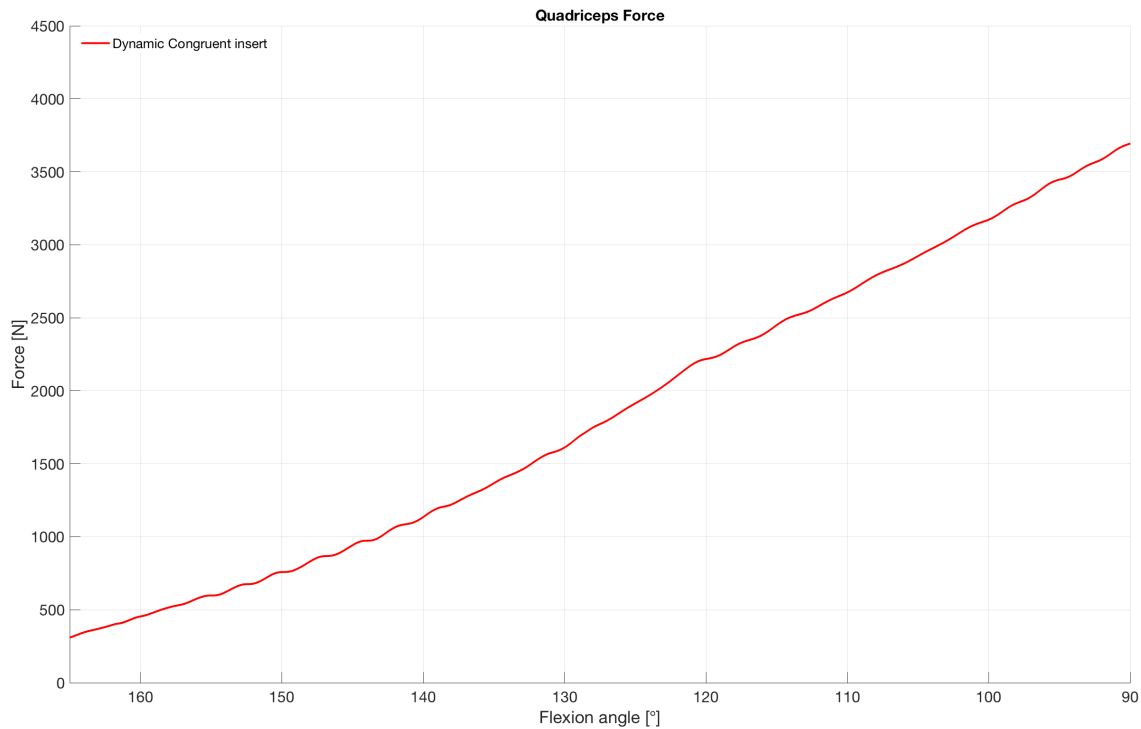


Figure 3. 16: Quadriceps force developed in the model with dynamic congruence insert

In both models, the force developed by the muscle grows as the flexion angle increases, reaching a maximum peak of 90 ° as reported also in the results relative to the Bersini multibody model [Bersini S. et al 2015]. In the model with ultracongruent insert the quadriceps strength starts from a minimum of 220.5 N reaching a maximum of 4000 N corresponding to 5 BW. In the model with dynamic congruent insert the maximum force developed is slightly lower reaching a maximum value of 2681 N corresponding to 4.6 BW. The values obtained are not totally congruent with those reported in the studies of Bersini and Innocenti related to two multibody models for knee flexion with muscle activation. In Bersini's study a peak of strength of 4.2 BW is reached, whereas in the models of knee prostheses tested by Innocenti we reach forces included in the range 3-5.5 BW [Innocenti B. et al 2011; Bersini S. et al 2015].

The non-perfect correspondence of the results obtained with those reported in the literature can be traced back to the different modeling of the same muscle: in this thesis work the strength of the quadriceps automatically adapts to the increase of the flexion in the multibody model of Bersini the strength of the quadriceps is made to vary manually.

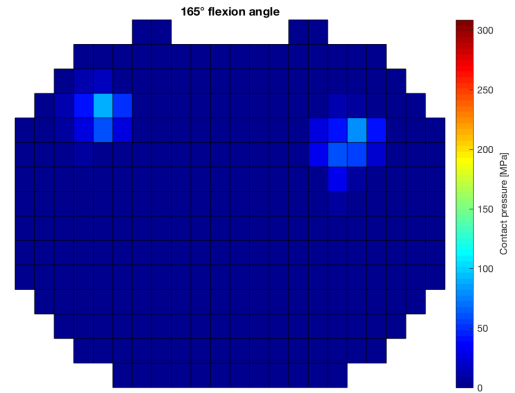
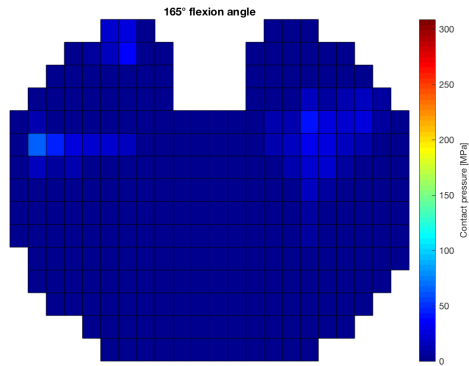
3.2.3 FORCES DISTRIBUTION DURING A SQUAT MOTION

**DYNAMIC
CONGRUENT INSERT**

**ULTRACONGRUE
INSERT**

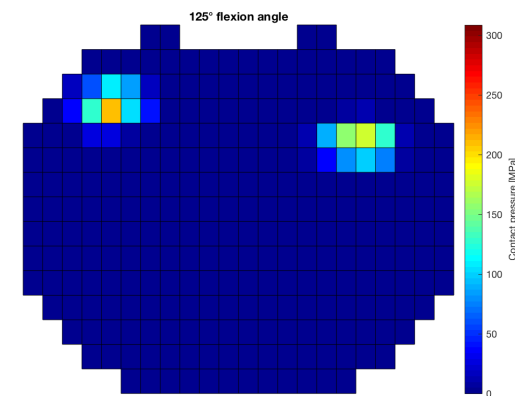
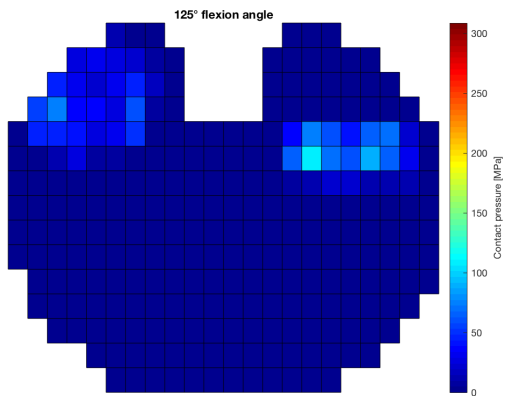
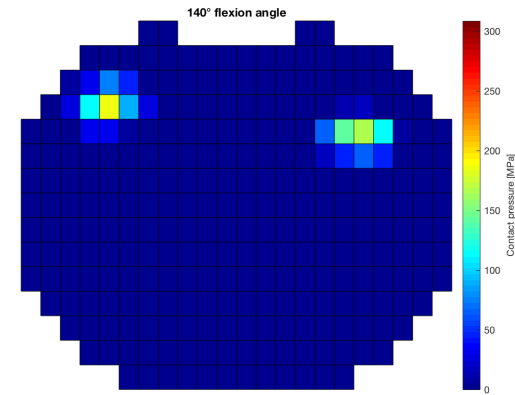
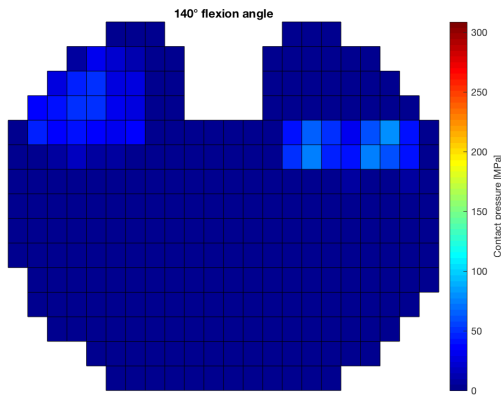
Posterior

Posterior



Anterior

Anterior



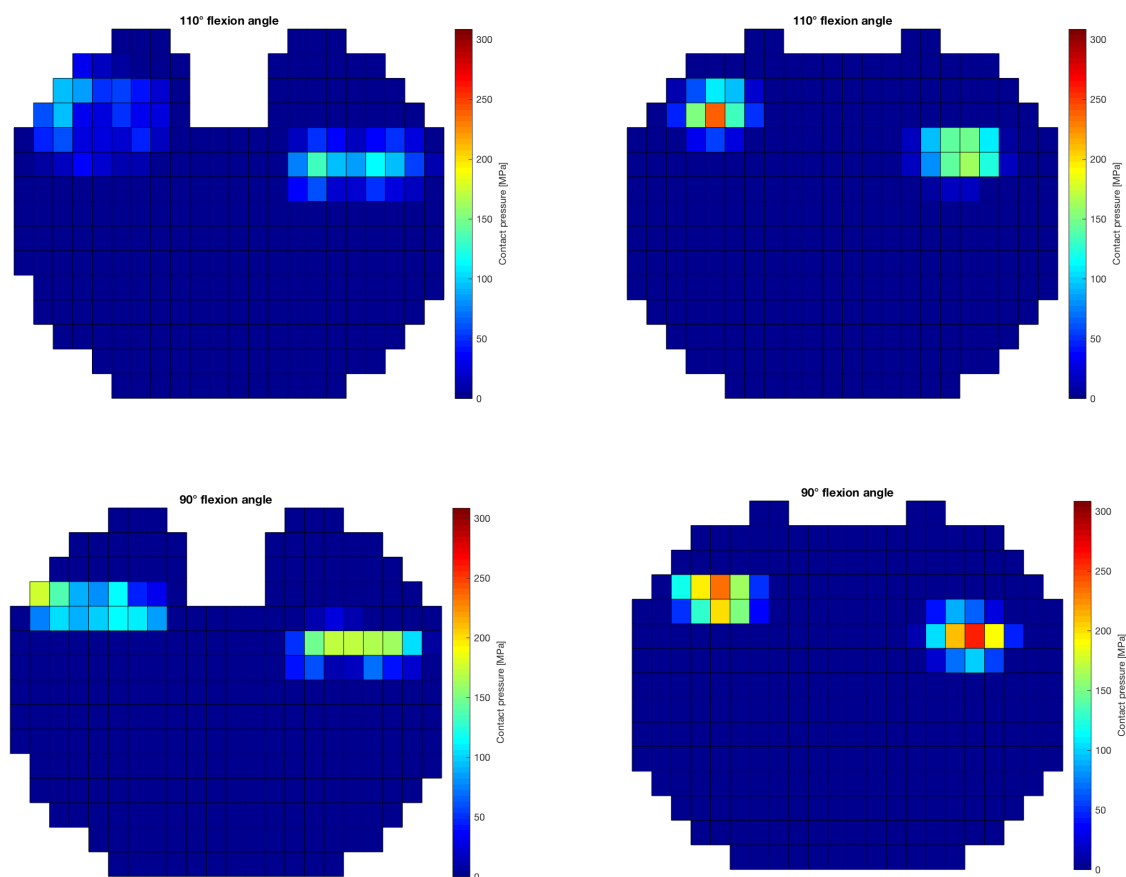


Figure 3. 17: Forces distribution at some flexion angles

The discretization of the inserts made it possible to obtain a map in which the distribution of the contact forces during the active flexion of the knee is evident (Figure 3.15). The pattern forces obtained in this work is not in agreement with that reported in another study related to a multibody model for the simulation of a squat activity [Stylianou A. P. et al 2013]. The contact pressure maps reported in this study show anterior movement of contact points during movement execution. However, this discrepancy can be attributed to the geometry of the inserts: in this thesis two knee prosthesis have been tested whose inserts have a raised front edge to ensure greater stability and avoid a front sliding which causes premature wear of the insert. This is why from the maps it is possible to observe a posterior femoral roll back: posterior translation of the contact points. This phenomenon is mainly manifested on the lateral side reflecting the physiological **medial pivot motion**.

3.3 CONCLUSIONS AND FUTURE DEVELOPMENTS

The aim of this thesis work was to compare two different types of total knee replacements. The two K-MOD prostheses of the Bioimpianti company in Milan have the same femoral and tibial components but two different inserts.

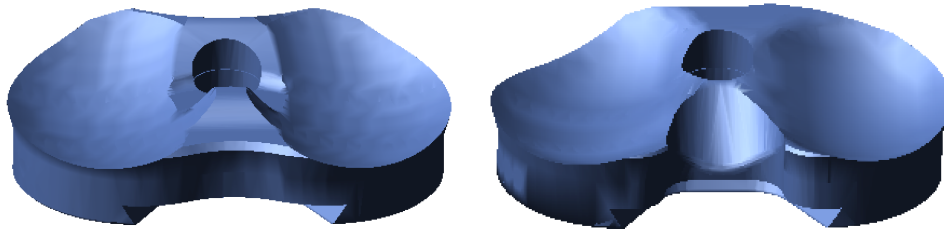


Figure 3. 18: Ultra Congruent and Dynamic congruence insert

The two inserts differ in their shape: the ultracongruent insert presents the medial compartment perfectly equal to the lateral compartment; the dynamic congruence insert shows two non-symmetrical compartments that are able to reproduce the physiological asymmetry of the articular interface. Both inserts have the most raised anterior portion that should increase stability and reduce the frontal slip.

A multibody approach was used to compare the two different types of prosthesis using MSC Adams Software, which allows the study of the dynamics and kinematics of solid bodies connected together through joints and after the application of external forces. The realized models allow to reproduce the flexion movement of the knee both without muscular activation (passive flexion) and with muscular activation (active flexion) through the use of specific joints between the different components and the application of appropriate loads.

To test whether the selected ligament positions and the selected parameters could be appropriate, the forces exerted by the single bundles of the collateral ligaments were evaluated in order to allow a balanced load distribution in the two medial and lateral compartments. The results obtained have allowed us to conclude that the final configuration chosen for the positioning of the ligaments can allow a bicompartamental balancing of the medial and lateral loads. From the passive flexion simulation, trends and amplitudes of the forces of the collateral ligament bundles were obtained and they were consistent with literature studies related to bicompartamental balancing.

Using the positions and parameters of the bundles of ligaments that favored loads balancing during a passive flexion model, a knee flexion model was implemented including the quadriceps activation. For both models containing the two different prosthetic models, it was

found that during active flexion, the contact forces (medial and lateral) increase up to 90° of flexion.

The analysis of the joint kinematics was conducted by quantifying the degrees of axial tibial rotation that can be observed during the knee flexion movement.

In both models, with the two different inserts, the "screw-home" mechanism was observed. The higher tibial internal rotation observed in the case of the dynamic congruence insert justifies that its asymmetric geometry allows a better reproduction of the physiological pivoting.

A greater posterior displacement of the lateral femoral condyle on the insert can be appreciated from the contact pressure maps obtained throughout the flexion range. This was observed both in the model containing the ultracongruent insert and in the model with dynamic congruence insert with the only difference that in the first case the contact forces are more concentrated than the other one. The reason for this difference in the distribution of contact forces can be attributed to the geometry of the two inserts: the dynamic congruent insert, with its most geometry closer to the real physiological shape, allows a less concentrated load distribution

The results obtained above all in terms of contact forces are to be considered satisfactory since they respect the limits imposed for the bicompartamental balancing in case of passive bending which is the fundamental prerequisite for the success of a knee prosthesis implant. Moreover, through the simulation of the weight bearing activity, it was possible to compare the results obtained with several studies reported in literature related to both the intact knee and the prosthetic knee.

However, the most critical aspect of the multibody models realized in this thesis project is represented by the implementation of the ligaments. For this reason, a further sensitivity analysis is needed involving the variation of the zero-load length of each ligament and the position of the points of origin and insertion of the ligaments. For this reason one of the possible future developments that can be foreseen for the models is their use for patient specific considerations following an identification of the areas of origin and insertion of the ligaments obtained directly from MRI images of the individual patient. In addition, the results obtained could be used as input for a finite element model (FEM) that can help predict, in a given load condition, the stress condition at the bone-prosthesis interface.

APPENDIX

!NOTE: The x,y,z components that define the position marker of the splitter box, have to point toward the geometry to split

```
! $splitter_box: T=geometry
! $geometry_to_split: T=geometry
! $cell_side: T=real: GT=0
! $target_geometry: T=geometry
! $fix_geometry: T=geometry
! $stiffness: T=real: GE=0: D=1.0E+05
! $damping: T=real: GE=0: D=10.0
! $exponent: T=real: GE=0: D=2.2
! $dmax: T=real: GE=0: D=0.1
! $static: T=real: GE=0
! $dynamic: T=real: GE=0
! $stiction: T=real: GE=0
! $friction: T=real: GE=0
! END_OF_PARAMETERS
```

```
defaults command_file echo=off
update=off
```

```
! INIT VARIABLE NAME
var cre
var=$_self.geo_to_split_name_copy
string=(UNIQUE_NAME("GEO1"))
var cre
var=$_self.splitter_geo_name_copy
string=(UNIQUE_NAME("GEO2"))
var cre var=$_self.int_part_name
string=(UNIQUE_NAME("INT"))
var cre var=$_self.int_geo_name
string=(UNIQUE_NAME("GEO3"))
var cre var=$_self.int_geo_name_copy
string=(UNIQUE_NAME("GEO4"))
var cre var=$_self.cell_name
string=(UNIQUE_NAME("CELL"))
var cre var=$_self.cell_geo_name
string=(UNIQUE_NAME("GEO5"))
var cre var=$_self.int_cell_geo_name
string=(UNIQUE_NAME("GEO6"))
var cre var=$_self.cell_marker_name
string=(UNIQUE_NAME("CELL_MARKER"))
var cre var=$_self.fix1_marker_name
string=(UNIQUE_NAME("FIX1_MARKER"))
```

```
var cre var=$_self.fix2_marker_name
string=(UNIQUE_NAME("FIX2_MARKER"))
var cre var=$_self.fix_name
string=(UNIQUE_NAME("FIX"))
var cre
var=$_self.measure_force_X_name
string=(UNIQUE_NAME("MEAS_FORCE_X"))
var cre
var=$_self.measure_force_Y_name
string=(UNIQUE_NAME("MEAS_FORCE_Y"))
var cre
var=$_self.measure_force_Z_name
string=(UNIQUE_NAME("MEAS_FORCE_Z"))
var cre var=$_self.measure_pos_X_name
string=(UNIQUE_NAME("MEAS_POS_X"))
var cre var=$_self.measure_pos_Z_name
string=(UNIQUE_NAME("MEAS_POS_Z"))
var cre var=$_self.contact_name
string=(UNIQUE_NAME("CONT"))
```

```
var cre var=$_self.model
object_value=(eval(DB_DEFAULT(.system_defaults,"model")))
var cre var=$_self.splitter_part
object_value=(eval(DB_ANCESTOR($splitter_box,"part")))
var cre var=$_self.fix_part
object_value=(eval(DB_ANCESTOR($fix_geometry,"part")))
var cre var=$_self.part_to_split
object_value=(eval(DB_ANCESTOR($geometry_to_split,"part")))
var cre var=$_self.splitter_X
real=(eval($splitter_box.diag_corner_coords[1]))
var cre var=$_self.splitter_Y
real=(eval($splitter_box.diag_corner_coords[2]))
var cre var=$_self.splitter_Z
real=(eval($splitter_box.diag_corner_coords[3]))
var cre var=$_self.corner
string=(eval($splitter_box.corner_marker))
var cre var=$_self.color_flag integer=1
```

```

var cre var=$_self.color_row_flag
integer=1

! PERMANENT VARIABLE
var cre var= cont_stiffness &
  real = $stiffness
var cre var= cont_damping &
  real = $damping
var cre var= cont_exponent &
  real = $exponent
var cre var= cont_dmax &
  real = $dmax
var cre var= cont_static &
  real = $static
var cre var= cont_dynamic &
  real = $dynamic
var cre var= cont_stiction &
  real = $stiction
var cre var= cont_friction &
  real = $friction

! CREATE A NEW GROUP
group create group_name = new_parts

group objects add group_name =
new_parts &
  objects_in_group = $splitter_box,
$geometry_to_split

! COPY BOTH SPLITTER
GEOMETRY AND GEOMETRY TO
SPLIT
geometry copy geometry=
$geometry_to_split &

new_geometry_name=(eval($_self.mode
l)).(eval($_self.part_to_split)).(eval($_sel
f_geo_to_split_name_copy))
geometry copy geometry= $splitter_box
&

new_geometry_name=(eval($_self.mode
l)).(eval($_self.splitter_part)).(eval($_self
.splitter_geo_name_copy))

! CREATE THE INTERSECTION
PART
part create rigid_body
name_and_position &

```

```

part_name=(eval($_self.int_part_name))

! INTERSECT SPLITTER GEOMETRY
AND GEOMETRY TO SPLIT
geometry create shape csg &

csg_name=(eval($_self.model)).(eval($_
self.int_part_name)).(eval($_self.int_geo
_name)) &

base_object=(eval($_self.geo_to_split_na
me_copy)) &

object=(eval($_self.splitter_geo_name_c
opy)) &
  type=intersection
part attributes
part_name=(eval($_self.int_part_name))
&
  color=green &
  name_vis=off

! UPDATE COPY NAMES
var set
var=$_self.geo_to_split_name_copy
string=(UNIQUE_NAME("GEO1"))
var set
var=$_self.splitter_geo_name_copy
string=(UNIQUE_NAME("GEO2"))

! ITERATE ALONG X
FOR var=$_self.count_2 start_value=0
increment_value=1
END_value=(EVAL(CEIL((eval($_self.s
plitter_X/$cell_side))))-1)

! IMPOSE FIRST CELL COLOR OF
THE ROW
IF condition=($_self.color_row_flag==1)
  variable set
  variable_name=$_self.color_row_flag
  integer_value=0
ELSE
  variable set
  variable_name=$_self.color_row_flag
  integer_value=1
END

```

```

variable set variable=$_self.color_flag
integer=(eval($_self.color_row_flag))

! ITERATE ALONG Z
FOR var=$_self.count_1 start_value=0
increment_value=1
END_value=(EVAL(CEIL((eval($_self.s
plitter_Z/$cell_side))))-1)

! CREATE CELL PART
part create rigid_body
name_and_position &
  part_name=(eval($_self.cell_name))
part modify rigid mass_properties &
  part_name=(eval($_self.cell_name))
&

material=(eval($_self.part_to_split.materi
al))
part attributes
part_name=(eval($_self.cell_name)) &
  name_vis=off
marker create
marker=(eval($_self.cell_marker_name))
&

location=(LOC_RELATIVE_TO({(eval(
$_self.count_2 *
$cell_side)),0,(eval($_self.count_1 *
$cell_side))),(eval($_self.corner)))) &

orientation=(ORI_RELATIVE_TO({0,0,
0},{(eval($_self.corner))))
marker attributes &
  marker_name =
(eval($_self.cell_marker_name)) &
  vis = off &
  name_vis = off
geometry create shape block &

block_name=(eval($_self.cell_geo_name
)) &

diag_corner_coords=($cell_side),(eval($_
self.splitter_Y)),$(cell_side) &

corner_marker=(eval($_self.cell_marker_
name))

! COPY INTERSECTION GEOMETRY

```

```

geometry copy
geometry=(eval($_self.int_geo_name)) &

new_geometry_name=(eval($_self.mode
l)).(eval($_self.int_part_name)).(eval($_s
elf.int_geo_name_copy))

! INTERSECT CELL GEOMETRY
AND INTERSECTION GEOMETRY
geometry create shape csg &

csg_name=(eval($_self.model)).(eval($_
self.cell_name)).(eval($_self.int_cell_geo
_name)) &

base_object=(eval($_self.int_geo_name_
copy)) &
  object=(eval($_self.cell_geo_name)) &
  type=intersection

!!! DETECT IF THE INTERSECTION
FAILS
IF
condition=(DB_EXISTS($_self.int_cell_
geo_name)==0)
  part delete
  part=(eval($_self.cell_name))
  geometry delete
  geometry=(eval($_self.model)).(eval($_s
elf.int_part_name)).(eval($_self.int_geo_
name_copy))

ELSE

! HIDE CELL CM MARKER
marker attributes &
  marker_name =
(eval($_self.cell_name).cm) &
  vis = off &
  name_vis = off

! CREATE FIXED JOINT BETWEEN
CELL AND REMAINING PART
marker create
marker=(eval($_self.model)).(eval($_sel
f.cell_name)).(eval($_self.fix1_marker_n
ame)) &

location=(LOC_RELATIVE_TO({$cell_
side/2,0,$cell_side/2},{(eval($_self.cell_m
arker_name)))) &

```

```

orientation=0.0, 0.0, 0.0
marker attributes &
  marker_name =
(eval($_self.fix1_marker_name)) &
  vis = off &
  name_vis = off
marker create
marker=(eval($_self.model)).(eval($_self.fix_part)).(eval($_self.fix2_marker_name)) &

location=(LOC_RELATIVE_TO({$cell_side/2,0,$cell_side/2},{eval($_self.cell_marker_name)})) &
orientation=0.0, 0.0, 0.0
marker attributes &
  marker_name =
(eval($_self.fix2_marker_name)) &
  vis = off &
  name_vis = off
constraint create joint Fixed &
  joint_name=(eval($_self.fix_name)) &

i_marker_name=(eval($_self.model)).(eval($_self.cell_name)).(eval($_self.fix1_marker_name)) &

j_marker_name=(eval($_self.model)).(eval($_self.fix_part)).(eval($_self.fix2_marker_name))
constraint attribute
constraint_name=(eval($_self.fix_name))
vis=off name_vis=off

! CREATE X REACTION FORCE
MEASURE
measure create object &

measure_name=(eval($_self.measure_force_X_name)) &

object=(eval($_self.model)).(eval($_self.fix_name)) &
  characteristic = "element_force" &
  component = "x_component" &
  from_first = no &
  &
  coordinate_rframe =
(eval($_self.model)).(eval($_self.fix_part)).(eval($_self.fix2_marker_name)) &
  comments="" &

```

```

create_measure_display = no

! CREATE Y REACTION FORCE
MEASURE
measure create object &

measure_name=(eval($_self.measure_force_Y_name)) &

object=(eval($_self.model)).(eval($_self.fix_name)) &
  characteristic = "element_force" &
  component = "y_component" &
  from_first = no &
  &
  coordinate_rframe =
(eval($_self.model)).(eval($_self.fix_part)).(eval($_self.fix2_marker_name)) &
  comments="" &
  create_measure_display = no

! CREATE Z REACTION FORCE
MEASURE
measure create object &

measure_name=(eval($_self.measure_force_Z_name)) &

object=(eval($_self.model)).(eval($_self.fix_name)) &
  characteristic = "element_force" &
  component = "z_component" &
  from_first = no &
  &
  coordinate_rframe =
(eval($_self.model)).(eval($_self.fix_part)).(eval($_self.fix2_marker_name)) &
  comments="" &
  create_measure_display = no

! CREATE X POSITION MEASURE
measure create point &

measure_name=(eval($_self.measure_pos_X_name)) &

point=(eval($_self.model)).(eval($_self.fix_part)).(eval($_self.fix2_marker_name)) &
  characteristic =
"translational_displacement" &

```

```

component = "x_component" &
comments="" &
create_measure_display = no

! CREATE Z POSITION MEASURE
measure create point &

measure_name=(eval($_self.measure_pos
_Z_name)) &

point=(eval($_self.model)).(eval($_self.f
ix_part)).(eval($_self.fix2_marker_name
) &
characteristic =
"translational_displacement" &
component = "z_component" &
comments="" &
create_measure_display = no

! CREATE CONTACT ON CELL
contact create contact_name
=(eval($_self.contact_name)) &
type = solid_to_solid &
i_geometry_name =
(eval($_self.model)).(eval($_self.cell_na
me)).(eval($_self.int_cell_geo_name)) &
j_geometry_name = $target_geometry
&
stiffness = (cont_stiffness) &
damping = (cont_damping) &
exponent = (cont_exponent) &
dmax = (cont_dmax) &
coulomb_friction = on &
mu_static = (cont_static) &
mu_dynamic = (cont_dynamic) &
stiction_transition_velocity =
(cont_stiction) &
friction_transition_velocity =
(cont_friction)
entity attributes
entity_name=(eval($_self.contact_name))
vis=off name_vis=off

var set var=$_self.contact_name
string=(UNIQUE_NAME("CONT"))

group objects add group_name =
new_parts &
objects_in_group =
(eval($_self.model)).(eval($_self.cell_na
me)),

```

```

.(eval($_self.model)).(eval($_self.fix_na
me))

END

! CHECK CELL COLOR
IF condition=($_self.color_flag==1)
variable set
variable_name=$_self.color_flag
integer_value=0
IF
condition=(DB_EXISTS($_self.cell_name))
geometry attributes
geometry=(eval($_self.int_cell_geo_name)) &
color=red
END
ELSE
variable set
variable_name=$_self.color_flag
integer_value=1
IF
condition=(DB_EXISTS($_self.cell_name))
geometry attributes
geometry=(eval($_self.int_cell_geo_name)) &
color=blue
END
END

! UPDATE VARIABLE NAMES
var set var=$_self.cell_name
string=(UNIQUE_NAME("CELL"))
var set var=$_self.cell_geo_name
string=(UNIQUE_NAME("GEO5"))
var set var=$_self.int_cell_geo_name
string=(UNIQUE_NAME("GEO6"))
var set var=$_self.cell_marker_name
string=(UNIQUE_NAME("CELL_MARKER"))
var set var=$_self.int_geo_name_copy
string=(UNIQUE_NAME("GEO4"))
var set var=$_self.fix1_marker_name
string=(UNIQUE_NAME("FIX1_MARKER"))
var set var=$_self.fix2_marker_name
string=(UNIQUE_NAME("FIX2_MARKER"))

```

```

var set var=$_self.fix_name
string=(UNIQUE_NAME("FIX"))
var set
var=$_self.measure_force_X_name
string=(UNIQUE_NAME("MEAS_FORCE_X"))
var set
var=$_self.measure_force_Y_name
string=(UNIQUE_NAME("MEAS_FORCE_Y"))
var set
var=$_self.measure_force_Z_name
string=(UNIQUE_NAME("MEAS_FORCE_Z"))
var set var=$_self.measure_pos_X_name
string=(UNIQUE_NAME("MEAS_POS_X"))
var set var=$_self.measure_pos_Z_name
string=(UNIQUE_NAME("MEAS_POS_Z"))

```

END

END

! DELETE INTERSECTION PART

```

part del
part=(eval($_self.int_part_name))

! DEACTIVATE AND HIDE SPLITTER
PART AND PART TO SPLIT
entity attr
entity_name=(eval($_self.splitter_part))
active=off dependents_active=off
part attributes
part_name=(eval($_self.splitter_part))
vis=off
entity attr
entity_name=(eval($_self.part_to_split))
active=off dependents_active=off
part attributes
part_name=(eval($_self.part_to_split))
vis=off

! DELETE ALL USED VARIABLES
var del var=$_self.*

```

!model verify

```

defaults command_file echo=on
update=on

```

REFERENCES

- Abulhasan J. F. and Grey M. J.**-*Anatomy and physiology of knee stability*. J. Funct. Morphol. Kinesiol. 2017, 2, 34; doi:10.3390/jfmk2040034
- Alice J. S. Fox, Asheesh Bedi and Scott A. Rodeo.** *The Basic Science of Human Knee Menisci : Structure, Composition, and Function*. 2012, Sports Health: A Multidisciplinary Approach, 340-351
- Ambrósio J., Silva M.** (2005) *Multibody Dynamics Approaches for Biomechanical Modeling in Human Impact Applications*. In: Gilchrist M.D. (eds) IUTAM Symposium on Impact Biomechanics: From Fundamental Insights to Applications. Solid Mechanics and Its Applications, 2005 vol 124. Springer, Dordrecht pp 61:80
- Asano T. Akagi M., tanaka K., Tamura J., and Nakamura T.**- *In vivo three-dimensional knee kinematics using a biplanar imagematching technique*. Clinical Orthopedics and related research (2001) Number 388; pp157-166
- Banks, S.A., Hodge, W.A.,** 1996, *Accurate measurement of three-dimensional knee replacement kinematics using single plane fluoroscopy*. IEEE Transactions on Biomedical Engineering, 43, pp. 638-649.
- Bei Y., Fregly B. j.**"*Multibody dynamic simulation of knee contact mechanics*. Medical Engineering & Physics 26 (2004) 777–789
- Bersini S. , Sansone V. & Carlo A. Frigo** (2015): *A dynamic multibody model of the physiological knee to predict internal loads during movement in gravitational field*, Computer Methods in Biomechanics and Biomedical Engineering, DOI: 10.1080/102558
- Bhaskar K. M., Srinivasa Rao Chalamalasetti, S. K. Sundara siva rao Bolla Pragada.** *Biomechanics of knee joint - A review*. Front. Mech. Eng. DOI 10.1007/s11465-014-0306-x. July 19, 2014
- Blankevoort L, Huiskes R and De Lange A.**- *Recruitment of Knee Joint ligaments*. Journal of Biomechanical Engineering FEBRUARY 1991, Vol. 113 94:103
- Blankevoort L, Huiskes R, de Lange A.** *The envelope of passive knee joint motion*. J Biomech 1988;21:705-20.
- Blankevoort L., Kuiper J.H., Huiskes R., Grootenboer H. J.** - *Articular contact in a three dimensional model of the knee*. 1991- 1. BiomechanicsV ol. 24, No. II. pp. 1019-1031.

- Bloemker K. H., Trent M. Guess, Lorin Maletsky, Kevin Dodd** - *Computational Knee Ligament Modeling Using Experimentally determined zero load lengths*. The Open Biomedical Engineering Journal, 2012, 6, 33-41 33
- Causero A., Di Benedetto P., Beltrame A., Gisonni R., Cainero V., Pagano M.** *Design evolution in total knee replacement: which is the future?*. Acta Biomed 2014; Vol. 85, Supplement 2: 5-19
- Chen Z., Jin Z.**-*Prediction of in-vivo kinematics and contact track of total knee arthroplasty during walking*. Biosurface and Biotribology 2(2016)86–94
- Chen Z., Xuan Zhang, Marzieh M Ardestani, Ling Wang, Yaxiong Liu, Qin Lian, Jiankang He, Dichen Li and Zhongmin Jin.** *Prediction of in vivo joint mechanics of an artificial knee implant with elastic contacts*. Journal of Engineering in Medicine. 2014
- Churchill D. L., Incavo S. J., Johnson C. C. and Beynnon B. D.**-*The Transepicondylar Axis Approximates the Optimal Flexion Axis of the Knee* . CLINICAL ORTHOPAEDICS AND RELATED RESEARCH Nurnber356, pp 111-118- (1998) Lippincott Williams & Wilkins
- Conditt, M. A., Noble, P. C., Bertolusso, R., Woody, J., and Parsley, B. S.** *The PCL significantly affects the functional outcome of total knee arthroplasty*. J. Arthro, 2004, 19(7, Suppl. 2), 107–112.
- Dennis D. A., Mahfouz M. R., Komistek R. D. and Hoff W.** -*In vivo determination of normal and anterior cruciate ligament-deficient knee kinematics*. Journal of Biomechanics 38 (2005) 241–253
- von Eisenhart-Rothe R1, Vogl T, Englmeier KH, Graichen H.**- *A new in vivo technique for determination of femoro-tibial and femoro-patellar 3D kinematics in total knee arthroplasty*. J Biomech. 2007;40(14):3079-88. Epub 2007 May 1.
- Felson David T.** *Developments in the clinical understanding of osteoarthritis*. Arthritis Res Ther. 2009; 11(1): 203
- Feng Y., Tsai T-Y, Li J-S, Wang S., Hu H., Zhang C, Rubash H. and Li G.** -*Motion of the Femoral Condyles in Flexion and Extension during a Continuous Lunge*. Journal of orthopedic research, April 2015, pp 591-8
- Freeman M. a. R. and Pinskerova V.**-*The movement of the normal tibio-femoral joint*. Journal of Biomechanics 38 (2005) 197–208
- Goldblatt J. P. and Richmond J. C.**-*Anatomy and biomechanics of the knee. Operative Techniques in Sports Medicine*, Vol 11, No 3 (July), 2003: pp 172-186

- Grood E.S., Suntay w.J.**-*A Joint Coordinate System for the Clinical Description of Three-Dimensional Motions- Application to the Knee.* Journal of Biomechanical Engineering MAY 1983, Vol. 105/136-144
- Guess Trent M. , Hongzeng Liu , Sampath Bhashyam & Ganesh Thiagarajan** (2013) *A multibody knee model with discrete cartilage prediction of tibio-femoral contact mechanics.* Computer Methods in Biomechanics and Biomedical Engineering, 16:3, 256-270
- Guess Trent M., Thiagarajan G., Kia M., Mishra M.** - *A subject specific multibody model of the knee with menisci.* Medical Engineering & Physics 32 (2010) 505–515
- Guess, T.M.** *Forward dynamics simulation using a natural knee with menisci in the multibody framework.* Multibody Syst Dyn (2012) 28: 37. <https://doi.org/10.1007/s11044-011-9293-4>
- Hill P.F., Vedi V., Williams A., Iwaki H., Pinskerova V., and Freeman M. A. R.**- *Tibiofemoral movement 2- the loaded and unloaded living knee studied by MRI.- J Bone Joint Surg* 2000; 82-B: 1196-8
- Hollister AM, Jatana S, Singh AK, et al.** *The axes of rotation of the knee.* Clin Orthop 1993;290:259.
- Innocenti B, Pianigiani S. , Labey L., Victor J., Bellemans J.** -*Contact forces in several TKA designs during squatting- A numerical sensitivity analysis.* JournalofBiomechanics44(2011)1573–1581
- Iwaki H, Pinskerova V.; Freeman M. A. R.**- *Tibiofemoral movement 1- the shapes and relative movements of the femur and tibia in the unloaded cadaver knee.* J Bone Joint Surg /Br/ 200; 82-B 1189-95
- Johal P., Williams A., Wragg P., Hunt D. and Gedroych W.** - *Tibio-femoral movement in the living knee. A study of weight bearing and non-weight bearing knee kinematics using ‘interventional’ MRI.* Journal of biomechanics 38 (2005) 269-276
- Kapandji I. The knee.** In: **Kapandji I,** editor. *The physiology of the joints.* Vol 2. Edinburgh: Churchill Livingstone; 1970. p 72-135.
- Kasumovic M. , Emir Gorcevic, Semir Gorcevic, Jasna Osmanovic**3. *Efficacy of Physical Therapy in the Treatment of Gonarthrosis in Physically Burdened Working Men.* Mater Sociomed. 2013 Sep; 25(3): 203-205
- Komistek R. D., Dennis D. A. and Mahfauz M.** -*In Vivo Fluoroscopic Analysis of the Normal Human Knee.- Clinical orthopedics and related research* 2003 Number 410, pp 69-81

- Kricun R., Kricun M. e., Arangio G. A., Salzman G. S. and Berman A. T.-** *Patellar Tendon Rupture with Underlying Systemic Disease.* AJR: 1 35, October 1980 pp 803:807
- Kutzner I., B.Heinlein, F.Graichen , A.Bender , A.Rohlmann , A.Halder, A. Beier, G.Bergmann-***Loading of the knee joint during activities of daily living measured in vivo in five subjects.* Journal of Biomechanics 43(2010)2164–2173
- Kweon C., Lederman E. S. and Chhabra A.-** *Anatomy and Biomechanics of the Cruciate Ligaments and their surgical implications.* 2013 In book: The Multiple Ligament Injured Knee Chapter 2
- Li G., Gil J., Kanamori A., Woo S. L.-Y.** *A Validated Three-Dimensional Computational Model of a Human Knee Joint.* Journal of Biomechanical Engineering. 1999, Vol. 121,657:662
- Li G., Zayontz S., DeFrate L. E., Most E., Suggs J. F., Rubash H. E. -***Kinematics of the knee at high flexion angles- an in vitro investigation.* Journal of orthopedic research 22 (2004) 90-95
- Marra MA, Vanheule V, Fluit R, Koopman BH, Rasmussen J, Verdonchot N, Andersen MS.-***A Subject-Specific Musculoskeletal Modeling Framework to Predict In Vivo Mechanics of Total Knee Arthroplasty.* J Biomech Eng. 2015 Feb 1;137(2):020904.
- Meyer, H. von,** 1853. Die Mechanik des Kniegelenkes. Archivfur Anatomie, Physiologie und Wissenschaftliche Meitian 20,497}547.
- Mizu-uchi H., MD, PhDa,b, Clifford W. Colwell Jr, MDa, Cesar Flores-Hernandez, BSa, Benjamin J. Fregly, PhDd, Shuichi Matsuda, MD, PhDc, and Darryl D. D’Lima, MD, PhD.-** *Patient-Specific Computer Model of Dynamic Squatting after Total Knee Arthroplasty.-* J Arthroplasty 2015 May; 30(5) 870-874.
- Mordecai SC, Al-Hadithy N, Ware HE, Gupte CM.** *Treatment of meniscal tears: an evidence based approach.* World J Orthop 2014;5:233-241
- Moro-oka T., Hamai S., Miura H., Shimoto T., Higaki H., Fregly B. J., Iwamoto Y.,S. A. Banks-** *Dynamic activity dependence of in vivo normal knee kinematics.* Journal of orthopaedic research april 2008 p
- Moti L. Tiku and Hatem E. Sabaawy.** *Cartilage regeneration for treatment of osteoarthritis- a paradigm for nonsurgical intervention.* her Adv Musculoskelet Dis. 2015 Jun; 7(3): 76–87

- Muller W.** *The knee: form, function and ligament reconstruction.* New York: Springer-Verlag; 1983. p 8, 9, 145-50
- Nagura T., Matsumoto H., Kiriyaama y., Chaudhari A., and Andriacchi T.P.-** *Tibiofemoral joint contact force in deep knee flexion and its consideration in knee osteoarthritis and joint replacement.* Journal of Applied Biomechanics, 2006;22:305-313
- Navarro MS, Navarro RD, Akita J Jr, Cohen M.** *Anatomical study of the lateral patellofemoral ligament in cadaver knees.* Rev Bras Ortop 2008%3B43-300-307.
- Noyes FR, Grood ES.** *Classification of ligament injuries: why an anterolateral laxity or anteromedial laxity is not a diagnostic entity.* In Griffin P, editor: AAOS Instructional Course Lectures, Vol XXXVI. Chicago: American Academy of Orthopaedic Surgeons;
- O'Connor J, Shercliff T, Fitzpatrick D, et al.** **Geometry of the knee.** In: **Akeson WH, O'Connor JJ, Daniel DM, editors.** *Knee ligaments: structure, function, injury and repair.* New York: Raven Pr; 1990. p 163-200.
- Otake N, Chen H., Yao X. and Shoumura A.** *-Morphologic study of the lateral and medial collateral ligaments of the human knee.* FEBRUARY 1991, Vol. 113
- Otto B. Y., Brantigan C. and Voshell A. F.-***The mechanics of the ligaments and menisci of the knee joint.* The journal of bone and joint surgery vol. xxiii, no. 1, january 1941 pp 44:66
- Papas PV, BS, Fred D. Cushner, MD, and Giles R. Scuderi, MD.** *The History of Total Knee Arthroplasty.* 2018, Techniques in Orthopaedics Volume 00, Number 00;1:5
- Petersen W. and Zantop T.-***Anatomy of the anterior cruciate ligament with regard to its two bundles.* CLINICAL ORTHOPAEDICS AND RELATED RESEARCH Number 454, pp. 35–47 © 2006 Lippincott Williams & Wilkins
- Salvadore G., Meere P. A., Verstraete M. A., victor . and Walker P. S.-** *Laxity and contact forces of total knee designed for anatomic motion: A cadaveric study.* (2018), <https://doi.org/10.1016/j.knee.2018.04.014>
- Schunke M., Schulte E., Schumacher U., Voll M. and Wesker K.-***Prometheus-Atlante di Anatomia-Anatomia Generale e Apparato Locomotore-* Utet 2006
- Shimmin A., Martinez-Martos S., Owens, Iorgulescu A. D., Banks S** - *Fluoroscopic motion study confirming the stability of a medial pivot design total knee arthroplasty.* The Knee 22 (2015) 522–526

- Smirk C and Morris H.** - *The anatomy and reconstruction of the medial patellofemoral ligament.* C. Smirk, H. Morris / *The Knee* 10 (2003) 221–227
- Smith PN, Refshauge KM, Scarvell JM.** *Development of the concepts of knee kinematics.* *Arch Phys Med Rehabil* 2003;84:1895-902.
- Smith S. M. , Cockburn R. A., Hemmerich A., Li R. M., Wyss U. P.**-*Tibiofemoral joint contact forces and knee kinematics during squatting.* *Gait & Posture* 27 (2008) 376–386
- Stiehl J. B.**-*Comparison of tibial rotation in fixed and mobile bearing total knee arthroplasty using computer navigation.* *International Orthopaedics (SICOT)* (2009) 33:679–685
- Stylianou AP, Guess TM, Kia M.** *Multibody muscle driven model of an instrumented prosthetic knee during squat and toe rise motions.* *J Biomech Eng.* 2013 Apr;135(4):041008
- Tamer T. M.** *Hyaluronan and synovial joint- function, distribution and healing.* *Interdisciplinary Toxicology.* 2013; Vol. 6(3): 111–125
- Todo S., Kadoya Y., Moilanen T., Kobayashi A., Yamano Y., Iwaki H., and Freeman M. A. R.** -*Anteroposterior and rotational movement of the femur during knee flexion.* 1999 *Clinical Orthopedics and Related Research* number 362, pp 162-170
- Trilha Junior M, Fancello EA, Roesler CRM, More ADO.** *Three-dimensional numerical simulation of human knee joint mechanics.* *Acta Ortop Bras.* [online]. 2009;17(2):18-23. Available from URL: <http://www.scielo.br/aob>.
- Verra WC, van den Boom LG, Jacobs W, Clement DJ, Wymenga AA, Nelissen RG.** *Retention versus sacrifice of the posterior cruciate ligament in total knee arthroplasty for treating osteoarthritis.* *Cochrane Database Syst Rev.* 2013 Oct 11;(10):CD004803. doi: 10.
- Verstraete M. A., Meere P. A., Salvadore G., Victor J and Walker P.S.**- *Tibiofemoral Force following Total Knee Arthroplasty- Comparison of Four Prosthesis Designs In Vitro.* *J. Biomech.* (2017), <http://dx.doi.org/10.1016/j.jbiomech.2017.05.008>
- Walker P. S. and Sathasivam S.** *Design forms of total knee replacement.* 2000 *Proc InstnMech Engrs* Vol 214 Part H 101:119
- Walker P.S, Sussman-Fort J.M, Yildirim G, MSc and Boyer J.** *Design features of total knees for achieving normal knee motion characteristics.* 2009- *The Journal of Arthroplasty* Vol. 24 No. 3 475:483

Wilson D. R., Feikes J. D., Zavatsky A. B., O' Connor J. J. *The components of passive knee movement are coupled to flexion angle.* Journal of Biomedics 33 (2000) 465-473

Wismans J.-A *Three dimensional mathematical model of the human knee joint.* Eindhoven: Technische Hogeschool Eindhoven DOI: 10.6100/IR155825 General

Wismans, J. (1980). *A Three-Dimensional Mathematical Model of the Human Knee Joint.* PhD, Eindhoven University of Technology.

Jones O. *The knee joint- TeachMeAnatomy.info- 2018* (The knee joint-Articulations-Movements-Injuries-TeachMeAnatomy)

Zaffagnini P. S., Dr. Giulio Maria Marcheggiani Muccioli, Dr.ssa Maria Pia Neri, Dr. Mirco Lo Presti, Dr. Alessandro Russo, Dr. Alessandro Di Martino, Dr. Alberto Grassi, Dr. Matteo Romagnoli, Dr. Massimiliano Mosca, Prof. Vittorio Vaccari-
Ginocchio: la protesi di ginocchio- 2017 (<http://www.ior.it/curarsi-al-rizzoli/ginocchio-la-protesi-di-ginocchio>)